

**A NUMERICAL STUDY OF BACTERIA TRANSPORT
THROUGH POROUS MEDIA USING
THE GREEN ELEMENT METHOD**

By

SURESH RAMSUROOP

Submitted in part fulfilment of the requirements for the degree of
Master of Science in Engineering (Water and Environmental Management)
in the Department of Civil Engineering in the Faculty of Engineering
at the University of Durban Westville

Supervisor : Professor O.O. Onyejekwe

July 2000

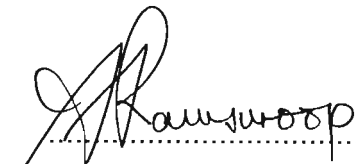


DECLARATION

The Registrar (Academic)
UNIVERSITY OF DURBAN WESTVILLE

Dear Sir

I, SURESH RAMSUROOP , REG. NO.: 9904708, hereby declare that the dissertation entitled **A NUMERICAL STUDY OF BACTERIA TRANSPORT THROUGH POROUS MEDIA USING THE GREEN ELEMENT METHOD**, is the result of my own investigation and research and that it has not been submitted in part or in full for any other degree or to any other University.


.....
S Ramsuroop

27-07-2000
.....
Date

This dissertation is dedicated to
my son Jyestha
and
wife Paranjothi

Acknowledgements

I wish to express my sincere gratitude to the following people, for their contribution towards this dissertation :

- ▶ Prof. O.O. Onyejekwe, my supervisor, for his invaluable input, guidance and encouragement, and for igniting my interest in the field of computational analysis.
- ▶ My colleagues in the Department of Chemical Engineering at the ML Sultan Technikon, for their assistance and advice, especially Sadhana Vallabh and Lingum Pillay for their constructive comments.
- ▶ My wife, Paranjothi Pillay, for her understanding, love and support throughout my studies.

Abstract

The continued widespread contamination of the subsurface environment by microbial pathogens and chemical wastes has resulted in an increased interest in the factors that influence microbial transport through porous media.

In this work a numerical study is undertaken to determine the influence of various processes that contribute to microbial transport in porous media. The evaluations were conducted by the simulation of a typical macroscopic transport model, using a novel numerical technique referred to as the Green Element Method (GEM). This computational method applies the singular boundary integral theory of the Boundary Element Method (BEM) to a discretised domain in a typical Finite Element Method (FEM) procedure.

Three models are presented to evaluate the effects of the various parameters and factors: a constant porosity model was formulated to verify the GEM formulation against an analytical solution, a variable porosity linear model was developed and used for the simulation of the transport process involving first order type clogging, and a variable porosity nonlinear model used to evaluate effects of nonlinear type clogging. All three models were validated by simulations in specific applications in which analytical or deduced solutions were available. The parameters and factors evaluated included the effects of substrate concentrations, decay rates, source concentrations (boundary conditions), flow velocity, clogging rates, dispersivity, point and distributed sources, and nonlinear clogging.

The results show that the trends predicted were consistent with the trends expected from theory. The conditions that enhanced bacteria transport included high velocities, low decay rate constants, high substrate concentrations, and low clogging rates. The range of dispersivities investigated showed little variation in the bacteria concentration

in the longitudinal direction. Reduction in porosity resulted in retardation of the migrating plume. Conditions that led to significant loss in porosity are high bacteria loadings and high growth rates.

The GEM formulation showed no restrictions or limitations in solving transient linear and transient nonlinear applications. In the nonlinear application, the Newton Raphson algorithm was successfully used for the iterative solution procedures. In addition, the GEM formulation easily facilitated the application of distributed and point sources in the problem domain.

Short Title : Bacteria Transport through Porous Media

Key words : bacteria transport, Green element method, biologically reactive contaminants, transport modelling.

Table of Contents

Abstract		
List of Figures		iv
List of Tables		vi
Nomenclature		vii
Chapter One	INTRODUCTION	
1.1	Background	1.1
1.2	Objectives	1.4
1.3	Approach and Thesis Organisation	1.4
Chapter Two	LITERATURE REVIEW	
2.1	Microbial Transport	2.1
2.2	Numerical Methods	2.6
2.3	Summary	2.6
Chapter Three	OVERVIEW OF BACTERIA TRANSPORT PROCESS	
3.1	Transport Processes	
	3.1.1 Physical Processes	3.1
	3.1.2 Chemical Processes	3.5
	3.1.3 Biological Processes	3.7
3.2	Transport Models	3.8
3.3	Summary	3.12
Chapter Four	GREEN ELEMENT FORMULATION	
4.1	Comparison of Numerical Techniques	4.1
4.2	Green Element Formulation of Transport Equation	4.2
4.3	Summary	4.11

Chapter Five	MODEL VERIFICATION AND COMPUTATIONAL PROCEDURES	
5.1	Model Verification Procedures	5.1
5.2	Numerical Procedures	5.4
	5.2.1 Linear Transport Equations	5.6
	5.2.1 Nonlinear Transport Equation	5.10
5.3	Computation Procedures	5.12
5.4	Summary	5.12

Chapter Six	APPLICATION OF GEM MODELS	
6.1	GEM Model Verification	6.1
	6.1.1 Constant Porosity Model Verification	6.2
	6.1.2 Variable Porosity and Nonlinear Model Verification	6.4
6.2	Effects of Various Parameters on Bacteria Transport	6.6
	6.2.1 Groundwater Flowrate	6.7
	6.2.2 Dispersivity	6.7
	6.2.3 Linear and Nonlinear Clogging	6.7
	6.2.4 Growth and Decay Rates	6.8
	6.2.5 Substrate Concentration	6.8
	6.2.6 Source Concentration (Boundary Conditions)	6.8
	6.2.7 Distributed and Point Sources	6.8
6.3	Summary	6.9

Chapter Seven	RESULTS AND DISCUSSION	
7.1	General Observations	7.1
7.2	Model Simulations	7.2
	7.2.1 Comparison of Constant Porosity and Variable Porosity Models	7.2
	7.2.2 General Illustration	7.5
	7.2.3 Influence of Model Parameters	7.6
	7.2.3.1 Flow velocity	7.7

7.2.3.2	Dispersivity	7.9
7.2.3.3	Source Concentration (Boundary conditions)	7.10
7.2.3.4	Substrate Concentration	7.13
7.2.3.5	Decay Rates	7.14
7.2.3.6	Clogging Process	7.15
7.2.3.7	Distributed and Point Sources	7.19
7.3	Summary	7.27
Chapter Eight	CONCLUSIONS AND RECOMMENDATIONS	8.1
REFERENCES		Ref-1
APPENDIX A	- Worked Example - Heterogeneous Heat Transfer	A-1
APPENDIX B	- Worked Example - Biofilm Mass Transfer	B-1
APPENDIX C	- Programme Details	C-1

List of Figures

Figure No.	Description	Page
Figure 1.1	Overview of Thesis Organisation	1-6
Figure 2.1	Inter-relationships of Parameters and Processes affecting Bacteria Transport through Porous Media	2-5
Figure 2.2	Classification of Major Numerical Techniques	2-7
Figure 3.1	Effect of Advection, Diffusion and Dispersion on Contaminant plume	3-3
Figure 3.2	The effects of advection and dispersion	3-3
Figure 3.3	The effects of sorption processes on concentration profile	3-6
Figure 3.4	Clogging and declogging processes in bacteria transport	3-6
Figure 4.1	Discretisation of spatial domain	4-5
Figure 4.2	Discretisation of spatial and temporal domains	4-10
Figure 5.1	Analytical Solutions for different times	5-3
Figure 5.2	Analytical solutions at different distances	5-3
Figure 5.3	Computational algorithm for linear transport models	5-9
Figure 5.4	Computation algorithm for nonlinear transport model	5-13
Figure 5.5	Computer programme algorithm for linear models	5-14
Figure 5.6	Computer programme algorithm for nonlinear models	5-15
Figure 6.1	Comparison of Analytical and constant porosity model at different times	6-3
Figure 6.2	Comparison of Analytical and constant porosity model at different positions	6-4
Figure 6.3	Comparison of the three GEM models	6-6
Figure 7.1	Comparison of constant porosity and variable porosity models	7-3

Figure 7.2	Typical porosity profile for application of significant porosity changes	7-4
Figure 7.3	Typical bacteria concentration profile	7-5
Figure 7.4	Effects of groundwater velocity on contaminant plume at five hours	7-8
Figure 7.5	Effects of groundwater velocity on contaminant plume at 24 hours	7-8
Figure 7.6	Effects of Dispersion concentration profile	7-9
Figure 7.7	Effects of bacteria loading on concentration profile	7-12
Figure 7.8	Effects of bacteria loading on porosity	7-12
Figure 7.9	Effects of substrate concentration on bacteria profile	7-14
Figure 7.10	Effects of decay rates on bacteria concentration profile	7.16
Figure 7.11	Effects of clogging rates on concentration profile	7-17
Figure 7.12	Effects of clogging reaction order on bacteria concentration profile	7-18
Figure 7.13	Effects of bacteria loading on nonlinear clogging	7-19
Figure 7.14	Effects of distributed source with net growth conditions	7-21
Figure 7.15	Effects of distributed source with net decay conditions	7-21
Figure 7.16	Effects of point source with net growth conditions	7-22
Figure 7.17	Effects of point source with net decay conditions	7.22
Figure 7.18	Effects of point sources / sinks on elements	7.23
Figure A.1	Sketch of heterogenous heat transfer problem	A-1
Figure A.2	Temperature Profile comparison between FEM and GEM	A-13
Figure A.3	Flux profile comparison between FEM and GEM	A-13
Figure B.1	Comparison of GEM and analytic solutions for mass transfer applications	B-6
Figure C.1	Sample of Input Data File for BactVaripore Programme	C-6
Figure C.2	Sample of Output File for BactVaripore Programme	C-7

List of Tables

Table No.	Description	Page No.
Table 2.1	Summary of solution procedures for contaminant and bacteria transport	2-8
Table 6.1	Comparison of analytical and GEM solutions for different times	6-2
Table 6.2	Comparison of analytical and GEM solutions for different distances	6-3
Table 6.3	Simulation parameters	6-5
Table 7.1	Simulation parameters	7-6
Table A.1	Comparison of GEM and FEM results	A-12
Table B-1	Results of GEM and analytical solutions	B-5

Nomenclature

C	bacteria concentration (g / ml or kg / m^3)
C_F	substrate concentration (g / ml or kg / m^3)
D	mechanical dispersion coefficient (cm^2 / s or m^2 / h)
D_B	diffusion coefficient (cm^2 / s or m^2 / h)
D_m	dispersion coefficient (cm^2 / s or m^2 / h)
D_T	motility coefficient (cm^2 / s or m^2 / h)
J	sum of fluxes ($g / s.cm^2$ or $kg / h.m^2$)
J_A	flux due to advection ($g / s.cm^2$ or $kg / h.m^2$)
J_B	flux due to Browian motion ($g / s.cm^2$ or $kg / h.m^2$)
J_C	flux due to chemotaxis ($g / s.cm^2$ or $kg / h.m^2$)
J_D	flux due to dispersion ($g / s.cm^2$ or $kg / h.m^2$)
J_T	flux due to tumbling ($g / s.cm^2$ or $kg / h.m^2$)
J_S	flux due to settling ($g / s.cm^2$ or $kg / h.m^2$)
K_S	substrate concentration when growth rate is half its maximum (g / ml or kg / m^3)
K_m	chemotatic coefficient (cm^2 / s or m^2 / h)
\tilde{K}_e	average diffusion coefficient within an element
k	net decay / growth rate (s^{-1} or h^{-1})
k_c	clogging rate (s^{-1} or h^{-1})
k_d	decay rate (s^{-1} or h^{-1})
k_y	declogging rate (s^{-1} or h^{-1})
L_{ij}	matrix coefficients
l	length of typical element (cm or m)
\tilde{l}	length of longest element (cm or m)
R_a	rate of deposition of particles on grains ($g / ml.s$ or $kg.m^3.h$)
R_{g_f}	bacteria growth rate in the bulk fluid ($g / ml.s$ or $kg.m^3.h$)

R_{d_f}	decay rate of bacteria in bulk fluid ($g / ml.s$ or $kg.m^3.h$)
R_{d_s}	decay rate of bacteria adsorbed on grains ($g / ml.s$ or $kg.m^3.h$)
R_{ij}	matrix coefficients
u	groundwater velocity (cm / s or m / h)
U_{ij}	matrix coefficients
α	weighting factor
δ	Dirac delta function
ϕ	primary variable
φ	primary variable gradient
μ	growth rate constant (s^{-1} or h^{-1})
μ_m	maximum growth rate (s^{-1} or h^{-1})
θ_0	initial porosity
θ_i	changed porosity
ρ_B	bacteria density (g / ml or kg / m^{-3})
σ	volume of adsorbed bacteria ($ml / ml\ solid$ or $m^{-3} / m^{-3}\ solid$)
τ	integrating constant
ξ	integrating constant
ζ	local co - ordinate system
Δt	time change interval (s or h)
Ω	linear interpolation function

Chapter One

Introduction

The continued widespread contamination of surface water and subsurface water (aquifer) by microbial pathogens and chemical wastes has resulted in an increased interest in the factors that influence microbial transport. The areas of application in South Africa in which microbial / bacteria transport through porous media is of significance include: environmental pollution, groundwater contamination, bioremediation, and artificial recharge of aquifers. In this study a new numerical procedure is presented for the simulation of biologically reactive contaminants in porous media.

1.1. Background

In South Africa, the provision of potable water to its previously excluded population is rapidly out-pacing its current available capacity. Furthermore, comparatively low and varied rainfall, averaging about 502mm per annum as compared to a world average of 802 mm per annum, makes South Africa a relatively arid country (Fuggle and Rabie, 1994). The need to consider groundwater as an additional source of water to peri-urban and rural areas, and to supplement the requirements in rapidly growing urban areas, is increasing. Several studies relating to groundwater utilization were undertaken by the Water Research Commission (WRC). These included:

A study to establish the magnitude of groundwater contamination originating from formal and semi-formal settlements (WRC, 1999a). The aquifers underlying some of these settlements could act as a cheap source of drinking water. The study found that the major source of pollutants emanating from these settlements were domestic (liquid and solid) and sanitation waste, and therefore the

significant pollutants were micro-organisms, organics and nutrients.

A study to determine the extent of groundwater and storm-water run-off contamination from septic tank and soak away systems (WRC,1999b), found these to be a major source of microbial pollution. It reported that, due to lack of legislation and control, poor location, poor design, and lack of maintenance of these systems, which are widely used in South African coastal resorts, were a major source of pollution to groundwater and lagoons.

A study to determine the extent of groundwater pollution from agricultural activities (WRC,1999c), namely, intensive animal husbandry, and the use of sewer sludge as fertilizer, reported elevated dissolved organic carbon (DOC) levels and faecal pollution in the groundwater.

The recharge of the Atlantis Aquifer (situated 50 km north of Cape Town) with purified sewer water and storm-water run-off, to meet the increase in domestic and industrial demands for water (Botha,1987), showed varying concentrations of faecal coliforms in samples drawn near the infiltration pans.

Additional sources of groundwater contamination by bacteria are contamination from landfill leachate and from sewer line leaks. A useful application for bacteria transport through porous media models, is in the process of bioremediation of contaminated soils. Van Zyl (1998) provides a comprehensive review of the status of bioremediation in South Africa.

The most obvious way to check on pollution of aquifers, would be to monitor it continuously. This method is time consuming, expensive and only yields passive information, i.e. pollution is detected only after an aquifer becomes contaminated. It does not provide the information to prevent or contain the pollution, or even clean up

contaminated environments (i.e. soils / aquifers).

The most viable approach to predict and manage microbial contamination of aquifers and bioremediation processes, is through the use of contaminant transport models. These models are a mathematical representation of the physical, chemical and biological processes that a pollutant undergoes in the subsurface environment. The mathematical models are attractive because they offer a relatively rapid and inexpensive way to assess potential contaminations of the subsurface environment.

The two ways of solving the transport equations/models are analytical methods and numerical methods. Whilst the strength of the analytical methods is the derivation of exact solutions, these can only be obtained for a narrow range of simplified applications. The usefulness of the exact solution is that they provide a check for the numerical solutions which can be subjected to a variety of errors. The two most widely used techniques for solving transport equations are the Finite Difference Method (FDM) and the Finite Element Method (FEM). Several modified and new techniques have emerged to overcome some of the inefficiencies of the traditional FDM and FEM. These include: Particle Tracking Method, Integrated Finite Difference Method, Moving Finite Element Method, Mixed Finite Element Method, Boundary Element Method (BEM), and the Green Element Method (GEM).

Sato (1992) and Ramchandran (1994), highlighted the principle differences between the domain methods (FDM and FEM) and the boundary method (BEM), by comparing the advantages and disadvantages of these methods in some applications. The most notable advantages listed by Sato (1992) is the high degree of accuracy and the simplicity of the BEM formulation in linear applications. Onyejekwe (1996a) and Taigbenu (1999) noted that the lack of applications of BEM to nonlinear applications was indicative of the numerical difficulty encountered in applying the BEM to nonlinear transient problems.

A numerical method that has the capacity to handle nonlinearity, heterogeneity, and point and distributed sources / sinks without any simplifications or restrictions is an essential requirement to solve practical applications of the transport equations.

A relatively new computational method, referred to as the Green Element Method (GEM), applies the singular boundary integral theory of the Boundary Element Method (BEM) to a discretised domain in a typical Finite Element Method (FEM) procedure. This methodology combines the accuracy of BEM and the flexibility of FEM, resulting in a more versatile computation technique. The applications of GEM to several nonlinear transient problems by Taigbenu (1998;1999), Onyejekwe (1995,1996;1998a,b,c,d), and Onyejekwe *et al.* (1998;1999), Taigbenu and Onyejekwe (1995; 1997a,b; 1998) have shown the ease of application, accuracy, and robustness of the method.

1.2. Objectives of Study

The objective of this study are three fold:

- i) To develop the mathematical model for Microbial transport through porous media.
- ii) To solve the transport model by the Green Element Method (GEM) and to validate the results by comparison to analytical or experimental results.
- iii) Using this procedure to evaluate the effects of the various mechanisms and processes (linear and non-linear) that contribute to microbial transport through porous media.

1.3. Approach and Thesis Organisation

Microbial transport through porous media is a complex phenomenon and it would not be possible to cover all aspects in detail in this limited study. This present study is therefore limited to:

- i) Literature review of bacteria transport models and numerical procedures used to solve contaminant transport models.

- ii) Review of bacteria transport model adopted by this study.
- iii) GEM formulation of adopted model.
- iv) Model verification by comparing the results to an analytical solution for a specific application.
- v) Simulation of the GEM transport model/s in different applications.

The remaining chapters will cover the following aspects:

Chapter Two provides a literature review on microbial transport models, factors influencing microbial transport, and numerical procedures used to solve transport equations.

Chapter Three gives an overview of the processes associated with microbial transport, and establishes the transport model adopted by this study.

In Chapter Four the GEM formulation for the adopted transport model is systematically developed.

Chapter Five provides an overview of the numerical, computational and verification procedures.

Chapter Six is devoted to the verification of the GEM model and the application of the model for different scenarios.

In Chapter Seven the results and the discussion thereof are presented.

The main results and conclusions are listed in Chapter Eight. This chapter also includes a discussion of possible future work.

The overall thesis organisation is depicted pictorially in Figure 1.1

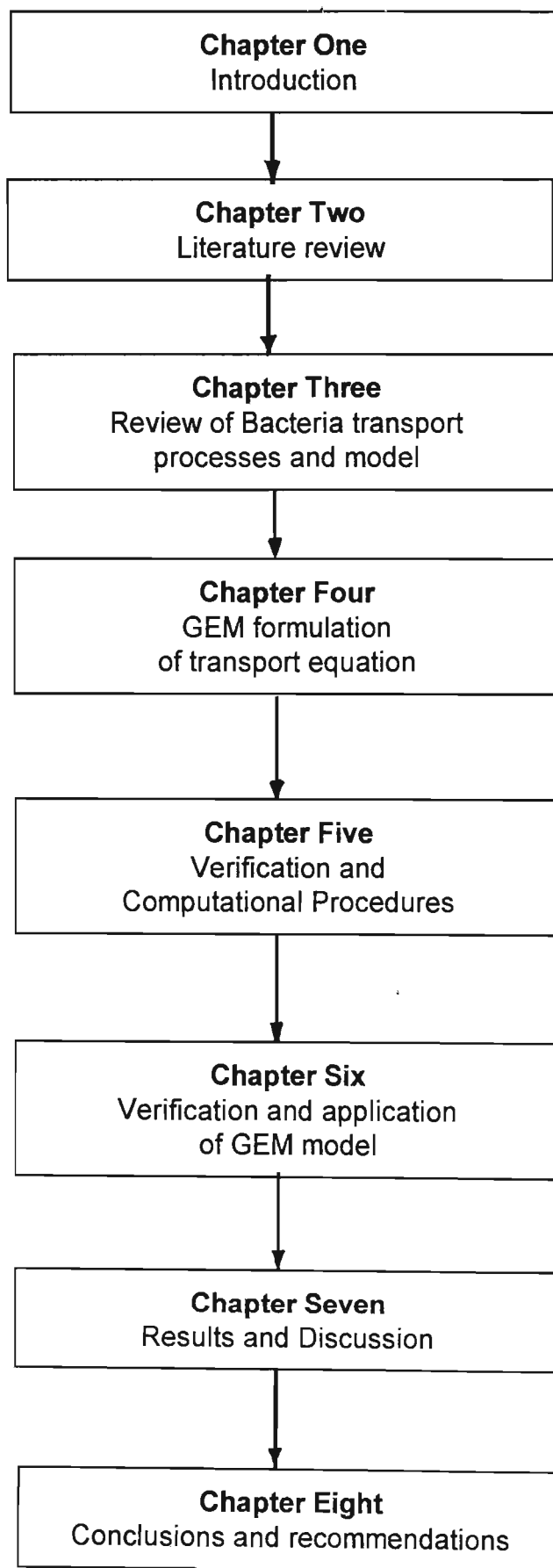


Figure 1.1. Overview of Thesis Organisation

Chapter Two

Literature Review

The purpose of this chapter is to present a literature review of microbial transport through porous media, factors that influence microbial transport, and numerical procedures used to solve contaminant and microbial transport models

2.1. Microbial Transport

Corapcioglu and Haridas (1984) reported on the various transport and retention mechanisms experienced by micro-organisms at a macroscopic level. The study analyzed the various transport processes of dispersion, convection, Brownian motion, chemotaxis and tumbling, deposition, adsorption, decay and growth kinetics of bacteria. These processes were expressed in mathematical terms that could be incorporated into physical transport models. The differences between bacteria and virus transport were also investigated.

Corapcioglu and Haridas (1985) developed mathematical models to predict the spatial and temporal distribution of the microbial concentration and nutrient concentration in porous media. The models presented included all the mechanisms outlined in their previous work (1984). The coupled models were solved by the Galerkin method and simulated for the case of a 14 cm soil column. The model developed included the effects of changing porosity due to clogging, however the changes to dispersivity were not included.

Molz *et al.* (1986) developed mathematical models that were based on pore scale transport processes. The models developed assumed that, bulk of the micro-organisms in an aquifer grow in micro-colonies attached to the matrix

surfaces where the growth and degradation processes occurred. The pore scale approach results in small values for the dispersions, and therefore the solutions to the models were obtained by an Eulerian - Lagrangian numerical procedure.

Baveye and Valocchi (1989) reported on the developments of mathematical models for microbial transport prior to 1989. The study highlighted the existence of three different conceptual frameworks for bacteria growth and biologically reacting solute transport in saturated porous media. The different frameworks were described as : the biofilm model, the micro-colony model, and the macroscopic model. The fundamental differences between these models are that the bio-film and micro-colony models are based on pore scale processes, whereas in the macroscopic model, the pore scale processes are neglected and the biomass is assumed to react with the macroscopic bulk fluid substrate concentrations. In the final analysis it was concluded that the macroscopic transport equations for each of the formulations are formally identical.

Taylor and Jaffe (1990a,b,c,d) adopted the bio-film model to investigate the changes to porosity, permeability, and dispersivity resulting from the bio-film growth. This work also investigated the effects of pulsed substrate loadings, and flow-rate and flow duration on the clogging of the porous media by the biomass. The equations derived to predict changes to dispersivity, porosity and permeability correlated to the tracer experiments conducted in a bio-film column reactor.

Harvey and Goradedian (1991) used colloid filtration theory to model the movement of bacteria through a contaminated sandy aquifer. The filtration model commonly used for packed bed filtration was modified and used to predict the transport of indigenous bacteria moving down-gradient within a plume of organically contaminated groundwater. It was concluded that there were several

uncertainties in applying filtration theory to problems involving the transport of bacteria in groundwater.

In a comprehensive review of transport models, Dickinson (1991) concluded that the use of existing contamination models and those describing colloidal transport are inadequate to describe microbial transport. The review also includes a list of field studies that were done, to quantify microbial transport and to determine realistic values for the transport parameters.

Hornberger *et al.* (1992) used a simplified form of the macroscopic model to fit solutions to a range of experimental results to establish the effects of grain size, type of organisms and ionic strength of water on the variability of dispersion, deposition and entrainment coefficients. The study concluded that the macroscopic model of Corapcioglu and Haridas (1985) successfully described some of the important characteristics of transport of bacteria through porous media.

The influence of the chemical and physical conditions of the groundwater and the solid matrix on the various microbial transport processes, has received considerable attention. These are briefly reviewed here:

Harvey (1991) and Mc Inerney (1991) provided comprehensive reviews of factors that influence microbial transport in groundwater. The reviews highlighted the complex interactions that exists between the processes that affect transport, and the chemical and physical properties of the subsurface environment. Scholl and Harvey (1992) investigated the effects of surface sediment characteristics and pH. Le Blanc (1993) reported on the field and laboratory studies of the physical, chemical and micro-biological processes that affect transport in a sewage contaminated aquifer at Cape Cod. Bengtsson and Lindquist (1995) investigated the effects of microbial concentration on the

sorption processes. Wan *et al.*(1995) reported on the significance of bacteria sedimentation on the transport process. Weiss *et al.*(1995) investigated the effect of bacteria cell shape on the transport process. Vandeverve *et al.*(1995) proposed models to predict the change in hydraulic conductivity due to microbial activity in different textured media. Ryan and Elimelech (1996) reviewed the various physio-chemical and engineering aspects of colloid mobilization and transport in groundwater. Wu *et al.* (1996) reported on experimental work done to determine the reduction in hydraulic conductivity due to microbial growth. Ryan *et al.* (1999) investigated the effects of chemical agents and chemical perturbations on the mobilization and transport of colloids. Keely *et al.* (1999) reviewed aspects of microbial physiology, and outlined the type of information needed to predict contaminant movement and transformation in groundwater.

The general conclusions from the literature review on factors that influence microbial transport can be summarised as : The transport of bacteria is controlled by the : specific bacteria type, the nature of the soil, and the climate of the environment. Specific factors affecting the survival of bacteria include temperature, organic matter, moisture content, pH and the presence of other microorganisms. Migration is controlled by moisture content, pH, salt species and concentration, soil properties (sand, silt, clay), organic matter and hydraulic conditions. Whilst all these factors have been shown experimentally to play a role in the transport of microorganisms in the subsurface, most of the data is described qualitatively rather than quantitatively. In some cases, too few data were generated to describe the results mathematically. In others the results are microorganism specific that they cannot easily be generalised to describe all situations. Figure 2.1 attempts to show the interactions and interrelationships of the parameters and factors involved in the transport of bacteria through porous media.

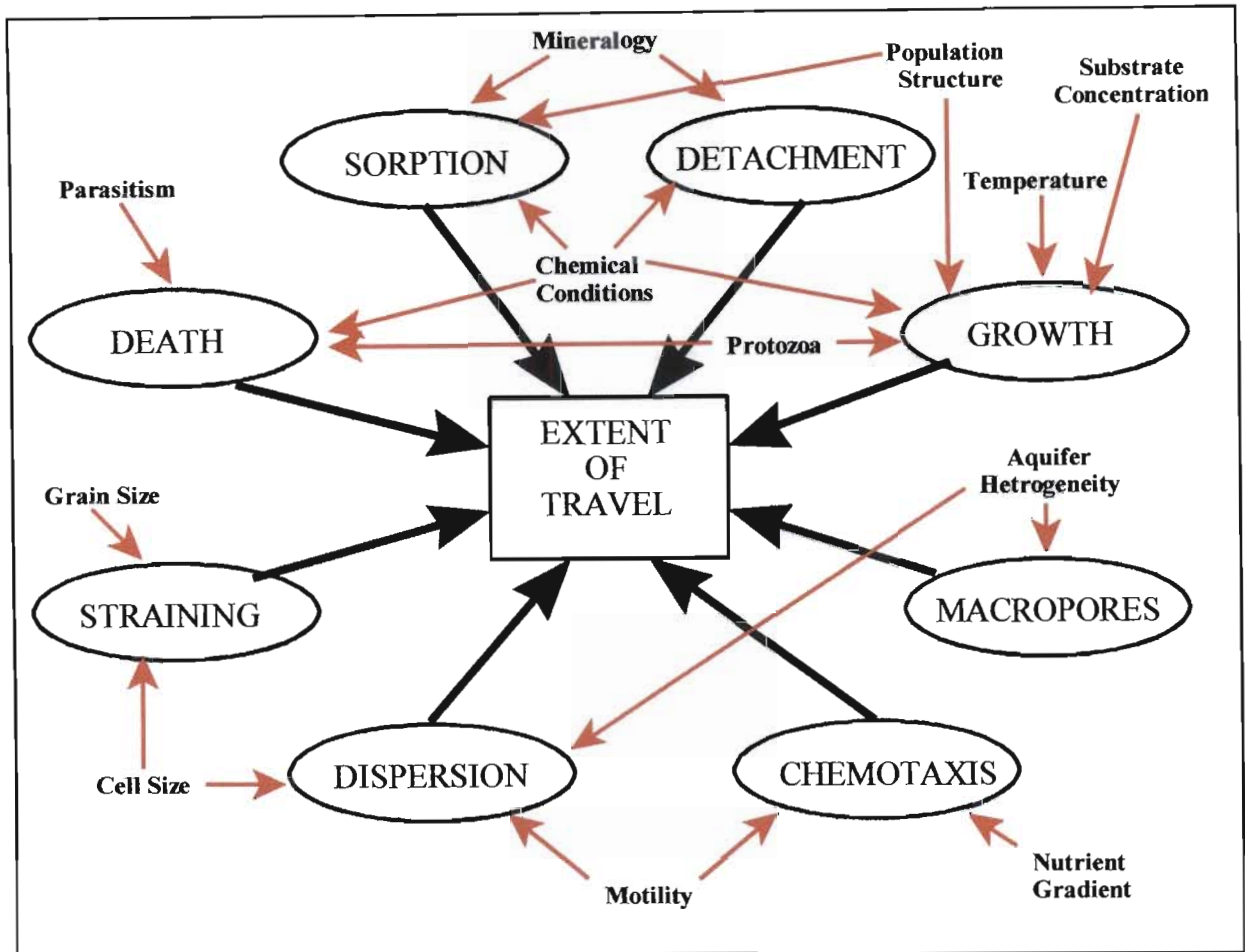


Figure 2.1 Schematic representation of the interrelationship of parameters and factors involved in the transport of bacteria through medium aquifers (Harvey, 1991)

2.2. Numerical Procedures

A variety of analytical and numerical solution procedures have been developed for use in groundwater applications. The procedures reviewed here are restricted to solutions of contaminant and microbial transport. As indicated in chapter one, the two most common techniques used to solve the transport equations are FDM and FEM. Due to the dual nature of the transport equation i.e. parabolic nature at diffusion domination and hyperbolic nature at advection domination, various hybrids of these techniques have been developed to improve the numerical efficiency of these methods. These include : Particle Tracking Method, Integrated Finite Difference Method, Moving Finite Element Method, Mixed Finite Element Method, Boundary Element Method (BEM), and Green Element Method (GEM). Figure 2.2 shows Ramachandran's (1994) classification of the major numerical solution techniques used to solve differential equations. A comprehensive discussion on each of the techniques is beyond the scope of this study, however, a comprehensive summary of the techniques is given in Table 2.1. A further comparison of the major techniques will be given in chapter four. This summary complements the summary given by the National Research Council (1990).

2.3. Summary

The literature review in this chapter has provided the necessary information to make an informed decision in selecting an appropriate model for the microbial transport process, and the appropriate numerical solution procedure for the governing partial differential equation. It is also evident from the review that there are several critical and complicating features which need to be considered when modeling microbial transport :

- Microbial growth is dependant on other species (substrate) being present, therefore it may be required that the fate of one or more substrate/s need to be modeled. The interactions between these models must be properly

determined.

- Biomass growth and accumulation lead to loss of permeability. This change to porosity may lead to change in flow paths and dispersivity. This requires models to be interactively coupled.
- The various constants and coefficients used in these models are highly application and location specific. Most of these values are not directly measurable and need to be determined from experimental studies.

In the next chapter , an overview of the transport processes of the adopted model will be given.

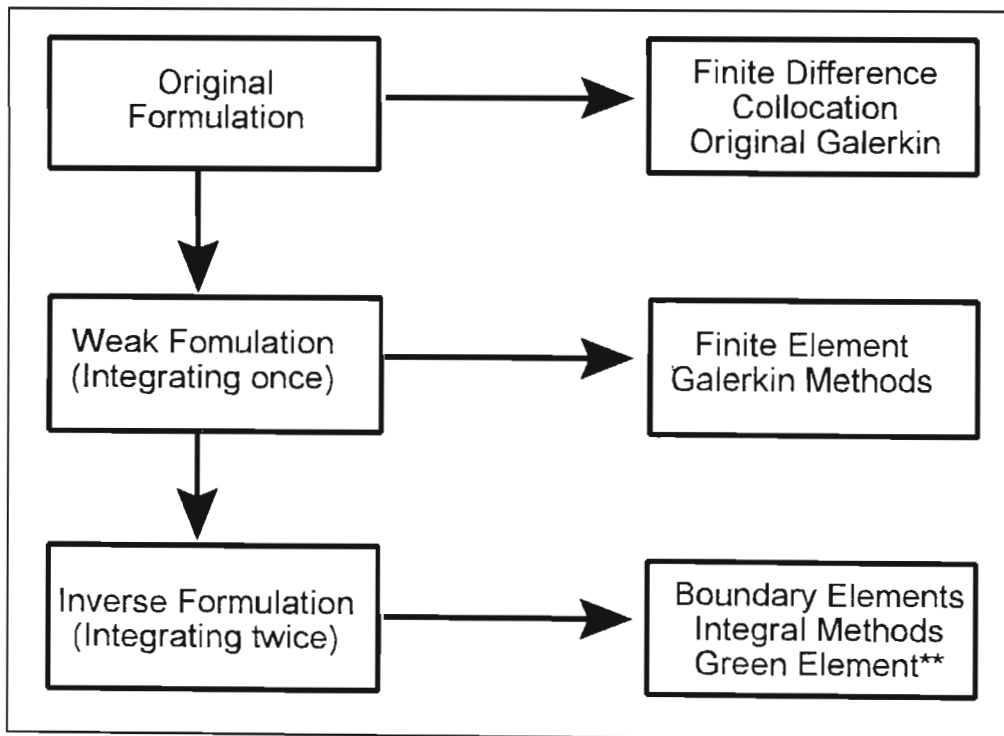


Figure 2.2 Classification of the major techniques for numerical solutions to differential equations (Ramachandran, 1994) (** added in by the author of this work)

Table 2.1. Summary of Solution Procedures for Contaminant and Bacteria Transport Models

Method	Description of method	Application	References
Analytical	a closed form solution of the governing equation, continuous in space and time [EPA,1997]	3D leachate migration Contaminant transport Virus transport	Huyakorn <i>et al.</i> (1987) ; Leiz and Dane (1990) ; Goltz and Roberts (1986) ; Sun and Chrysikopoulos (1995)
Semi - analytical	analytical solutions are evaluated using approximative techniques, resulting in a solution discrete in either space or time domain [EPA,1997]	contaminant transport landfill leachate	Celia <i>et al.</i> (1989) ; Rowe and Booker (1995)
Finite Element Method	a discrete technique for solving the given PDE wherein the domain of interest is represented by a finite number of mesh- or grid points, and the information between these points is obtained by interpolation using piecewise continuous polynomials; the resulting set of linear or nonlinear algebraic equations is solved using directly or iterative solving techniques [EPA,1997]	contaminant transport Bacteria transport	Guymon (1970) ; Gohardi and Venutielli (1995) ; Pepper and Stephenson(1995) ; Arbogast and Wheeler (1995) Corapcioglu and Haridas (1985); Taylor and Jaffe (1990)
Finite Difference Method	a discrete technique for solving the given PDE by : 1) replacing the continuous domain of interest by a finite number of mesh- or grid points representing the average sub-domain properties, and 2) by approximating the derivatives of the PDE for each of these points using finite differences; the resulting set of linear or nonlinear algebraic equations is solved using directly or iterative solving techniques [EPA,1997]	landfill leachate Contaminant transport Bacteria Transport	Straub and Lynch (1982) Oster <i>et al.</i> (1970) ; Buikis <i>et al.</i> (1995) Tan <i>et al.</i> (1994)
Boundary Element Method	a method in which the boundary value problem is expressed in terms of an integral equation; this equation is solved by approximating the boundary by series of straight lines or flat surfaces, and making simplifying assumptions regarding the behavior of the solutions along the boundary elements [EPA,1997]	Contaminant transport	Taigbenu and Liggett (1986)
Methods of characteristics	Breaks the equation into two parts, one accounting for dispersion and one accounting for advection, and replacing each of these with an equivalent system of ODE's [EPA,1997]	Contaminant transport microbial transport	Morshed and Kaluarachi (1995) ; Vachabe <i>et al.</i> (1995) Clement <i>et al.</i> (1996) ; Molz <i>et al.</i> (1986)
Green Element Method	a method in which the singular integral theory of the boundary element method is implemented in an element by element method over the whole domain [Onyejekwe, (1996a)]	Contaminant transport	Onyejekwe (1995, 1996b, 1998d) Taigebenu (1998, 1999)

Chapter Three

Overview of Bacteria Transport Processes

The purpose of this chapter is to present a brief overview of the processes that are associated with microbial transport in porous media. The transport model adopted by this work will also be analyzed.

3.1. Transport Processes

The transport of any species in porous media is controlled by a variety of physical, chemical and biological processes. Some of these processes enhance the spreading of a contaminant plume, and some may retard the spread of the plume. The processes involved will depend on the type of species being investigated, i.e. is the species miscible, immiscible, suspended solids, colloidal, organic, inorganic, etc. and on the chemical and physical properties of the subsurface environment. A brief description of some of the processes will now be presented.

3.1.1. Physical Processes

Advection - is the movement of the contaminant caused by the actual flow of the bulk fluid. Advection is the primary process by which contaminants move in the subsurface. The overall impact of advection is the movement of contaminants away from the source. The net flux due to advection in a control volume can be expressed mathematically as:

$$J_A = v_f \theta C \quad (3.1)$$

where v_f is the bulk fluid velocity (cm/s or m/h), θ is the

porosity, and C is the species concentration (g / ml or kg / m^3).

Diffusion - is the movement of contaminant in response to a concentration gradient. Diffusion transport will dominate in situations of low flow-rates and in low permeability media. Diffusion is also a dominating mechanism in micro-colony and bio-film models. The net flux due to diffusion in a control volume can be expressed mathematically as:

$$J_B = -D_B \nabla \theta C \quad (3.2)$$

where D_B is the diffusion (cm^2 / s or m^2 / h) coefficient, and ∇C is the species concentration gradient

Dispersion - is the mixing and spreading of contaminant caused by a variation of velocity of the bulk fluid. This is due to the tortuous nature of flow through porous media. Figure 3.1 attempts to illustrate this mechanism. The net flux due to diffusion in a control volume can be expressed mathematically as:

$$J_D = -D_m \nabla \theta C \quad (3.3)$$

where D_m is the dispersion coefficient (cm^2 / s or m^2 / h)

Figure 3.2 gives a visual indication of the effect of advection, diffusion and dispersion will have on a typical contaminant concentration profile in the subsurface environment.

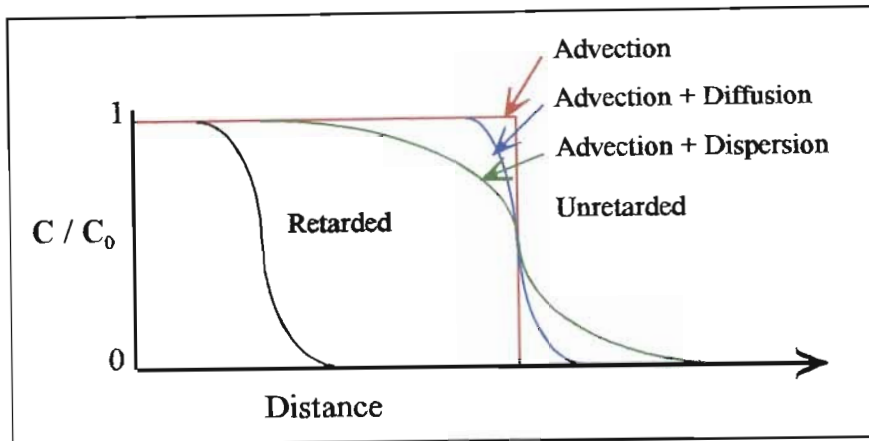


Figure 3.1. Effect of Advection, Diffusion, Dispersion on contaminant profile

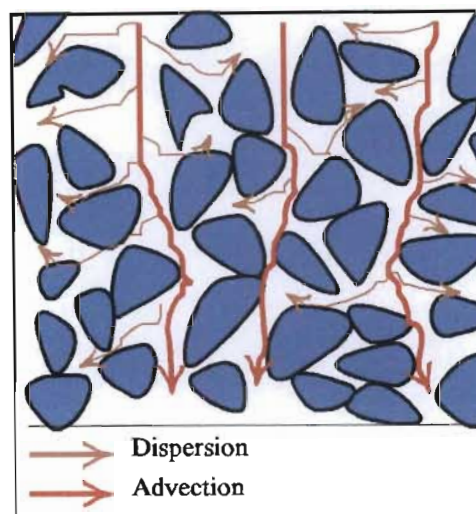


Figure 3.2. The effects of advection and dispersion

Straining - is the physical trapping of suspended solids / colloids within the solid matrix. This generally results when the suspended particles are bigger than the pore opening.

Sedimentation - settling of suspended solids / colloids due to lack of buoyancy offered by the bulk fluid. This usually results from sudden reduction in velocity or change in flow path of the bulk fluid. The net flux due to sedimentation in a control volume can be expressed mathematically as:

$$J_S = v_g \theta C \quad (3.4)$$

where v_g is the settling velocity (cm / s or m / h)

Declogging - is the release of trapped solids / colloids from the solid matrix into the bulk fluid.

Chemotaxis - is the movement of bacteria, induced by the presence of substrate gradient. Bacteria tend to propel themselves towards a richer food supply. The net flux due to advection in a control volume can be expressed mathematically as:

$$J_C = v_m \theta C \quad (3.5)$$

where $v_m = k_m \nabla \ln C_F$, C is the species (biomass) concentration, k_m is called the migration rate or chemotactic coefficient, and C_F is the substrate concentration.

Tumbling - is the chaotic, random movement of bacteria. It may be viewed as analogous to Brownian motion. The net flux due to tumbling in a control volume can be expressed mathematically as:

$$J_T = -D_T \nabla \theta C \quad (3.6)$$

where D_T is the effective diffusivity or motility coefficient, and ∇C is the species concentration gradient

3.1.2. Chemical Processes

- Sorption** - this is the general term that is used to describe the process by which a species from the bulk fluid is attached to the solid matrix or detached from the solid matrix into the bulk fluid. It includes:
- adsorption - attachment of species to the surface of the solid matrix by physical or chemical forces.
 - Absorption - transport of species into the interior of the solid matrix.
 - Ion exchange - adsorption, with a charge for charge replacement of ionic species on a surface by other species from the bulk fluid.
 - Desorption - is the opposite of the above mechanisms.

The effects of the sorption processes on a typical contaminant profile is illustrated in figure 3.3.

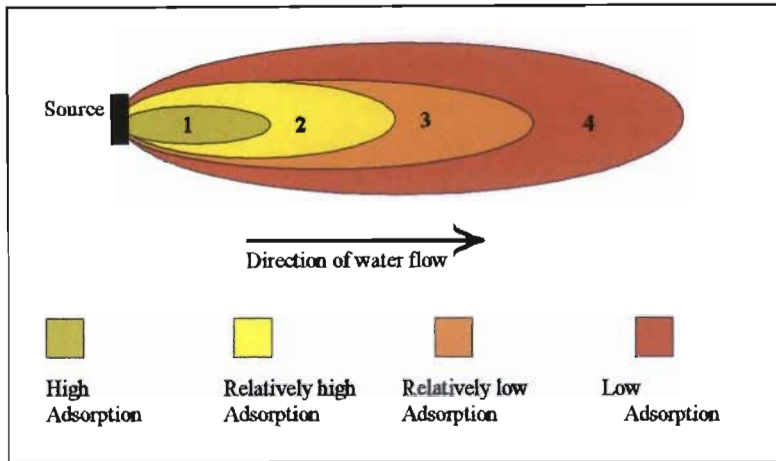


Figure 3.3. The effects of sorption processes on contaminant profile

The various mechanisms that contribute to the clogging and de-clogging processes in bacteria transport is depicted pictorially in figure 3.4.

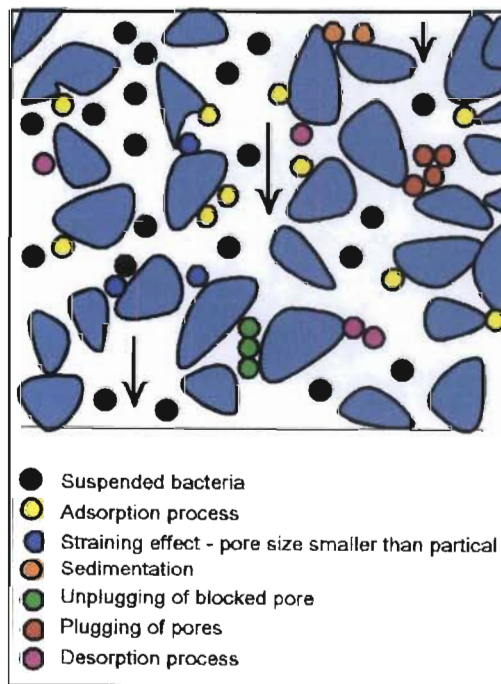


Figure 3.4. Clogging and de-clogging processes in bacteria transport

Transformation - contaminants can be transformed into other compounds by complex reactions. The main types of reactions are; hydrolysis reactions, oxidation - reduction reactions, acid- base reactions, dissolution, precipitation, and complex formations.

3.1.3. Biological Processes

Biodegradation - is the conversion of other organic and or inorganic species by micro-organisms. This is generally achieved via enzymatic reactions.

Biomass growth - under the right conditions (availability of substrate and electron donor), there will be growth of the biomass. This generally means the production of new cell mass. The growth of biomass is assumed to follow Monod's equation, which describes a relationship between the concentration of a limiting substrate and the growth rate of micro-organisms. This relationship referred to as the specific growth rate, is expressed as:

$$\mu = \frac{\mu_m C_F}{K_S + C_F} \quad (3.7)$$

where μ_m is the maximum growth rate achievable when $C_F \gg K_S$, when the concentration of all other essential nutrients are unchanged, C_F is the essential substrate concentration, and K_S is that value of the concentration of the substrate when μ_m has half its maximum value.

Biomass Decay - this is a natural life cycle process, and the life span is different for different organisms. The decay of biomass / micro-organisms is

often expressed as an irreversible first order reaction. The rate of decay is proportional to the specific decay rate constant k_d and the concentration of the biomass.

3.2. Transport Model

In this study the macroscopic model of Corapcioglu and Haridas (1985) is adopted. The application of the continuity equation will be used to introduce the various factors or processes that are included in the macroscopic model. In the macroscopic model, only processes that affect the microbial concentration in the bulk fluid will be considered.

The continuity equation states:

The sum of all fluxes into and out of the control volume plus / minus any processes which consume or create species within the control volume must equal a change in the concentration of the species within the volume.

The **sum of fluxes** J (in 1- dimension) comprises of: diffusion, dispersion, advection, chemotaxis, tumbling, and gravitational settling. This can be expressed as:

$$\begin{aligned}
 J &= J_B + J_C + J_T + J_D + J_A + J_S \\
 &= \left(-D_B \theta \frac{\partial C}{\partial x} \right) + \theta \left(C k_m \frac{\partial \ln C_F}{\partial x} - D_T \frac{\partial C}{\partial x} \right) + \left(-D_D \theta \frac{\partial C}{\partial x} \right) + \left(\theta v_f C \right) + \left(\theta v_g C \right) \\
 &\quad \text{Brownian} \qquad \text{Chemotaxis and Tumbling} \quad \text{Diffusion} \quad \text{Advection} \quad \text{Sedimentation}
 \end{aligned}$$

Which can be written as

$$\begin{aligned}
J &= -(D_B + D_T + D_D)\theta \frac{\partial C}{\partial x} + (v_m + v_f + v_g)\theta C \\
&= -D\theta \frac{\partial C}{\partial x} + u\theta C
\end{aligned}
\tag{3.8}$$

where $u = v_m + v_f + v_g$

The **sorption processes** can be expressed as:

$$R_a = k_c(n - \delta)C - k_y\rho_B\sigma \tag{3.9}$$

where: R_a is the rate of deposition of particles on grains,
 k_c and k_y are the clogging (includes adsorption, straining, entrapment, etc) and declogging rates respectively,
 σ is the volume of deposited bacteria per volume of bulk solid,
and ρ_B is the density of the bacteria.

The **sources of micro-organisms**, namely microbial growth can be expressed as

$$R_{g_f} = \mu\theta C \tag{3.10}$$

where: μ is the specific growth rate, and is related to the essential substrate concentration C_F by the following expression:

$$\mu = \frac{\mu_m C_F}{K_s + C_F}$$

and μ_m is the maximum growth rate achievable when $C_F \gg K_i$, and the concentration of all the other essential nutrients is unchanged, C_F is the essential substrate concentration, and K_i is that value of the concentration of the substrate where the

specific growth rate has half its maximum value.

The **sinks of micro-organisms**, namely microbial decay, can be expressed as

$$R_{d_f} = -k_d \theta C \quad (3.11)$$

where: k_d is the specific decay rate of the suspended bacteria.

The macroscopic mass conservation equation in one dimension for bacteria in a porous medium is given by:

$$\begin{aligned} \frac{\partial \theta C}{\partial t} + k_c \theta C - k_y \rho_B \sigma &= -\frac{\partial}{\partial x} \left[-D\theta \frac{\partial C}{\partial x} + u\theta C \right] + R_{d_f} + R_{g_f} \\ &= D\theta \frac{\partial^2 C}{\partial x^2} - u\theta \frac{\partial C}{\partial x} - k_d \theta C + \mu \theta C \\ &= D \frac{\partial^2 \theta C}{\partial x^2} - u \frac{\partial \theta C}{\partial x} + (\mu - k_d) \theta C \end{aligned} \quad (3.12)$$

which can be written as:

$$\frac{\partial C^*}{\partial t} + k_c C^* - k_y \sigma^* = D \frac{\partial^2 C^*}{\partial x^2} - u \frac{\partial C^*}{\partial x} + k C^* \quad (3.13)$$

where: $C^* = \theta C$, $k = \mu - k_d$, and $\sigma^* = \rho_B \sigma$

In order to solve the bacteria transport model, the volume of the absorbed or deposited bacteria needs to be determined. To determine the volume of the deposited bacteria, we apply the continuity equation to the adsorbed bacteria. Performing a material balance, for the bacteria absorbed on the grains, we have

$\text{rate of change of bacteria on the solid} = \text{rate of deposition} + \text{rate of growth} - \text{rate of decay}$

$$\frac{\partial \rho_B \sigma}{\partial t} = R_a + R_{g_s} - R_{d_s} \quad (3.14)$$

where: R_a is the net deposition rate, and is mathematically expressed by equation 3.9 as:

$$R_a = k_c(n - \delta)C - k_y \rho_B \sigma$$

R_{g_s} is the growth rate of the deposited bacteria, and is expressed as:

$$R_{g_s} = \mu \rho_B \sigma \quad (3.15)$$

R_{d_s} is the decay rate of the deposited bacteria, and is expressed as:

$$R_{d_s} = k_d \rho_B \sigma \quad (3.16)$$

which can finally be expressed as

$$\begin{aligned} \frac{\partial \sigma^*}{\partial t} &= k_c C^* - k_y \sigma^* + \mu \sigma^* - k_d \sigma^* \\ &= \left[\mu - (k_d + k_y) \right] \sigma^* + k_c C^* \end{aligned} \quad (3.17)$$

where: $C^* = \theta C$, and $\sigma^* = \rho_B \sigma$ (3.18)

For the purpose of completeness, the model for the essential substrate will be given. This is done to show the interactions between the various equations. The transport equation for the essential substrate will not be deduced as has been done above but merely stated.

The substrate transport equation can be expressed as:

$$\frac{\partial(\rho_s S_F)}{\partial t} + \frac{\partial(\theta C_F)}{\partial t} = - \frac{\partial}{\partial x} \left[\underbrace{-D_d \theta \frac{\partial C_F}{\partial x}}_{\text{Mechanical Diffusion}} - \underbrace{D_m \theta \frac{\partial C_F}{\partial x}}_{\text{diffusion}} + \underbrace{v_f \theta C_F}_{\text{advection}} \right] + R_F \quad (3.19)$$

substrate adsorbed on grains Dispersion to bacteria growth

where, $R_F = [-\mu Y^{-1} \theta C] + [-\mu Y^{-1} \rho \sigma]$, i.e it is the substrate consumption by the suspended bacteria, and the adsorbed bacteria respectively, and Y^{-1} is the true cell yield i.e. the mass of cell produced per unit mass of substrate removed.

The amount of substrate absorbed onto the grains can be approximated using the adsorption isotherm relationship of:

$$S_F = k_a C_F^m \quad (3.20)$$

where the values for k_a and m are determined experimentally. Assuming that $m=1$, we have

$$\frac{\partial(\rho_s k_a C_F)}{\partial t} + \frac{\partial(\theta C_F)}{\partial t} = D_F \frac{\partial^2 \theta C_F}{\partial x^2} - v_f \frac{\partial \theta C_F}{\partial x} - \mu Y^{-1} \theta C - \mu Y^{-1} \rho_B \sigma \quad (3.21)$$

which can be written as

$$\frac{\rho_s k_a \partial C_F^*}{\theta \partial t} + \frac{\partial(C_F^*)}{\partial t} = D_F \frac{\partial^2 C_F^*}{\partial x^2} - v_f \frac{\partial C_F^*}{\partial x} - \mu Y^{-1} C^* - \mu Y^{-1} \sigma^* \quad (3.22)$$

3.3. Summary

In this chapter the models for bacteria and substrate transport were stated. The various processes of these transport equations were briefly discussed. The equations clearly show the interactions that exists between these models, namely:

- the dependance of the substrate equation (3.22) on the bacteria concentration,
- the dependance of bacteria growth (3.13) on substrate concentration,

- both transport equations require the value of the volume of adsorbed bacteria σ ,
- the volume of the adsorbed bacteria (3.17) is a function of substrate and bacteria concentrations.

Chapter Four

Green Element Formulation

The numerical procedure adopted by this study to solve the equations presented in chapter three, is the Green Element Method (GEM). In addition to the review on numerical procedures given in chapter two, a brief comparison of Finite Difference Method, Finite Element Method, Boundary Element Method, and Green Element Method will be given in this chapter for completeness, and the GEM formulation of the bacteria transport equation (eqn.3.12) will be systematically developed.

4.1. Comparison of Numerical Techniques

All the above numerical procedures involve replacing the continuous form of the governing partial differential equation by a finite number of algebraic equations. The resulting set of linear or non linear algebraic equations are solved using direct or iterative solving techniques.

The two most commonly used numerical methods applied in developing numerical models are the finite difference and finite element methods. Both these methods approximate differential operators on subregions in the domain, hence direct connections exist only between neighbouring elements, therefore the coefficient matrices generated by these methods have relatively few non zero coefficients in any given matrix row. The finite difference approach is less cumbersome to implement, but the method usually requires special modifications to define irregular boundaries, heterogenous domains and complex boundary conditions. The finite difference method is applied to the original differential equation without any reduction in the order of the differential equation. In the finite element method the order of the differential equation is usually reduced by one.

Equations in the differential form can often be replaced by equations in integral form. The Boundary Element Method utilizes this fact by transforming the differential operator defined in the domain to integral operators defined on the boundary. In this method only the boundary is discretized. However, the method requires that the solution at one node must directly involve every node on the boundary, hence the resulting coefficient matrix is fully populated. A comprehensive comparison of Boundary Element Method to Finite Difference Method and Finite Element Method are given by Ramachandran (1994), and Sato (1992).

Onyejekwe (1996a) classified the Green Element Method (GEM) as a coupled boundary element - finite element procedure in that it implements the singular integral theory of Boundary Element Method in an element by element method over the whole domain. This method as with Finite Element Method results in a sparsely populated matrix. A comprehensive comparison of the Green Element Method to the Boundary Element Method is given by Taigbenu (1999).

The robustness of GEM and its advantages over other methods in a range of applications are comprehensively covered in studies by Taigbenu (1998;1999), Onyejekwe (1995; 1996a,b; 1997a,b; 1998a,b,c; 1999), Taigbenu and Onyejekwe (1995;1997a,b; 1998;1999). A worked example in Appendix A illustrates the computational capability and accuracy of the GEM as compared to FEM.

4.2. Green Element Formulation of the Bacteria Transport Equation

The Green element formulation converts a differential equation (that is at least twice differentiable) into an integral form using Green's second identity. The application of GEM to solve the bacteria transport equation (3.12) requires the following steps:

- 1) Integral representation of the governing differential equation.
- 2) Discretisation of the resulting equation over the problem domain.
- 3) A finite element solution to determine the field variables.

The bacteria transport equation is restated here, and is recast into a form that will facilitate its transformation.

$$\frac{\partial C^*}{\partial t} + k_c C^* - k_y \sigma^* = D \frac{\partial^2 C^*}{\partial x^2} - u \frac{\partial C^*}{\partial x} + k C^* \quad (4.1)$$

which can be rewritten as:

$$\frac{\partial^2 \phi}{\partial x^2} = \frac{1}{D} \left[\frac{\partial \phi}{\partial t} + (k_c - (\mu - k_d)) \phi - k_y \sigma^* + u \frac{\partial \phi}{\partial x} \right]$$

or
$$\frac{\partial^2 \phi}{\partial x^2} = \frac{1}{D} \left[\frac{\partial \phi}{\partial t} + u \frac{\partial \phi}{\partial x} + K \phi - k_y \sigma^* \right] \quad (4.2)$$

where:
$$K = k_c - (\mu - k_d) \quad (4.3)$$

To cast the bacteria transport equation into an integral form, Green's second identity is used. For two functions $G(x, x_i)$ and $\phi(x, t)$ which are twice differentiable, the Green's second identity is given by:

$$\int_{x_0}^{x_i} \left[\phi(x, t) \frac{d^2 G(x, x_i)}{dx^2} - G(x, x_i) \frac{d^2 \phi(x, t)}{dx^2} \right] dx = \left[\phi(x, t) \frac{dG(x, x_i)}{dx} - G(x, x_i) \frac{d\phi(x, t)}{dx} \right]_{x=x_0}^{x=x_i} \quad (4.4)$$

where $\frac{d^2 G(x, x_i)}{dx^2}$ is the proposed complementary differential equation, and is of the

form

$$\frac{d^2 G(x, x_i)}{dx^2} = \delta(x - x_i) \quad \text{for } -\infty \leq x \leq \infty \quad (4.5)$$

where δ is the Dirac delta function. Equation 4.5 has a fundamental solution, referred to as the free space Green's function, of the form:

$$G(x, x_i) = \frac{1}{2}(|x - x_i| + k) \quad (4.6)$$

Where k is an arbitrary constant, and its value is usually chosen to be the length of the longest element of the domain. The derivative of free space Green's function with respect to x can be expressed as:

$$\frac{dG(x, x_i)}{dx} = \frac{1}{2} [H(x - x_i) - H(x_i - x)] \quad (4.7)$$

where H is the Heaviside function and is defined as

$$H(x, x_i) = \begin{cases} 1, & x \succ x_i \\ 0, & x \prec x_i \end{cases}$$

Introducing equations 4.2, 4.5, 4.6, and 4.7 into equation 4.4, yields

$$\begin{aligned} & \int_{x_0}^{x_i} \left[\phi(x, t) \delta(x - x_i) - \left(\frac{1}{2}(|x - x_i| + k) \right) \frac{1}{D} \left[\frac{\partial \phi}{\partial t} + u \frac{\partial \phi}{\partial x} + K\phi - k_y \sigma^* \right] \right] dx \\ & = \left[\phi(x, t) \frac{1}{2} [H(x - x_i) - H(x_i - x)] - \left(\frac{1}{2}(|x - x_i| + k) \right) \frac{d\phi(x, t)}{dx} \right]_{x=x_0}^{x=x_i} \end{aligned} \quad (4.8)$$

Using the sieving properties of the Dirac delta function, and an extended definition of the Heaviside function, we have

$$\int_{x_0}^{x_i} \phi(x, t) \delta(x - x_i) dx = \lambda \phi(x, t) \quad (4.9)$$

$$\begin{aligned} H(x_L - x_i) - H(x_i - x_L) &= \begin{cases} 1, & x_i \prec x_L \\ 0, & x_i = x_L \end{cases} \\ H(x_0 - x_i) - H(x_i - x_0) &= \begin{cases} -1, & x_i \succ x_0 \\ 0, & x_i = x_0 \end{cases} \end{aligned} \quad (4.10)$$

where λ has a value of 1 if the source point x_i is within the computational domain or 0.5 if it is located at the boundaries. Recasting equation 4.8 in a compact form, we have

$$-\lambda \phi(x_{i,t}) + \int_{x_0}^{x_i} G(x, x_i) \frac{1}{D} \left[\frac{\partial \phi}{\partial t} + u \frac{\partial \phi}{\partial x} + K\phi - k_y \sigma^* \right] dx + \left[\phi(x, t) \frac{dG(x, x_i)}{dx} - G(x, x_i) \frac{d\phi(x, t)}{dx} \right]_{x=x_0}^{x=x_i} = 0 \quad (4.11)$$

Equation 4.11 is the integral representation of the governing transport equation. This equation is now applied to a discretised domain. Discretising the problem domain into M line elements, a typical element is denoted by the interval $[x_2^e - x_1^e]$, where x_1^e and x_2^e represent nodes 1 and 2, respectively, of a typical element in the problem domain.

The pictorial representation of the discretisation of the spatial domain is shown in figure 4.1.

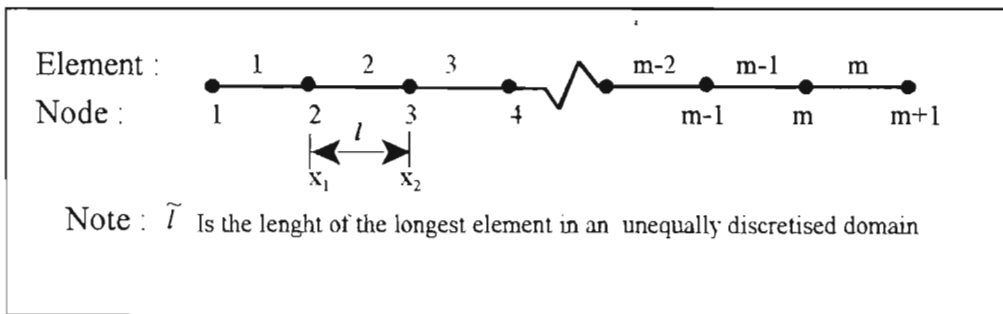


Figure 4.1. Discretisation of the Spatial Domain

To evaluate the line integral over a typical element, there is the need to prescribe a distribution for u , ϕ , σ^* and $\frac{d\phi}{dx}$ over each element. To accomplish this, the

following set of linear element interpolation functions are used,

$$\phi(x,t) \approx \Omega_j(\zeta)\phi(t) = \Omega_1(\zeta)\phi(t) + \Omega_2(\zeta)\phi(t)$$

$$\frac{d\phi(x,t)}{dx} \approx \phi(x,t) \approx \Omega_j(\zeta)\phi(t) = \Omega_1(\zeta)\phi(t) + \Omega_2(\zeta)\phi(t)$$

$$\sigma^*(x,t) \approx \Omega_j(\zeta)\sigma^*(t) = \Omega_1(\zeta)\sigma^*(t) + \Omega_2(\zeta)\sigma^*(t) \quad (4.12)$$

$$\frac{d\phi(x,t)}{dt} \approx \Omega_j(\zeta)\frac{d\phi(t)}{dt} = \Omega_1(\zeta)\frac{d\phi(t)}{dt} + \Omega_2(\zeta)\frac{d\phi(t)}{dt}$$

$$u(x,t) \approx \Omega_j(\zeta)u(t) = \Omega_1(\zeta)u(t) + \Omega_2(\zeta)u(t)$$

where $\Omega_1(\zeta)$ and $\Omega_2(\zeta)$ are shape functions, and are defined as

$$\Omega_1(\zeta) = 1 - \zeta \quad \Omega_2(\zeta) = \zeta \quad (4.13)$$

where ζ is a local co-ordinate system whose origin is at x_1^e , and is expressed as

$$\zeta = \frac{x - x_1^e}{l^e} \Rightarrow dx = l^e d\zeta \quad \text{where } l^e \text{ is the length of the element.} \quad (4.14)$$

Substituting equations 4.7; 4.9, 4.12, and 4.13 in equation 4.11, and applying it to a typical element, yields the discretised form of the integral equation representing the governing transport equation. This is given by:

$$\begin{aligned} & \sum_{e=1}^M -2D\lambda_i^e \phi^e(x_i, t) + \int_{x_1}^{x_2} (|x - x_i^e| + k^e) \Omega_j^e \left[\frac{\partial \phi_j^e}{\partial t} + \Omega_n u_n^e \phi_j^e + K \phi_j^e - k_y \sigma^{*e}_j \right] dx + \\ & D \left[\phi_2^e(x, t) \left[H(x - x_2^e) - H(x_2^e - x) \right] - \phi_1^e(x, t) \left[H(x - x_1^e) - H(x_1^e - x) \right] \right] \\ & - D \left[(|x - x_2^e| + k) \phi_2^e - (|x - x_1^e| + k) \phi_1^e \right] = 0 \end{aligned} \quad (4.15)$$

Since information is required from each of the nodes in an element, two discretised

equations are obtained from equation 4.15, by considering the position of the source nodes at x_1 and x_2 respectively. If the source node x_i is at the location x_1 , we obtain:

$$\sum_{e=1}^M D \left(-\phi_1^e + \phi_2^e + \tilde{l} \phi_1^e - (l + \tilde{l}) \phi_2^e \right) + \int_0^1 l^e \left(l^e \zeta + \tilde{l} \right) \Omega_j^e \left[\frac{\partial \phi_j^e}{\partial t} + \Omega_n u_n^e \phi_j^e + K \phi_j^e - k_y \sigma_j^{*e} \right] d\zeta = 0 \quad (4.16)$$

Similarly, if the source node x_i is at the location x_2 , we obtain:

$$\sum_{e=1}^M D \left(\phi_1^e - \phi_2^e + (l + \tilde{l}) \phi_1^e - \tilde{l} \phi_2^e \right) + \int_0^1 l^e \left(l^e (1 - \zeta) + \tilde{l} \right) \Omega_j^e \left[\frac{\partial \phi_j^e}{\partial t} + \Omega_n u_n^e \phi_j^e + K \phi_j^e - k_y \sigma_j^{*e} \right] d\zeta = 0 \quad (4.17)$$

We note that:

$$\left(|x - x_2| + k \right) = \left(|x - (x_1 + l^e)| + k \right) = \left(|(x - x_1) - l^e| + k \right) = \left(|l^e (1 - \zeta)| + k \right)$$

and we, let $k = \tilde{l}$, where \tilde{l} is the length of the longest element. If the domain is equally discretised, then $\tilde{l} = l$.

Equations 4.16 and 4.17 are combined to give a system of discrete element equations. Expressing the system of equations in compact matrix form yields:

$$\sum_{e=1}^M \left(DR_{ij}^e + T_{ij}^e K \right) \phi_j^e + \left(DL_{ij}^e + U_{inj}^e u_n^e \right) \phi_j^e + T_{ij}^e \left[\frac{\partial \phi_j^e}{\partial t} - k_y \sigma_j^{*e} \right] = 0 \quad (4.18)$$

Where

$$R_{ij}^e = \begin{bmatrix} -1 & 1 \\ 1 & -1 \end{bmatrix} \quad L_{ij}^e = \begin{bmatrix} \tilde{l} & -(l + \tilde{l}) \\ (l + \tilde{l}) & -\tilde{l} \end{bmatrix}$$

$$T_{ij}^e = l \int_0^1 \Omega_j^e G(\zeta, \zeta_i) d\zeta = \frac{l}{6} \begin{bmatrix} \binom{3\tilde{l}+l}{3\tilde{l}+l} & \binom{3\tilde{l}+2l}{3\tilde{l}+2l} \\ \binom{3\tilde{l}+2l}{3\tilde{l}+2l} & \binom{3\tilde{l}+2l}{3\tilde{l}+2l} \end{bmatrix}$$

$$U_{ij}^e = l \int_0^1 \Omega_i^e \Omega_j^e G(\zeta, \zeta_1) d\zeta = \frac{l}{12} \begin{bmatrix} \binom{4\tilde{l}+l}{2\tilde{l}+l} & \binom{2\tilde{l}+l}{4\tilde{l}+3l} \\ \binom{2\tilde{l}+l}{4\tilde{l}+3l} & \binom{4\tilde{l}+l}{2\tilde{l}+l} \end{bmatrix}$$

$$U_{2ij}^e = l \int_0^1 \Omega_i^e \Omega_j^e G(\zeta, \zeta_2) d\zeta = \frac{l}{12} \begin{bmatrix} \binom{4\tilde{l}+3l}{2\tilde{l}+l} & \binom{2\tilde{l}+l}{4\tilde{l}+l} \\ \binom{2\tilde{l}+l}{4\tilde{l}+l} & \binom{4\tilde{l}+3l}{2\tilde{l}+l} \end{bmatrix}$$

If the velocity of the transporting fluid is uniform, that is $U(t) = u(x, t)$, it is no longer necessary to express the velocity in terms of interpolation functions. Therefore equation 4.18 will taken on the following form:

$$\sum_{e=1}^M \left(DR_{ij}^e + T_{ij}^e K \right) \phi_j^e + (DL_{ij}^e + T_{ij}^e U) \phi_j^e + T_{ij}^e \left[\frac{\partial \phi_j^e}{\partial t} - k_y \sigma_j^{*e} \right] = 0 \quad (4.19)$$

Various techniques can be used to the evaluate the temporal term in equation 4.19. In this work, the temporal derivative will be approximated using the finite difference scheme. This results in the temporal derivative being replaced by:

$$\left. \frac{d\phi^e}{dt} \right|_{t=t_1+\alpha\Delta t} \approx \frac{\phi_j^e(t_{m+1}) - \phi_j^e(t_m)}{\Delta t} = \frac{\phi_j^{(e,m+1)} - \phi_j^{(e,m)}}{\Delta t} \quad 0 \leq \alpha \leq 1 \quad (4.20)$$

Where t_{m+1} is the current time level where the solution is required, t_m is the previous time level, α is a weighting factor which determines the position within the temporal element at which the temporal derivative will be determined, and $\Delta t = t_{m+1} - t_m$. Whilst the value for α varies from 0 to 1, the conventional values used in FDM and FEM are: 0 (fully explicit scheme), 0.5 (Crank-Nicholson scheme), 0.67 (Galerkin's scheme), and 1 (fully implicit scheme). Since the temporal derivative is being evaluated at $t_{m+1} = t_m + \alpha\Delta t$, all the other terms will be evaluated at this time as well. Therefore the discretised weighted expression for the transport equation is given by:

$$\begin{aligned} & \sum_{e=1}^M \alpha \left(DR_{ij}^e + T_{ij}^e K \right) \phi_j^{(e,m+1)} + \alpha \left(DL_{ij}^e + T_{ij}^e U \right) \phi_j^{(e,m+1)} + \\ & (1 - \alpha) \left(DR_{ij}^e + T_{ij}^e K \right) \phi_j^{(e,m)} + (1 - \alpha) \left(DL_{ij}^e + T_{ij}^e U \right) \phi_j^{(e,m)} + \quad (4.21) \\ & T_{ij}^e \left[\frac{\phi_j^{(e,m+1)} - \phi_j^{(e,m)}}{\Delta t} - \left[\alpha k_y \sigma_j^{*(e,m+1)} + (1 - \alpha) k_y \sigma_j^{*(e,m)} \right] \right] = 0 \end{aligned}$$

The resulting discretisation of the temporal domain and the spatial domain is shown schematically in figure 4.2.

Equation 4.21 represents the Green Element Method formulation of the Bacteria transport equation. We note that in the above expression, only the primary dependant variable at the current time $\phi_j^{(e,m+1)}$, and the concentration gradient at the current time $\phi_j^{(e,m+1)}$ are the only unknowns. The inclusion of a source term $f(x, t)$, will result in a GEM model of the following form:

$$\begin{aligned}
& \sum_{e=1}^M \alpha \left(DR_{ij}^e + T_{ij}^e K \right) \phi_j^{(e,m+1)} + \alpha \left(DL_{ij}^e + T_{ij}^e U \right) \phi_j^{(e,m+1)} + \\
& (1 - \alpha) \left(DR_{ij}^e + T_{ij}^e K \right) \phi_j^{(e,m)} + (1 - \alpha) \left(DL_{ij}^e + T_{ij}^e U \right) \phi_j^{(e,m)} + \\
& T_{ij}^e \left[\frac{\phi_j^{(e,m+1)} - \phi_j^{(e,m)}}{\Delta t} - \left[\alpha k_y \sigma_j^{*(e,m+1)} + (1 - \alpha) k_y \sigma_j^{*(e,m)} \right] + \right. \\
& \left. \left(\alpha f_j^{(e,m+1)} + (1 - \alpha) f_j^{(e,m)} \right) \right] = 0
\end{aligned} \tag{4.22}$$

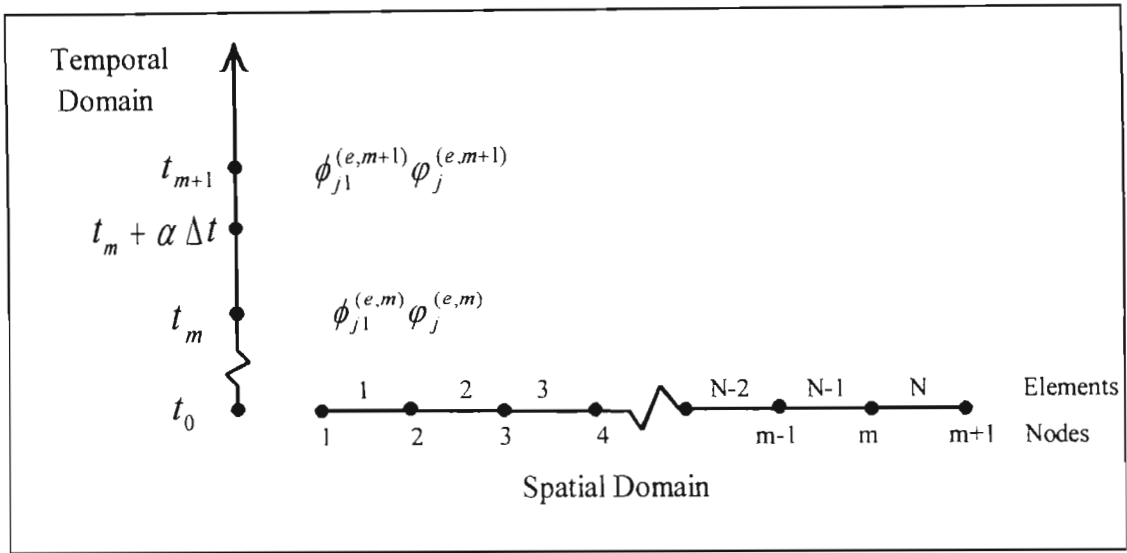


Figure 4.2. Spatial and temporal discretisation

A global matrix system representing the problem, can be expressed as:

$$[A]_{ij} \cdot \begin{Bmatrix} \phi_j^{m+1} \\ \phi_j^{m+1} \end{Bmatrix} = \{B_i\} \tag{4.23}$$

where A_{ij} is the coefficient matrix, and B_i is the right hand side vector which receives contributions from boundary conditions, initial data and sources or sinks.

4.3 Summary

In this chapter, we briefly compared the common numerical techniques, and developed the GEM model for bacteria transport. We note that the model consists of the following terms: a diffusive term, a convective term, two linear reaction terms, a transient term, and a source term.

In Appendixes A and B, simpler applications are formulated and solved using the Green Element method. A linear homogenous steady state problem, and a heterogenous steady state problem are solved by manual calculations. These worked examples serve to show: the computational procedures, ease, and the capabilities of GEM.

In the next chapter, the computational and verification procedures will be briefly discussed.

Chapter Five

Computational and Model Verification Procedures

Although the mathematical development of the GEM formulation for bacteria transport has been discussed in the previous chapter, the ability of the GEM formulation to describe bacteria transport through porous media needs to be verified. In this chapter the procedure to verify the model is discussed. The numerical and computational procedures to implement the GEM formulation is also provided in this chapter.

5.1. Model Verification Procedures

The verification of the transport can be done in two ways: it can be tested against field data, or it can be tested against an analytical solution. Since fully defined data is lacking, the GEM formulation will be tested against an analytical solution. In this work, the GEM formulation for bacteria transport is verified against a simplified analytical solution presented by Corapcioglu and Haridas (1985). The analytical solution is given for a semi-infinite column with the following boundary and initial conditions:

$$\begin{aligned} C^*(0, t) &= C_0^* & C^*(\infty, t) &= 0 \\ C^*(x, 0) &= 0 & \sigma^*(x, 0) &= 0 \end{aligned}$$

Corapcioglu and Haridas' solution is given by:

$$\begin{aligned} \frac{C^*}{C_0^*} &= \frac{2}{\sqrt{\pi}} \exp\left[\frac{ux}{2D} + kt\right] \int_{\frac{x}{2\sqrt{Dt}}}^{\infty} \exp\left\{-\xi^2 - \left(\frac{ux}{4D\xi}\right)^2 - \frac{x^2 k_c}{4D\xi^2} - k_y \left(t - \frac{x^2}{4D\xi^2}\right)\right\} \times \\ &\left\{ I_0 \left[\sqrt{\frac{x^2 k_c k_y (t - x^2/4D\xi^2)}{D\xi^2}} \right] + (k_y - k) \exp\left[-(k_y - k) \left(t - \frac{x^2}{4D\xi^2}\right)\right] \right\} \times \\ &\int_0^{t - x^2/4D\xi^2} \exp\left[-(k_y - k)\tau\right] I_0 \left[\sqrt{\frac{x^2 k_c k_y \tau}{D\xi^2}} \right] d\tau \Bigg\} d\xi \end{aligned} \quad (5.1)$$

where I_0 is the first-kind zero-order modified Bessel function.

The numerical solutions obtained via the GEM formulation will be compared to the analytical solutions for the condition of constant porosity and the following parameter values:

$$\begin{aligned} D &= 0.04 \text{ cm}^2 / \text{s} & u &= 0.003 \text{ cm} / \text{s} & k &= -1 \times 10^{-6} \text{ s}^{-1} \\ k_c &= 6 \times 10^{-3} \text{ s}^{-1} & k_y &= 6 \times 10^{-5} \text{ s}^{-1} \end{aligned}$$

The boundary and initial conditions will be as stated above.

During the simulation of the equation 5.1, overflow and singularity problems were experienced. The overflow problem was due to the upper limit of the first integral being set at infinity. When this upper limit was replaced with a finite limit, results obtained were the same as Corapcioglu and Haridas (1985). The singularity problem arose when the lower limit of integration in time was zero. To overcome this, the lower limit was set at a non-zero value. The analytical results obtained are shown in Figures 5.1 and 5.2. The oscillating effect observed in Figure 5.2 for the first section of the temporal domain results from the software used to plot these graphs:

It is noted that the analytical solution provided by Corapcioglu and Haridas (1985) is based on the assumption that the porosity is constant through the spatial and temporal domains. Whilst this may be valid for low bacteria loadings and negligible growth rates, this may not be true for sewage plumes and in bioremediation applications. Therefore in this study two numerical procedures are proposed: a model that neglects changes to porosity, which will be used to verify the GEM with the analytical model, and a model that includes changes to porosity, which will be used by this study.

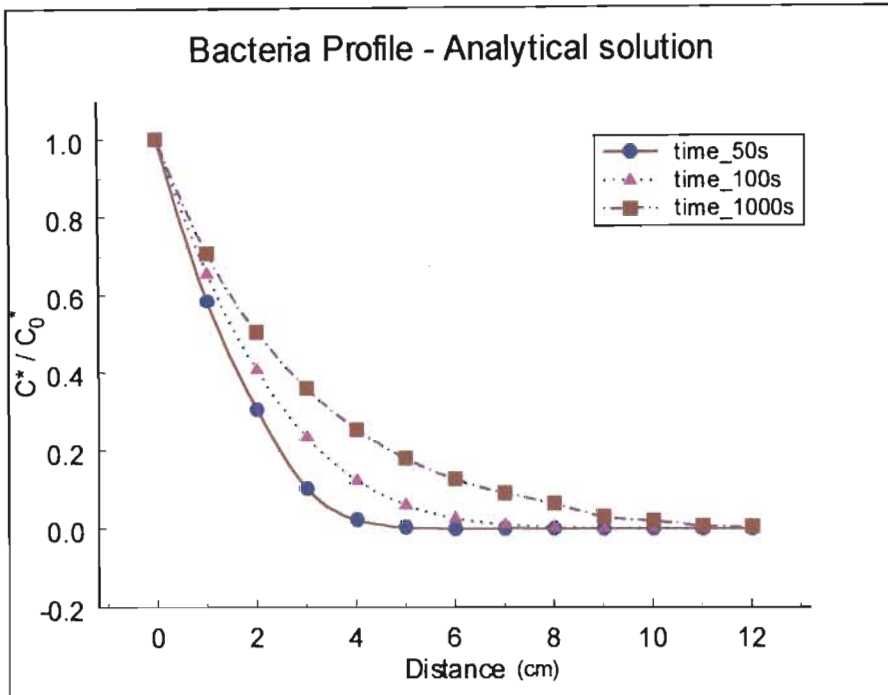


Figure 5.1. Analytical Solution obtained for 50s, 100s, and 1000s

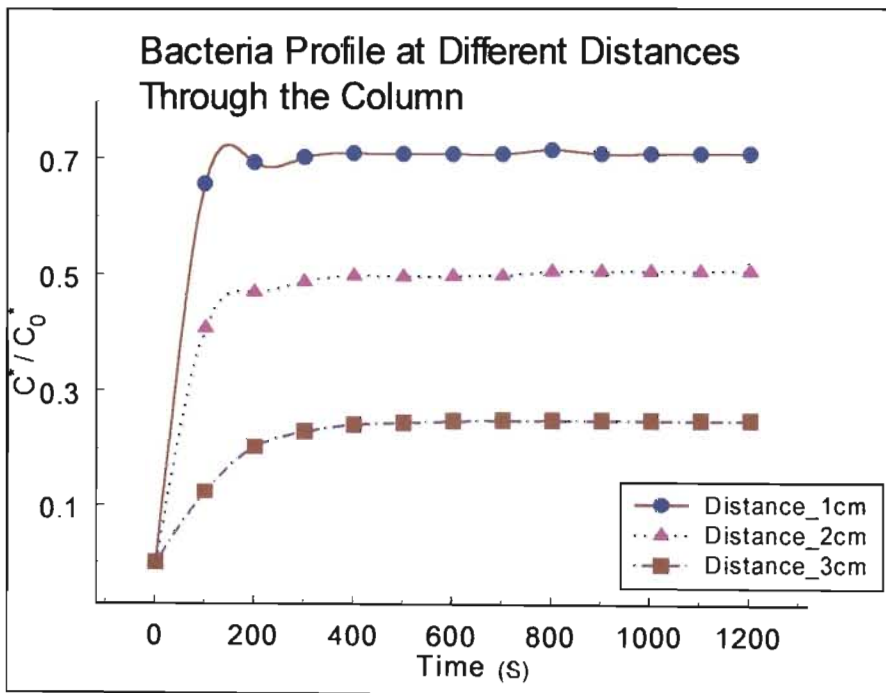


Figure 5.2. Analytical Solution Profile at 1 cm, 2 cm, and 4 cm

In addition, several studies have reported that some of the processes (adsorption, straining, sedimentation, etc) that lumped into the clogging term, deviate from linear kinetics. Saiers and Hornberger (1994) reported that the clogging process of some colloidal matter can be expressed by second order kinetics. Yates and Yates (1991) reported that all attempts to predict the degree of adsorption on the basis of either soil properties (such as pH, organic matter content and clay content) or characteristics of the microorganisms (such as its isoelectric point) have not been successful.

It is suggested by this study that the option to express the clogging process as a non-linear should be considered. Therefore an additional GEM model which includes clogging as a non linear process will be presented. In this work non linear clogging term will be defined as $k_c C^{n^*}$.

5.2. Numerical Procedures

In order to formulate a computational procedure, we need to revisit the governing PDE describing bacteria transport through porous media, and its associated equations, to establish the interactions between the equations. In chapter three, the three equations that fully described the transport of bacteria were established. These were equations 3.12, 3.16, and 3.17.

As has been alluded earlier, three bacteria transport models will be presented:

- i) A model in which the porosity remains constant throughout the spatial and temporal domains.
- ii) A model that includes changes to porosity throughout the spatial and temporal domains.
- iii) A model that will evaluate the effect of non linear type clogging.

The models listed in (i) and (ii) will be referred to as the linear transport model, and the model in (iii) will be referred to as the non linear transport model.

In this work, it is assumed that all the essential substrates are in abundance (as will be case in sewage plumes). Therefore it will be assumed that the substrate transport equation does not interact with bacteria transport equation. The equation that will be interacting with the bacteria transport equation is the adsorbed species continuity equation. Restating the bacteria transport equation and absorbed species continuity equations, we have:

$$\frac{\partial C^*}{\partial t} + k_c C^* - k_y \sigma^* = D \frac{\partial^2 C^*}{\partial x^2} - u \frac{\partial C^*}{\partial x} + k C^* \quad (5.2)$$

where: $C^* = \theta C$, $k = \mu - k_d$, and $\sigma^* = \rho_B \delta$

and

$$\begin{aligned} \frac{\partial \sigma^*}{\partial t} &= k_c C^* - k_y \delta^* + \mu \sigma^* - k_d \sigma^* \\ &= [k - k_y] \sigma^* + k_c C^* \end{aligned} \quad (5.3)$$

where: $C^* = \theta C$, $\sigma^* = \rho_B \delta$, and $k = \mu - k_d$

Since the substrate are in abundance, μ will be constant, and therefore k will be constant. This term will represent either the net growth or net decay depending on the values assigned to k .

Whilst the GEM formulation for bacteria transport has been developed, a solution procedure for the adsorbed species continuity equation is required. In this study we adopted a numerical method to solve the initial value differential equation. The numerical method solution can be stated as:

$$\sigma_j^{*(e,m+1)} = \sigma_j^{*(e,m)} + \Delta t \cdot f \left\{ \sigma_j^{*(e,m)}; C_j^{(e,m)} \right\} \quad 5.4$$

5.2.1. Numerical procedure for linear transport equation

The equations applicable to the linear transport model are equations 5.2 and 5.3. The essential difference between the constant porosity and variable porosity models is that, the variable porosity model accounts the variation in the porosity and velocity in the problem domain.

In the constant porosity model we determine the values of the lumped variables:

$$\phi = \theta C = C^* \quad \text{and} \quad \phi = \frac{\partial \theta C}{\partial x} = \frac{\partial C^*}{\partial x} \quad (5.5)$$

In the final representation of the results we have

$$\frac{C_i^*}{C_0^*} = \frac{\theta_0 C_i}{\theta_0 C_0} = \frac{C_i}{C_0} \quad (5.6)$$

For the variable porosity model we recast our equations in the following form:

$$\begin{aligned} \frac{\partial C}{\partial t} + k_c C - \frac{k_y \sigma^*}{\theta_i} &= D \frac{\partial^2 C}{\partial x^2} - u \frac{\partial C}{\partial x} + kC \\ \frac{\partial \sigma^*}{\partial t} &= k_c \theta_i C - k_y \delta^* + \mu \sigma^* - k_d \sigma^* \\ &= [k - k_y] \sigma^* + k_c \theta_i C \end{aligned} \quad (5.7)$$

We note that in this model, the variation in porosity will result in the variation of the velocity. In this work, the change to velocity will be accounted for in a simple ratio relationship, which is represented by:

$$u_i = \frac{\theta_i}{\theta_0} u_0 \quad (5.8)$$

where $\frac{\theta_i}{\theta_0}$ is the ratio of the changed porosity to the initial (original) porosity.

The value of the changed porosity can be determined by:

$$\theta_i = \theta_0 - \sigma_i \quad \text{where} \quad \sigma_i = \frac{\sigma_i^*}{\rho_B} \quad (5.9)$$

Even though the velocity is porosity dependant, applying the law of mass conservation indicates that, in a one dimensional application, the velocity should remain constant throughout the problem domain. The change in porosity at the beginning of the problem domain dictates the value for the velocity through the rest of the domain. Therefore the change in velocity can be determined as:

$$u = \frac{\theta_1}{\theta_0} u_0 \quad (5.11)$$

The transport model in its GEM formulation has been developed in chapter four, but will be restated here:

Constant porosity model:

$$\begin{aligned} & \sum_{e=1}^M \alpha \left(DR_{ij}^e + T_{ij}^e K \right) \phi_j^{(e,m+1)} + \alpha \left(DL_{ij}^e + T_{ij}^e U \right) \phi_j^{(e,m+1)} + \\ & (1 - \alpha) \left(DR_{ij}^e + T_{ij}^e K \right) \phi_j^{(e,m)} + (1 - \alpha) \left(DL_{ij}^e + T_{ij}^e U \right) \phi_j^{(e,m)} + \\ & T_{ij}^e \left[\frac{\phi_j^{(e,m+1)} - \phi_j^{(e,m)}}{\Delta t} - \left[\alpha k_y \sigma_j^{*(e,m+1)} + (1 - \alpha) k_y \sigma_j^{*(e,m)} \right] + \right. \\ & \left. \left(\alpha f_j^{(e,m+1)} + (1 - \alpha) f_j^{(e,m)} \right) \right] = 0 \end{aligned} \quad (5.12)$$

Variable porosity model:

Whilst the GEM formulation for this model has not been derived from first principles, the procedure is identical to those outlined in chapter four. The final formulation is merely stated here.

$$\begin{aligned}
 & \sum_{e=1}^M \alpha \left(DR_{ij}^e + T_{ij}^e K \right) \phi_j^{(e,m+1)} + \alpha \left(DL_{ij}^e + T_{ij}^e U \right) \phi_j^{(e,m+1)} + \\
 & (1 - \alpha) \left(DR_{ij}^e + T_{ij}^e K \right) \phi_j^{(e,m)} + (1 - \alpha) \left(DL_{ij}^e + T_{ij}^e U \right) \phi_j^{(e,m)} + \\
 & T_{ij}^e \left[\frac{\phi_j^{(e,m+1)} - \phi_j^{(e,m)}}{\Delta t} - \left[\frac{\alpha k_y \sigma_j^{*(e,m+1)}}{\theta_j^{e,m+1}} + \frac{(1 - \alpha) k_y \sigma_j^{*(e,m)}}{\theta_j^{e,m}} \right] + \right. \\
 & \left. \left(\frac{\alpha f_j^{(e,m+1)}}{\theta_j^{e,m+1}} + \frac{(1 - \alpha) f_j^{(e,m)}}{\theta_j^{e,m}} \right) \right] = 0
 \end{aligned} \tag{5.13}$$

The numerical methodology to solve these models will be as follows: The values for C^* and σ^* are known at $t=0$ for the whole spatial domain, therefore we

- i) solve the adsorbed bacteria continuity equation for the next temporal node i.e obtain the values of δ^{*m+1} for the whole spatial domain,
- ii) If the formulation includes porosity changes then, determine $\theta_j^{m+1} = \theta_0 - \sigma_j^{*m+1}$ and $u = (\theta_i / \theta_0) * u_0$
- iii) solve the bacteria transport equation for this temporal node to obtain values for C^{*m+1} for the whole spatial domain

This procedure is illustrated in figure 5.3.

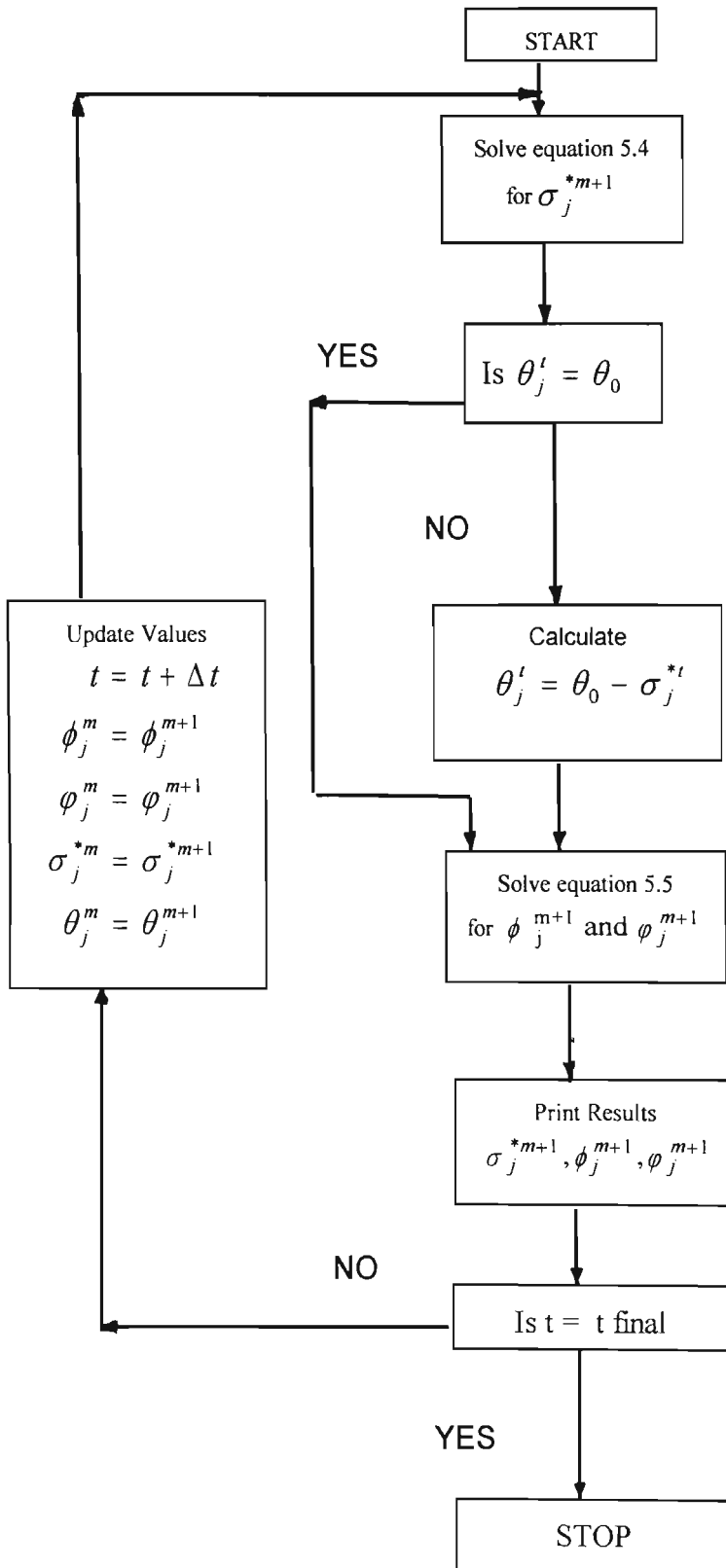


FIGURE 5.3. Computation Algorithm for Linear Transport Models

5.2.2. Numerical procedure for non linear transport equation

The proposed non linearity to the transport equation is in the clogging term. Therefore equations 5.2 and 5.3 will be modified as follows:

$$\frac{\partial C}{\partial t} + k_c C^n - \frac{k_y \sigma^*}{\theta} = D \frac{\partial^2 C}{\partial x^2} - u \frac{\partial C}{\partial x} + kC \quad (5.13)$$

where: $k = \mu - k_d$, and $\sigma^* = \rho_B \delta$

and

$$\begin{aligned} \frac{\partial \sigma^*}{\partial t} &= k_c C^{n*} - k_y \delta^* + \mu \sigma^* - k_d \sigma^* \\ &= [k - k_y] \sigma^* + k_c C^{n*} \end{aligned} \quad (5.14)$$

where $k_c C^{*n} = k_c \theta C^n = k_c \left(\theta_0 - \frac{\sigma^*}{\rho_B} \right) C^n$ (5.15)

The development of the GEM formulation for non linear transport equation is identical to the procedure outlined in chapter four. Therefore just the final expression will be stated here:

$$\begin{aligned} &\sum_{e=1}^M \alpha \left(DR_{ij}^e - T_{ij}^e k \right) \phi_j^{(e,m+1)} + \alpha \left(DL_{ij}^e + T_{ij}^e U \right) \phi_j^{(e,m+1)} + \\ &(1 - \alpha) \left(DR_{ij}^e - T_{ij}^e k \right) \phi_j^{(e,m)} + (1 - \alpha) \left(DL_{ij}^e + T_{ij}^e U \right) \phi_j^{(e,m)} + \\ &T_{ij}^e \left[\frac{\phi_j^{(e,m+1)} - \phi_j^{(e,m)}}{\Delta t} - \left[\frac{\alpha k_y \sigma_j^{*(e,m+1)}}{\theta_j^{e,m+1}} + \frac{(1 - \alpha) k_y \sigma_j^{*(e,m)}}{\theta_j^{e,m}} \right] + \right. \\ &\left. \left[\alpha k_c \phi_j^{n(e,m+1)} + (1 - \alpha) k_c \phi_j^{n(e,m)} \right] + \left(\frac{\alpha f_j^{(e,m+1)}}{\theta_j^{e,m+1}} + \frac{(1 - \alpha) f_j^{e,m}}{\theta_j^{e,m}} \right) \right] = 0 \end{aligned} \quad (5.16)$$

To solve the non linear model, an iterative solution procedure is required. The iterative procedures that could be used include: Newton Raphson, Picard, and the Chord slope methods. In this work the Newton Raphson algorithm will be used. The Newton Raphson procedure can be summerized as:

$$J_{ij}^{(m+1,k)} \cdot \Delta u_j^{(m+1,k+1)} = -g_i^{(m+1,k)} \quad (5.17)$$

where:

$$J_{ij}^{(m+1,k)} = \begin{cases} \left. \frac{\partial g_i}{\partial \phi_j} \right|_{\phi_j = \phi_j^{(m+1,k)}} = \alpha DR_{ij} - \alpha T_{ij} k + \frac{T_{ij}}{\Delta t} + \alpha nk_c T_{ij} \phi_j^{n-1,m+1} \\ \left. \frac{\partial g_i}{\partial \varphi_j} \right|_{\varphi_j = \varphi_j^{(m+1,k)}} = \alpha [DL_{ij} + T_{ij} U] \end{cases} \quad (5.18)$$

$$\Delta u_j^{(m+1,k+1)} = \begin{cases} \Delta \phi_{Sj}^{(m+1,k+1)} \\ \Delta \varphi_{Sj}^{(m+1,k+1)} \end{cases} \quad (5.19)$$

and

$$\begin{aligned} g_i^{m+1,k} = & \left[\alpha (D_S R_{ij} - T_{ij} k) + \frac{T_{ij}}{\Delta t} \right] \phi_{Sj}^{m+1} + \left[\omega (D_S R_{ij} - T_{ij} k) - \frac{T_{ij}}{\Delta t} \right] \phi_{Sj}^m \\ & + \alpha [D_S L_{ij} + T_{ij} U] \varphi_{Sj}^{m+1} + \omega [D_S L_{ij} + T_{ij} U] \varphi_{Sj}^m + \\ & T_{ij} \left[\alpha k_c \phi_j^{n,m+1} + \omega nk_c \phi_j^{n,m} \right] - T_{ij} \left[\frac{\alpha k_y \sigma_j^{*m+1}}{\theta_j^{m+1}} + \frac{\omega k_y \sigma_j^{*m}}{\theta_j^m} \right] + \\ & T_{ij} \left[\frac{f_j^{m+1}}{\theta_j^{m+1}} + \frac{f_j^m}{\theta_j^m} \right] \end{aligned} \quad (5.20)$$

We note that in determining the Jacobian matrix, the primary variable that appears in the adsorbed species continuity equation 5.15 is omitted. This is due to the numerical procedure adopted (equation 5.4) to solve equation 5.15. Equation 5.4 does not require

the current value for the primary variable (i.e $\phi_j^{n,m+1}$) in its solution procedure. The numerical procedure for solving the non linear model is illustrated in figure 5.4.

5.3. Computational Procedures

The computational code used for this work is based on the code developed by Onyejekwe (2000) for other linear and non-linear GEM applications. Modifications to the original code include:

- increasing data input requirements
- inclusion of vab subroutine - this subroutine computes the values for σ_j^{*m+1} .
- Inclusion of procedures to determine changes in porosity
- changes to the coefficient matrix subroutine (ASSMBLN) and to the subroutine(RIGHTLN) that computes the right hand side of the global matrix for the linear model.
- changes to the coefficient matrix subroutine (ASSMBL) and to the subroutine(RIGHT) that computes the right hand side of the global matrix for the non linear model.

The resulting structure for the computational code for the linear and non linear models are shown in Figure 5.4. and Figure 5.5 respectively. A brief description of the computational code for the 3 models presented, and sample input and output files are outlined in Appendix C.

5.4. Summary

In this chapter the approach to solving the coupled system was given. This included: a description of the verification and numerical procedures, and a brief overview the computer programme structures.

In the Chapter Six , the GEM model will be validated against analytical results, and several applications will be considered.

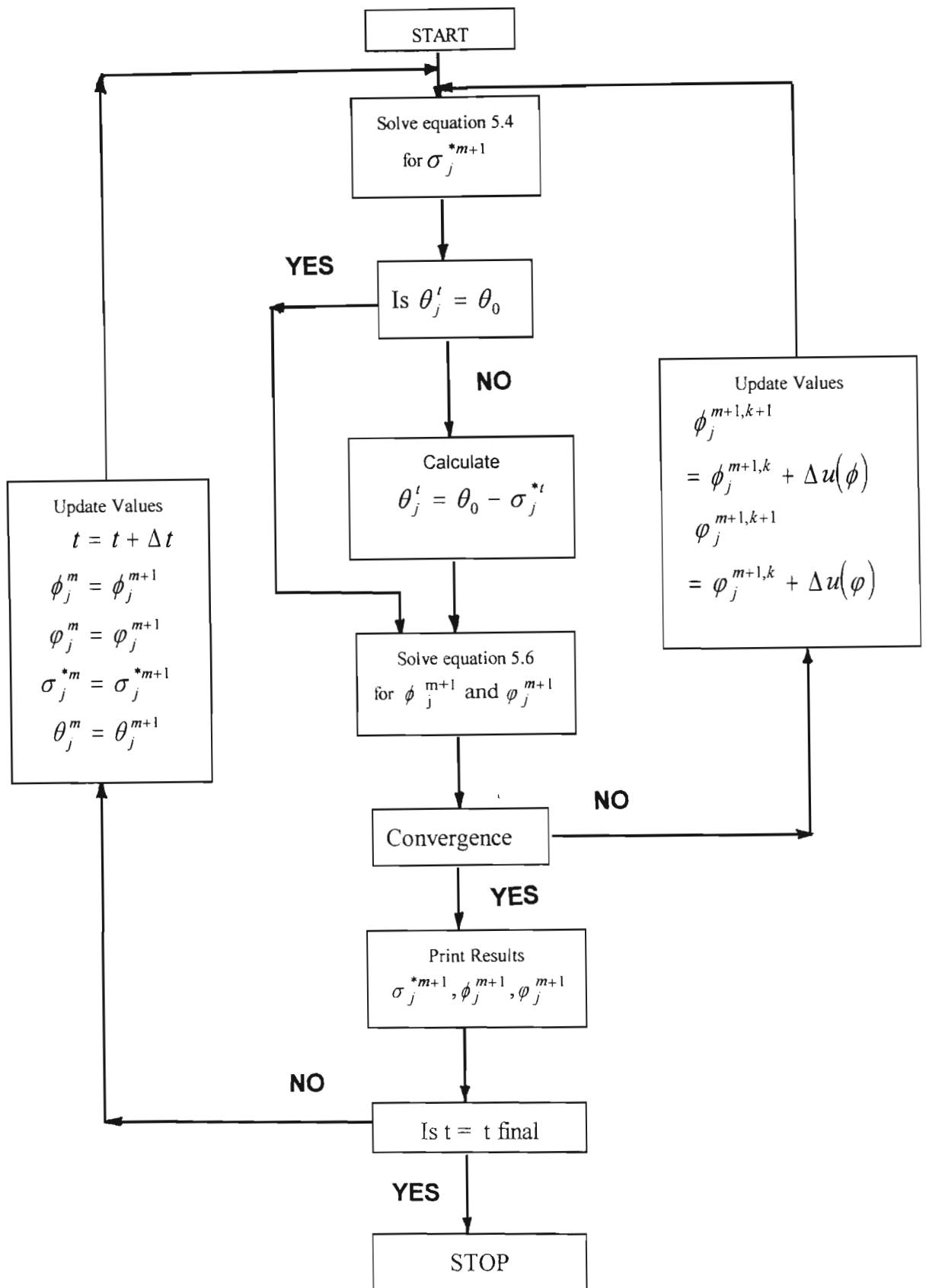


FIGURE 5.4. Computation Algorithm for Non Linear Transport Model

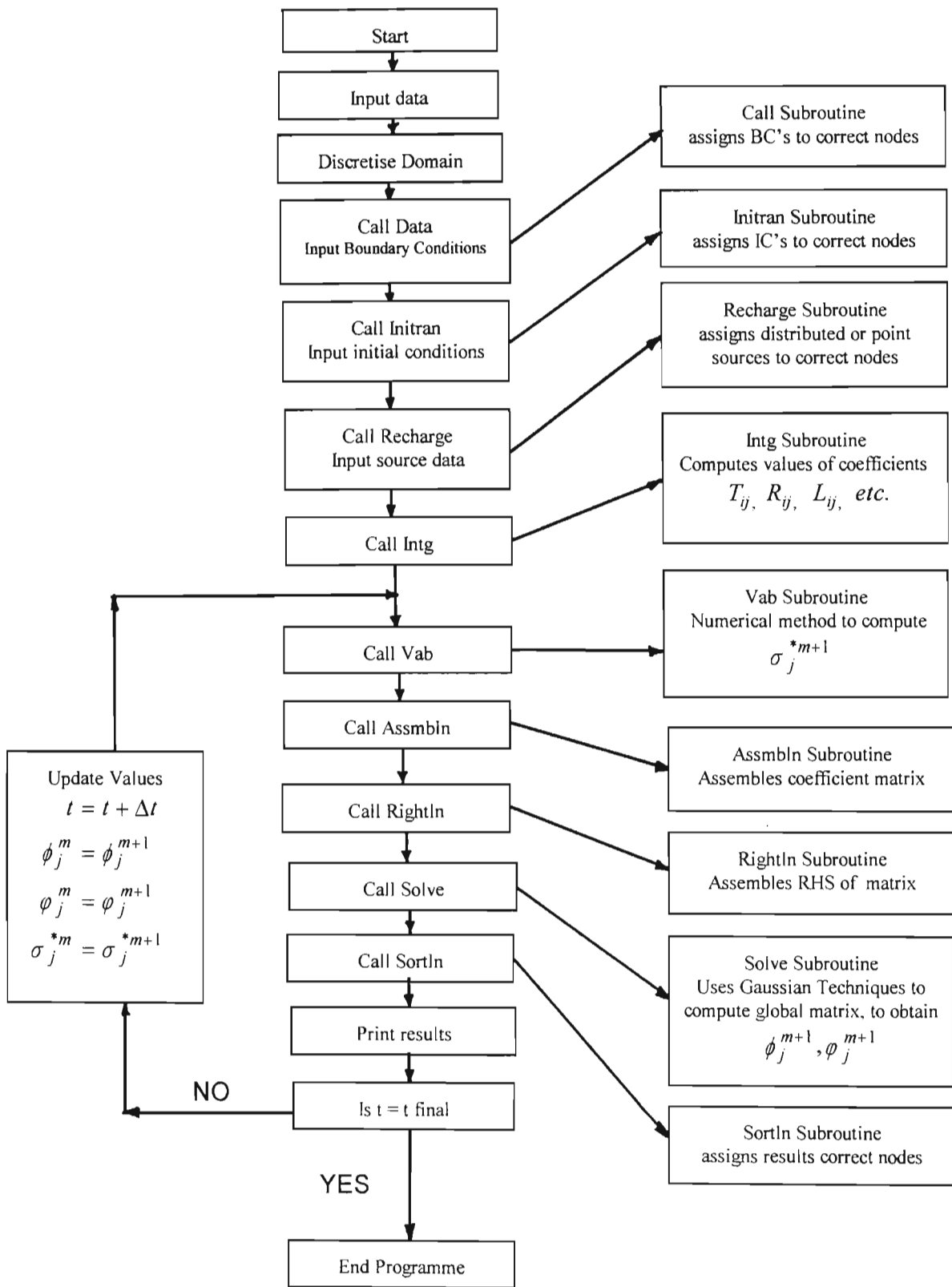


Figure 5.5 Computer Programme Algorithm for linear models

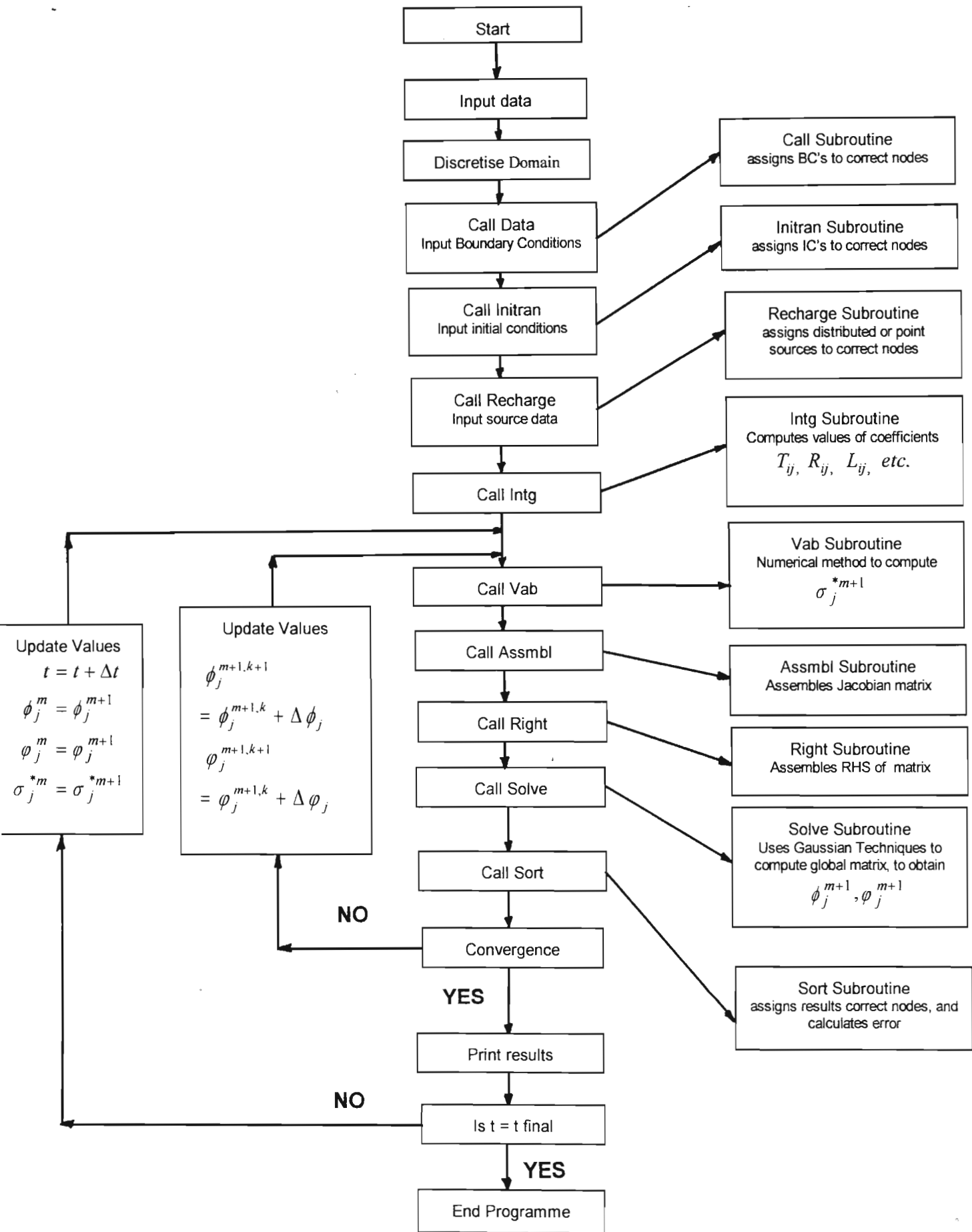


Figure 5.5. Programme Flowchart for Nonlinear Model

Chapter Six

Application of GEM Model

The merit of any transport model lies in its flexibility to simulate various applications. In this chapter, the GEM formulation will be compared to analytical results obtained by Corapcioglu and Haridas (1985). The validated model will then be used to evaluate the effects of the various parameters on bacteria transport. These include:

- The effects of ground water flow-rate and dispersivity on the bacteria concentration profile.
- The effect of the net growth / net decay rate on the concentration profile and the changes to the porosity.
- The effects of clogging and declogging rates on the bacteria concentration profile and the changes to porosity.
- The effects of non - linear clogging on the bacteria concentration profile and the changes to porosity.
- The effect of substrate concentration on the bacteria concentration profile.
- The effect of source concentrations on the bacteria concentration profile

Thus far, references have been made to the GEM formulation's accuracy and range of applicability. In addition to this, the formulation has its strength in being able to compute distributed sources, and concentrated point sources at any point in its domain.

6.1. GEM Model Verification

As indicated in chapter five , the analytical solution for a specific application will be used to verify the GEM formulation. It should be noted that the analytical solution provided is based on the assumption that there are no changes to the porosity.

Therefore a constant porosity GEM formulation will be tested against the analytical

solution.

6.1.1 Constant Porosity Model Verification

The GEM model and the numerical and computational procedures were outlined in chapter five. The constant porosity is simulated for the same conditions as those used by Corapcioglu and Haridas (1985) for the simulation of the analytical model. Therefore the following conditions and parameters were used for the verification:

$$D = 0.04 \text{ cm}^2 / \text{s} \quad u = 0.003 \text{ cm} / \text{s} \quad k = -1 \times 10^{-6} \text{ s}^{-1}$$

$$k_c = 6 \times 10^{-3} \text{ s}^{-1} \quad k_y = 6 \times 10^{-5} \text{ s}^{-1}$$

$$C^*(0,t) = C_0^* \quad C^*(\infty,t) = 0 \quad C^*(x,0) = 0 \quad \sigma^*(x,0) = 0$$

The results obtained from the simulations of the analytical and GEM models are shown in Table 6.1 and Table 6.2.

Table 6.1 Comparison of Analytical and GEM solutions at 50, 100, and 1000 seconds

Time	50 seconds		100 seconds		1000 seconds	
	Analytical	GEM	Analytical	GEM	Analytical	GEM
0	1.000	1.000	1.000	1.000	0.993	1.000
2	0.305	0.305	0.406	0.401	0.502	0.503
4	0.024	0.044	0.125	0.128	0.252	0.252
6	0.006	0.002	0.027	0.027	0.126	0.125
8	0.000	0.000	0.003	0.003	0.063	0.060
10	0.000	0.000	0.000	0.000	0.055	0.025
12	0.000	0.000	0.000	0.000	0.051	0.000

Table 6.2. Comparison of Analytical and GEM solutions at 1 cm, 2 cm, and 4 cm

Distance	1 centimeter		2 centimeter		4 centimeter	
	Analytical	GEM	Analytical	GEM	Analytical	GEM
0	0.00	0.00	0.00	0.00	0.00	0.00
200	0.691	0.691	0.470	0.471	0.203	0.204
400	0.707	0.705	0.498	0.495	0.242	0.241
600	0.705	0.709	0.498	0.501	0.248	0.250
800	0.713	0.712	0.506	0.506	0.252	0.254
1000	0.706	0.714	0.501	0.510	0.252	0.258
1200	0.706	0.717	0.509	0.513	0.254	0.261

Graphical comparisons of the results are shown in Figure 6.1 and Figure 6.2.

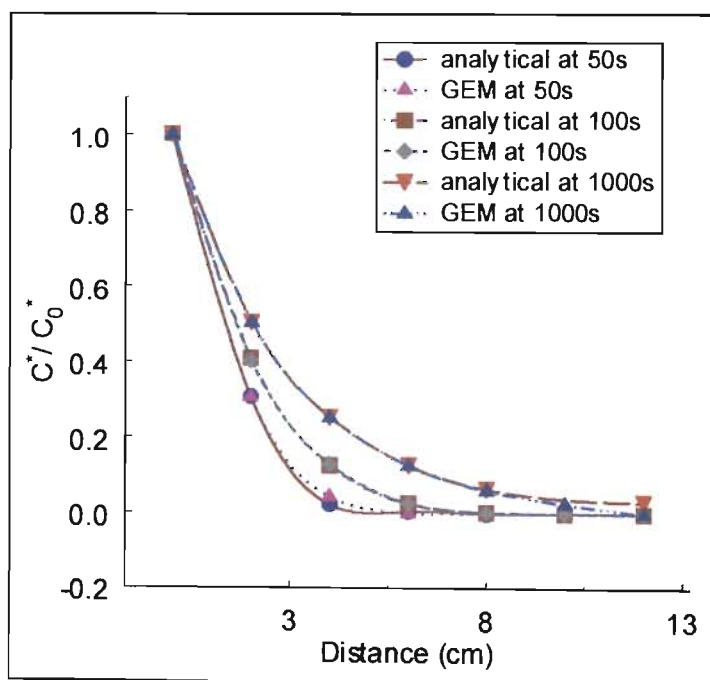


Figure 6.1 Comparison of Analytical and Constant Porosity Model solutions at 50s, 100s, and 1000s

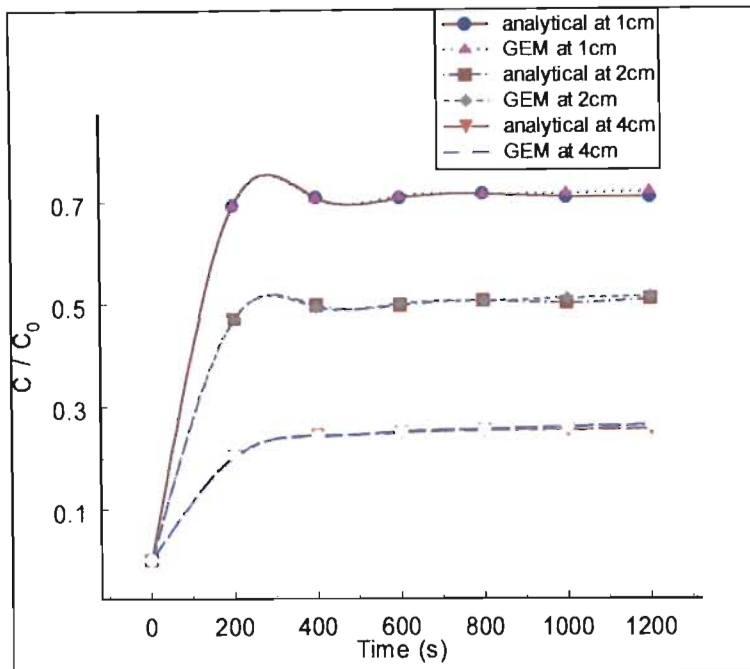


Figure 6.2 Comparison of Analytical and Constant Porosity Model solutions at 1cm, 2cm and 4cm

The results shown in the figures 6.1 and 6.2 show excellent correlation between the analytical and GEM models. This indicates that the GEM formulation can be used with confidence. The difference between the analytical and numerical solutions increases at larger times. This is explained by the boundary condition at 12 cm for the numerical solution which forces the solution to zero at all times, while the analytical solution for a semi-infinite domain attains non-zero values at every x at larger times.

6.1.2 Variable porosity model and Nonlinear Model Verification

Since analytical solutions do not exist for variable porosity and nonlinear applications, the verification will be done differently. It is assumed that since the constant porosity model has been verified against an analytical solution, this

model can be used for verifying the variable porosity and nonlinear models. The variable porosity model and the nonlinear model were verified by comparing the solutions obtained from these models for an application in which the changes in porosity are negligible. The results obtained were then compared to the solution obtained by the constant porosity model at the same conditions. For the nonlinear model, the reaction order of clogging will be assigned the value of one. The parameters used to simulate all three models is presented in Table 6.3. The comparison of the results is shown in Figure 6.3.

Table 6.3 Simulation parameters

Parameter	Symbol	Simulation values
Dispersion coefficient	D	$0.02 \text{ m}^2 \text{ h}^{-1}$
Density of Bacteria	ρ_B	1000 kg.m^{-3}
Clogging rate constant	k_c	23.4 h^{-1}
Declogging rate constant	k_y	1566 h^{-1}
Specific decay constant	k_d	$36 \times 10^{-4} \text{ h}^{-1}$
Monod half constant	K_S	2 kg.m^{-3}
Maximum growth constant	μ_m	0.15 h^{-1}
Flow velocity	u	1.0 m.h^{-1}
Initial porosity	n	0.6
Bacteria source concentration	C	0.1 kg.m^{-3}
Substrate concentration	C_s	0.1 kg.m^{-3}
Domain length		4.0 m
Number of elements		40
Number of iterations		5
Convergence Tolerance		1×10^{-6}
Differencing weight	α	0.67
Time step	Δt	0.5 hours

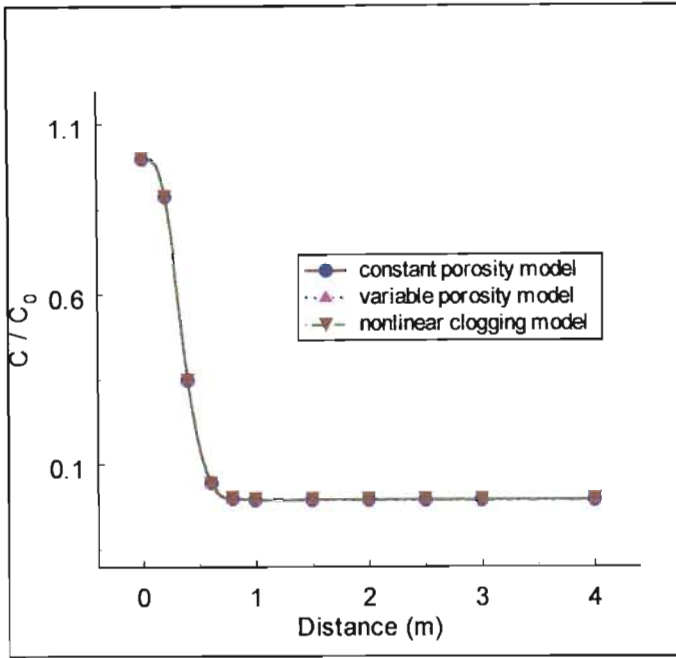


Figure 6.3 Comparison of the 3 GEM models for the parameter values given in table 6.3

6.2. The effects of the various parameters on bacteria transport.

From the governing partial differential equation (equation 3.12) which is restated here, it can be seen that several parameters influence the transport of bacteria in the subsurface environment. The GEM formulation will be used to evaluate the effects of some of these parameters.

$$\begin{aligned}
 &\frac{\partial \theta C}{\partial t} + k_c \theta C - k_y \rho_B \sigma = D \theta \frac{\partial^2 C}{\partial x^2} - u \theta \frac{\partial C}{\partial x} - k_d \theta C + \mu \theta C \pm F \quad (6.1) \\
 &\begin{array}{cccccccc}
 \uparrow & \uparrow & \uparrow & \uparrow & \uparrow & \uparrow & \uparrow & \uparrow \\
 \text{Transient} & \text{Clogging} & \text{Declogging} & \text{Dispersion} & \text{Advection} & \text{Decay} & \text{Growth} & \text{Source / Sink} \\
 \text{Term} & \text{Term} & \text{Term} & \text{Term} & \text{Term} & \text{Term} & \text{Term} & \text{Term}
 \end{array}
 \end{aligned}$$

6.2.1. The effects of groundwater flow-rate

The transport microbial contaminants will be influenced by the movement of groundwater. The factors that influence groundwater flow in an existing aquifer are: the rate of abstraction from aquifer, the rate of recharge (natural or artificial) of the aquifer, the hydraulic gradient and the changes to porosity (due to bacterial growth). Most of these influences can be the result of seasonal variations in water levels. The degree of influence of the groundwater flow-rate will be evaluated by considering reasonable variation in velocities. It will be assumed that all other parameters are constant.

6.2.2. Variation to Dispersivity

This parameter is greatly influenced by changes to the porosity of the aquifer. These changes in relation to bacteria transport, could result from microbial growth of species attached to solid matrix, clogging (adsorption, sedimentation and filtration) and de-clogging of the pores. Since this study is restricted to a one dimensional model, only the effects of longitudinal dispersivity can be evaluated.

6.2.3. Variation in Clogging and De-clogging Rates

The clogging process being a lumped parameter (consisting adsorption, sedimentation, and filtration effects) has been the focus of many studies. Most studies concluded that the processes of clogging and de-clogging are greatly influenced by the chemical and physical properties of the subsurface environment. In the study by Saiers and Hornberger (1994) it was reported that the clogging process of some colloidal matter can be expressed by higher order kinetics. In this work the evaluation will be two fold:

- i) the effect of clogging rates, using the linear model
- ii) the effect of clogging reaction order, using the nonlinear clogging model.

6.2.4. Variation in net growth / decay rate.

The effect of this parameter on the transport equation is two fold:

- it is directly related to the primary variable, and
- it impacts on the changes to porosity

As has been indicated previously, there are many factors that influence the growth and decay rates, especially presence of substrate, presence of predators, and the chemistry (toxicity) of the subsurface environment. Therefore the rates can be considered to be site specific, and need to be determined experimentally. In this application, the following range will be assumed: negative rate, zero rate, and positive rate. This will give some indication of the bacteria concentration profile and changes to porosity.

6.2.5 Variation in substrate concentrations

The survival and growth of bacteria has a primary dependency on the substrate concentrations. Whilst this study assumes a constant substrate concentration in the migrating plume, the effects of different concentrations will be evaluated.

6.2.6 Variation in source concentrations (Boundary conditions)

This application is very relevant to bioremediation applications, where the rate of clean up is dependant on bacteria concentration. The movement of bacteria in a remediation site is key to the efficiency of the process. Hence, the variation in bacteria loading will be evaluated.

It should be noted that factors in 6.2.4, 6.2.5, and 6.2.6 are interrelated.

6.2.7 Effect of Distributed and point sources

In chapter one, potential sources of microbial contamination of the groundwater were discussed. These included, septic tanks and soak systems, ruptured sewer lines, informal settlements, use of sewage sludge as fertilisers, landfill sites, and

artificial recharge of aquifers using purified sewage water. Therefore, the contamination of a typical aquifer may have many source points. In this application, the GEM formulation is tested on its capacity to handle distributed and concentrated sources.

6.3 Summary

In this chapter, the three models developed in this work namely:

- the constant porosity model
- the variable porosity model and,
- the nonlinear clogging model

were verified, and the parameters and processes to be evaluated using these models were outlined.

Chapter Seven

Results and Discussion

From the work presented thus far, it is evident that the phenomenon of bacteria transport through porous media possesses more complications than the transport of conservative substances. Whilst attempts to investigate the impact of the various factors on bacteria transport will be made, it must be noted that most of these factors cannot be studied in isolation. In chapter six, the three transport models were validated, and the factors to be evaluated were outlined. In this chapter, the results and the analysis of the results are presented.

7.1 General Observations

Several factors may complicate the simplified modelling approach described thus far. A brief discussion of some of these factors is provided here to indicate the potential problems associated with microbial transport modelling in the subsurface environment.

- ▶ The diverse range of bacteria with varying growth and decay rates, adsorption and desorption rates, and sizes of bacteria may exist in a typical sewage plume. Some of the differences are several orders of magnitude. The use of average values for computational purposes may render the model inadequate to correctly predict the migration of a sewage plume.

- ▶ Harvey (1991) reported that the verification of existing models by field observations is problematic, owing to the complexity of the models and the number of parameters that need to be determined a priori.

- ▶ The complex nature, both physical and chemical will have a major impact on almost all the processes that are used to describe bacteria transport. For example, the chemical condition of the groundwater will affect the following processes - decay, growth, attachment, and detachment. Under the same conditions some of the processes are enhanced, whilst others are retarded. Therefore the lack of correct information on an aquifer may render the model inadequate to predict the behaviour of a migrating plume.
- ▶ The ability of microbial movement by self propulsion in response to a stimuli, may contribute vast difference between simulation results and field observations, especially in low velocity and stagnant groundwaters.

7.2. Transport Model Simulations

Notwithstanding the above list of complications, the GEM formulations of the transport model were simulated in a range of applications to determine the general trends in bacteria transport through porous media. A typical set of default settings, listed in Table 7.1, were established and used throughout this work. Deviations from the default values were necessary to establish effects of the various parameters, and when certain phenomenon / process are being illustrated.

7.2.1 Comparison of Constant Porosity and Variable Porosity Models

The motivation for developing the variable porosity model described by equation 5.13 was based on the assumption that the contribution to the reduction to porosity by some of the processes will be significant. The processes most likely to contribute to reduction in porosity are: source concentration, clogging rates, declogging rates, growth rate, decay rate and substrate concentration. It must be noted that most of these processes are interrelated.

It has already been shown in chapter six that for the conditions in which the changes to porosity were negligible, both the constant porosity model (eqn. 5.12) and variable porosity model (eqn. 5.12) produced exactly the same results (see Figure 6.3). However, if there is significant changes to the porosity, then the ability of the constant porosity model to produce meaningful results is questioned. Both the models have been tested in an application in which the resulting change in porosity is approximately 33 %. The parameter values used were: source concentration (10 kg.m^{-3}), clogging rate constant (80 h^{-1}), and velocity (1.5 m.h^{-1}), the rest of the values are default setting values shown in Table 7.1. The comparison of the results obtained from the simulations of both models is shown in Figure 7.1.

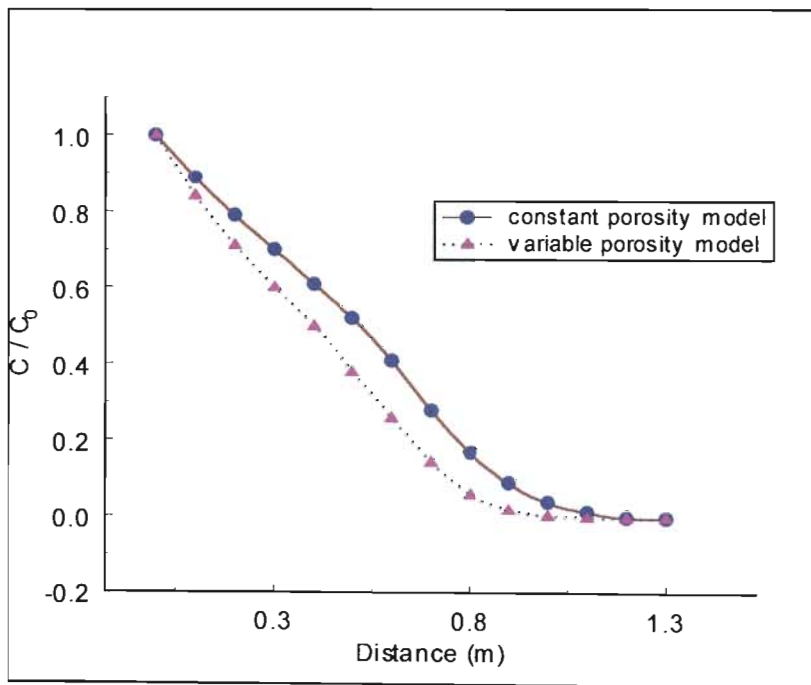


Figure 7.1 Comparison of constant porosity and variable porosity models in an application with significant decrease (33%) in porosity

The comparison shown in Figure 7.1 shows that the difference in predictions may be as large as 15% in this application. Whilst this over-prediction may be considered as a safety factor in the applications of groundwater pollution, this may lead to high inefficiencies in bio-remediation applications.

In this work, the variable porosity model (eqn. 5.130) will be used in all simulations except those involving nonlinear clogging. The added advantage of the variable porosity model is that, additional information regarding porosity changes, velocity changes and dispersivity changes can be obtained from this model. Figure 7.2 shows the changes to the porosity in the problem domain for the application evaluated above.

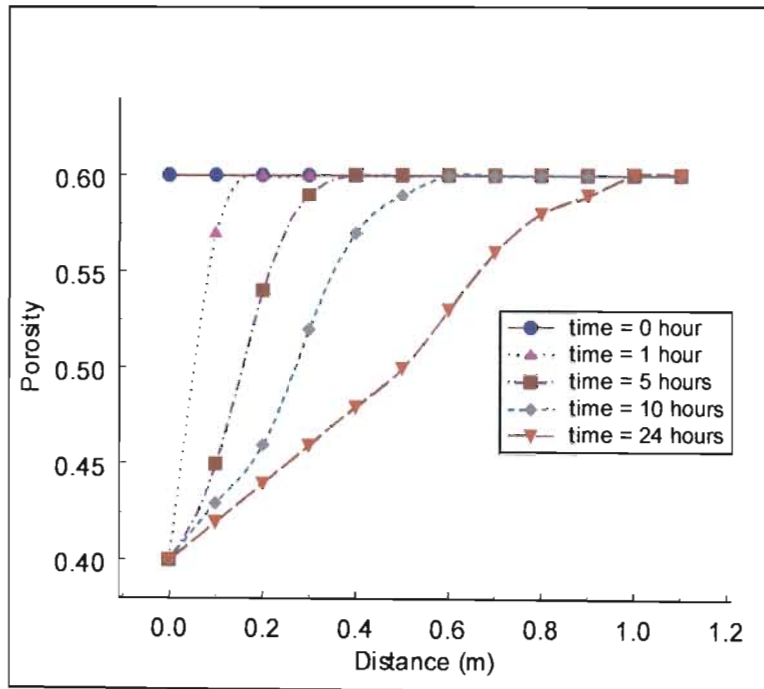


Figure 7.2 Typical porosity profile for applications with significant changes to porosity

7.2.2. General illustration

There are several factors influencing the transport of bacteria through the subsurface environment. Some of these will retard the migrating plume, whilst others may enhance this migration. To illustrate the potential seriousness of bacteria contamination, a simulation under favourable conditions has been done.

The results for a simulation of the variable porosity model (eqn. 5.13) to illustrate the behaviour of a typical plume, is shown in Figure 7.3. The bacteria concentration profile obtained were for conditions of net positive growth (i.e. growth rate is higher than decay rate) within the contaminant plume. The values for the model parameters are listed in Table 7.1 as simulation values.

The simulation results indicate that under the right conditions, the transport of bacteria through the subsurface environment could be fairly significant.

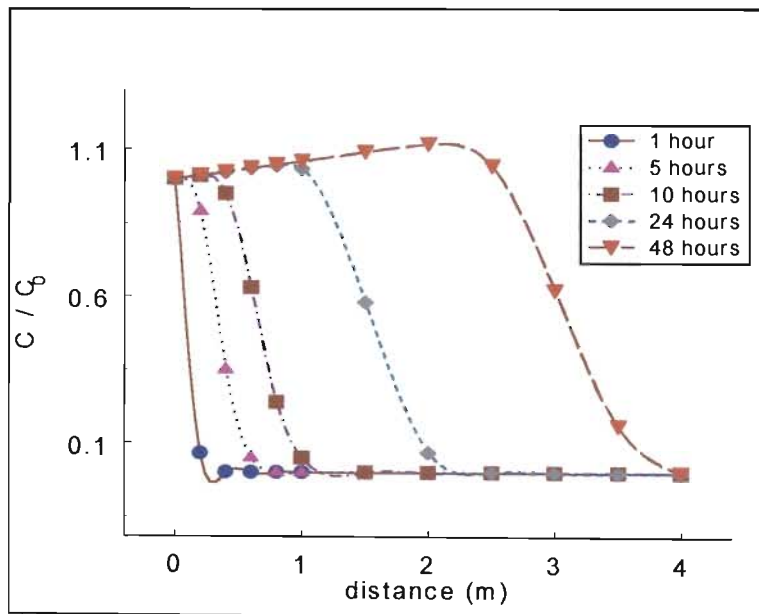


Figure 7.3. Typical bacteria concentration profile for conditions in table 7.1

Table 7.1 Simulation parameters

Parameter	Symbol	Default Settings	Simulation values
Dispersion coefficient	D	$0.02 \text{ m}^2 \text{ h}^{-1}$	$0.02 \text{ m}^2 \text{ h}^{-1}$
Density of Bacteria	ρ_B	$1000 \text{ kg} \cdot \text{m}^{-3}$	$1000 \text{ kg} \cdot \text{m}^{-3}$
Clogging rate constant	k_c	23.4 h^{-1}	23.4 h^{-1}
Declogging rate constant	k_y	1566 h^{-1}	1566 h^{-1}
Specific decay constant	k_d	$36 \times 10^{-3} \text{ h}^{-1}$	$36 \times 10^{-4} \text{ h}^{-1}$
Monod half constant	K_S	$2 \text{ kg} \cdot \text{m}^{-3}$	$2 \text{ kg} \cdot \text{m}^{-3}$
Maximum growth constant	μ_m	0.15 h^{-1}	1.5 h^{-1}
Flow velocity	u	$1.0 \text{ m} \cdot \text{h}^{-1}$	$1.0 \text{ m} \cdot \text{h}^{-1}$
Initial porosity	n	0.6	0.6
Bacteria source concentration	C	$0.1 \text{ kg} \cdot \text{m}^{-3}$	$0.1 \text{ kg} \cdot \text{m}^{-3}$
Substrate concentration	C_s	$0.01 \text{ kg} \cdot \text{m}^{-3}$	$0.1 \text{ kg} \cdot \text{m}^{-3}$
Domain length		4.0 m	4.0 m
Time step	Δt	0.5 hours	0.5 hours
Number of elements		40	40
Number of iterations		5	5
Convergence tolerance		1×10^{-6}	1×10^{-6}
Differencing weighting	α	0.67	0.67

7.2.3 Influence of model parameters on bacteria transport

As alluded to earlier, several factors influence the movement of bacteria in the subsurface environment. The degree of influence of these factors will now be presented. The governing PDE is restated here, and will be used as a point of reference for most of the discussions that follow.

$$\frac{\partial \theta C}{\partial t} + k_c \theta C - k_y \rho_B \sigma = D \theta \frac{\partial^2 C}{\partial x^2} - u \theta \frac{\partial C}{\partial x} - k_d \theta C + \mu \theta C \pm F \quad (7.1)$$

↑
Transient
Term

↑
Clogging
Term

↑
Declogging
Term

↑
Dispersion
Term

↑
Advection
Term

↑
Decay
Term

↑
Growth
Term

↑
Source
/ Sink

7.2.3.1. Flow velocity

The impact of flow velocity on bacteria transport was determined by simulating the variable porosity model (eqn 5.13) at three different velocities. The values used for the simulation were :

velocity range : 0.5 m.h^{-1} , 1.0 m.h^{-1} , and 1.5 m.h^{-1}

The other parameter values will be those given in Table 7.1. as default values.

The results obtained from the variable porosity model are shown in Figure 7.4. and Figure 7.5. The profiles obtained are at 5 hours and 24 hours after initial discharge, and at conditions that results in a net decay.

The results presented are consistent with theory - higher velocities will increase the advective transport of bacteria, resulting in a greater migration of the bacteria. Changes in velocity may also affect the rates of sedimentation, chemotaxis and tumbling, and declogging. The results indicate that for a set velocity, the profile of the advancing plume will be similar throughout the domain. Any changes to the porosity will result in a velocity reduction. This reduction of velocity may lead to a higher hydraulic gradient, which may eventually lead to higher declogging rates. To determine the effects of the hydraulic gradient on bacteria transport, the model will need to be coupled to the groundwater flow model.

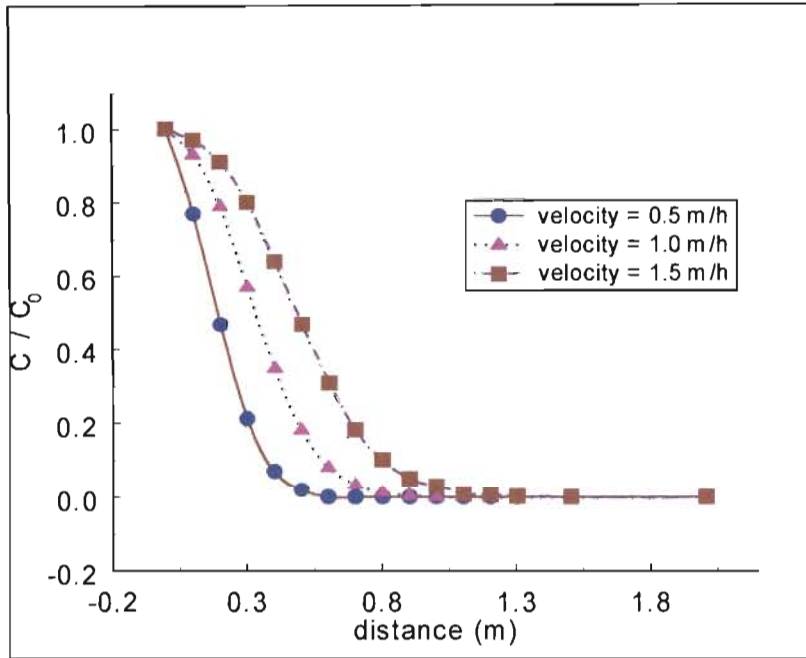


Figure 7.4 Effects of groundwater velocity on bacteria transport at 5 hours

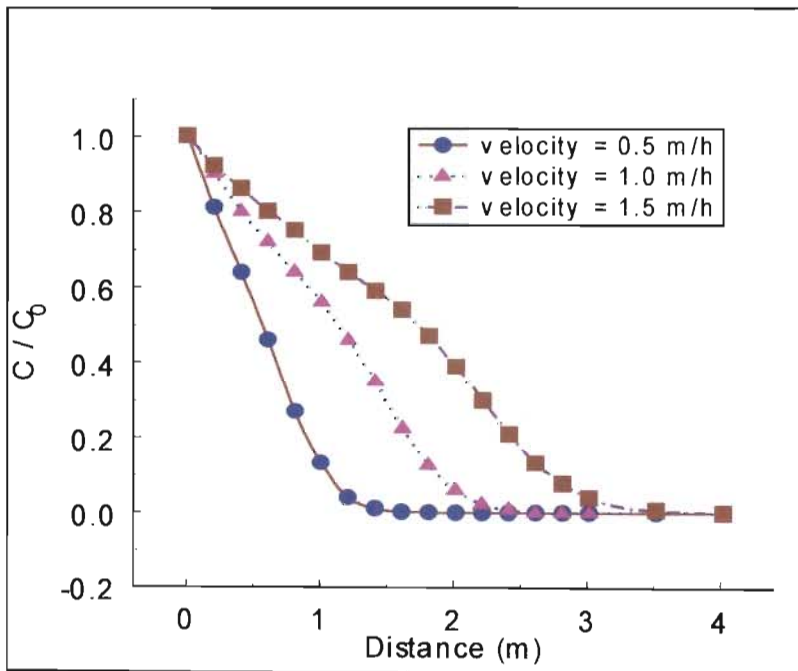


Figure 7.5 Effects of groundwater velocity on bacteria transport at 24 hours

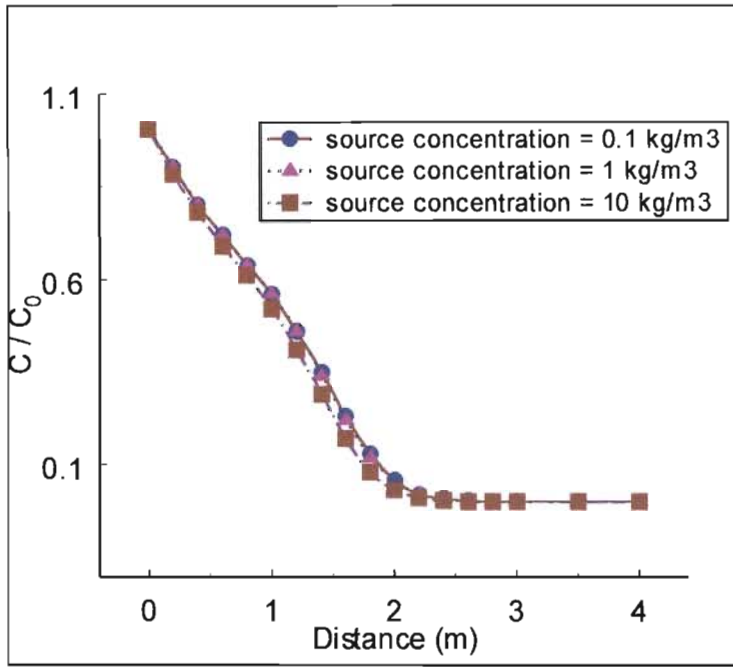


Figure 7.7. Effect of source concentration bacteria profile

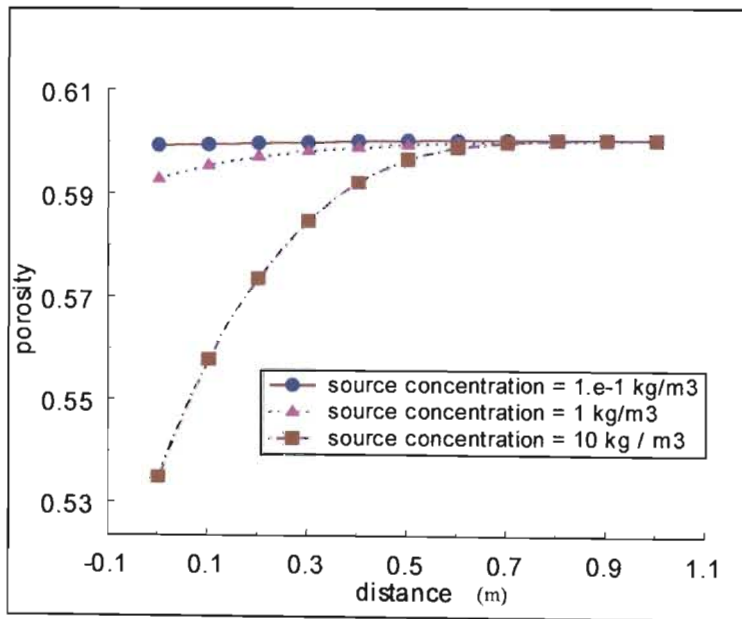


Figure 7.8. Effect of source concentrations on porosity

7.2.3.4. Substrate Concentration

The relationship between the substrate concentration and the bacteria growth rate is shown in equation 3.7. The relationship shows that higher substrate concentrations will result in higher growth rate constants. The influence of the substrate concentration on bacteria transport was determined by simulating the variable porosity model (eqn. 5.13) for three substrate concentrations. The values used for the simulation are:

$$1 \times 10^{-2} \text{ kg.m}^{-3}, \quad 1 \times 10^{-1} \text{ kg.m}^{-3} \quad \text{and} \quad 1 \text{ kg.m}^{-3}$$

The other parameter values will be those given in Table 7.1. as default values. The results obtained from the variable porosity model are shown in Figure 7.9. The profiles obtained are at 24 hours after initial discharge.

The influence of the substrate concentration results from its influence on the growth rate constant which given by:

$$\mu = \frac{\mu_m C_S}{K_S + C_S} \quad (7.3)$$

The growth rate constant affects both the transport equation and adsorbed species continuity equation shown in equation 7.1 and equation 7.2 respectively.

The results show that for concentrations greater than the minimum substrate concentration, there is substantial growth within the migrating plume. Unlike the retarded plume that was encountered for high source concentrations, the profile of the migrating plume for high substrate concentrations will be similar to that shown in Figure 7.1. It should be noted that in these simulations, it is assumed that substrate concentration is constant throughout the migrating plume.

The kinetic "constants" in the Monod equation can be subject to change in response to changes in temperature, the nature of the substrate, and the

chemical and physical properties of the subsurface environment. Therefore caution should be used in the application of Monod growth kinetics when there are temporal and spatial changes in any of these conditions in the aquifer.

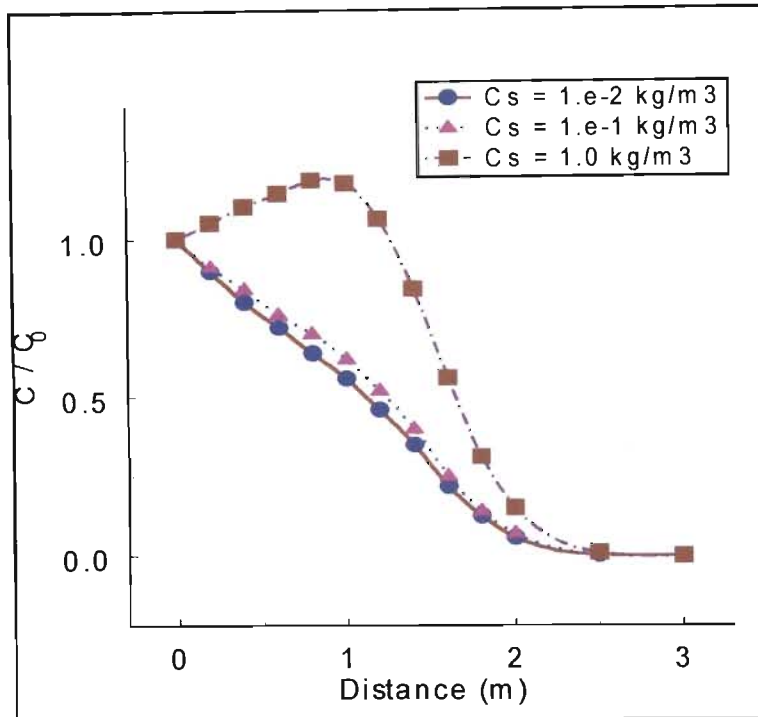


Figure 7.9. The effect of substrate concentration on the bacteria concentration profile

7.2.3.5. Decay

The process of decay is a natural process with living organisms. However the rate at which this occurs is very dependant on the physical and chemical conditions of the subsurface environment. The influence of decay rate constants on bacteria transport was determined by simulating the variable porosity model (eqn. 5.13) for three decay rate constant values . The values used for the simulation were:

$36 \times 10^{-4} h^{-1}$, $36 \times 10^{-3} h^{-1}$, and $36 \times 10^{-2} h^{-1}$

The other parameter values will be those given in table 7.1. as default values.

The results obtained from the variable porosity model are shown in Figure 7.10.

The profiles obtained are at 24 hours after initial discharge.

The influence of the decay rate is only significant when it exceeds the growth rate of the bacteria . This can be seen from the following relationship that relates the growth and decay terms:

$$\begin{aligned} \text{Net Growth Rate} &= \mu - k_d \\ &= \frac{\mu_m C_S}{K_S + C_S} - k_d \end{aligned} \quad (7.4)$$

The migration of the bacteria plume will be influenced by the amount of substrate present, immaterial of whether all other conditions promote growth or decay .The decay rate constants simulated here, all result in a negative growth rate, and will be $- 2.83 \times 10^{-3} h^{-1}$, $- 0.035 h^{-1}$, and $- 0.36 h^{-1}$ respectively. The results indicate that with high decay rates, the concentration of bacteria in the migrating plume is greatly reduced. Another factor which affects the bacteria population is the presence of predators.

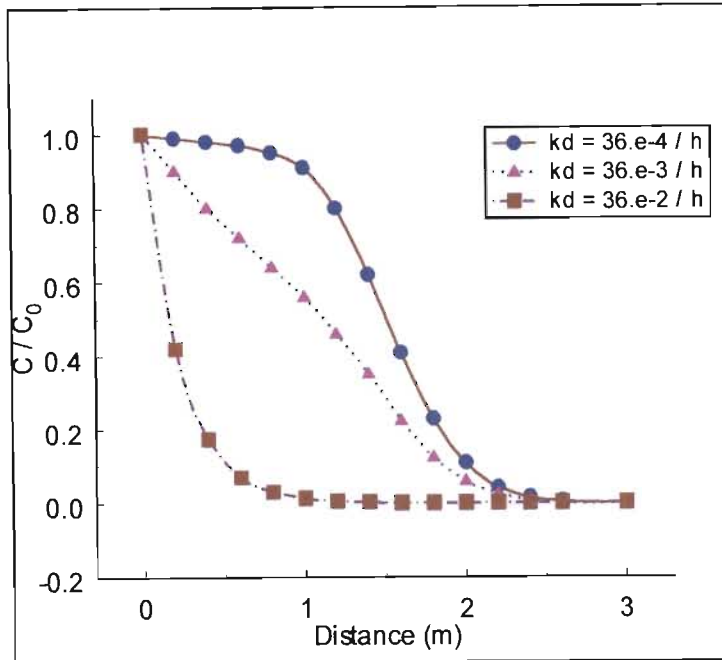


Figure 7.10. Effect of decay rates on the bacteria concentration profile

7.2.3.6. Clogging process

The evaluation of the clogging process has been approached in two ways: the effect of clogging rates, and the effect of nonlinear clogging. The influence of clogging rates on bacteria transport was determined by simulating the variable porosity model (eqn. 5.13) for three clogging rate values. The values used for the simulation were:

$$10 \text{ h}^{-1}, \quad 23.4 \text{ h}^{-1}, \quad \text{and} \quad 50 \text{ h}^{-1}$$

The other parameter values will be those given in Table 7.1. as default values. The results obtained from the variable porosity model are shown in Figure 7.11. The profiles obtained are at 5 hours after initial discharge, and at conditions that results in a net decay.

The clogging process is greatly affected by the chemical and physical properties of the subsurface environment eg. The filtering effect is dependant on the pore sizes, the adsorption of bacteria onto the solid matrix will be dependent on the type of grains, the ph and ionic strength of the ground water . Since clogging is a retarding effect, an increase the clogging constant will result in decreasing migration of the bacteria plume.

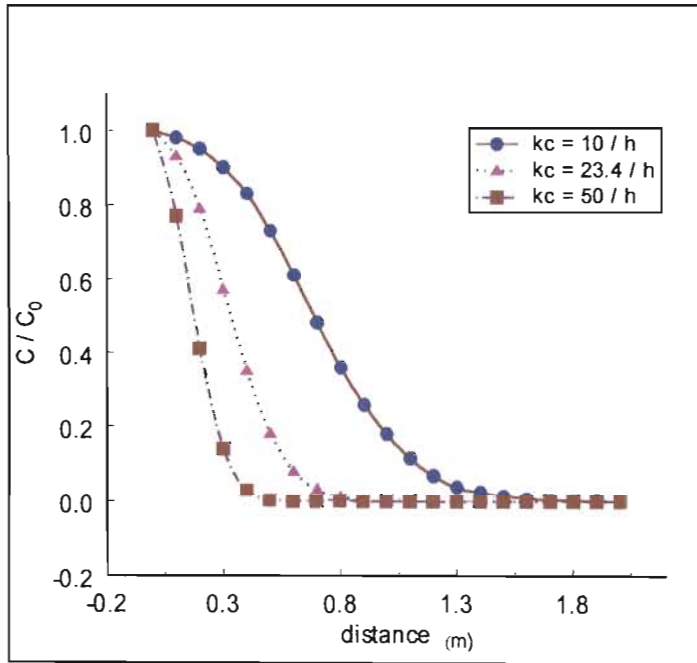


Figure 7.11 Effect of clogging rates on the bacteria concentration profile

In the evaluation of nonlinear clogging, the nonlinear model described by equation 5.16 was simulated for conditions where the clogging order was varied from 1 to 1.5. It should be noted that due to the lack of information in literature relating to non linear clogging, the rate constants used are assumed to equal that used for the linear model. However , irrespective of the actual values, the resulting trends will be similar to those shown in Figure 7.12. The simulation was done at default values shown in Table 7.1. The profiles obtained are at 5 hours

after initial discharge, and at conditions that results in a net decay.

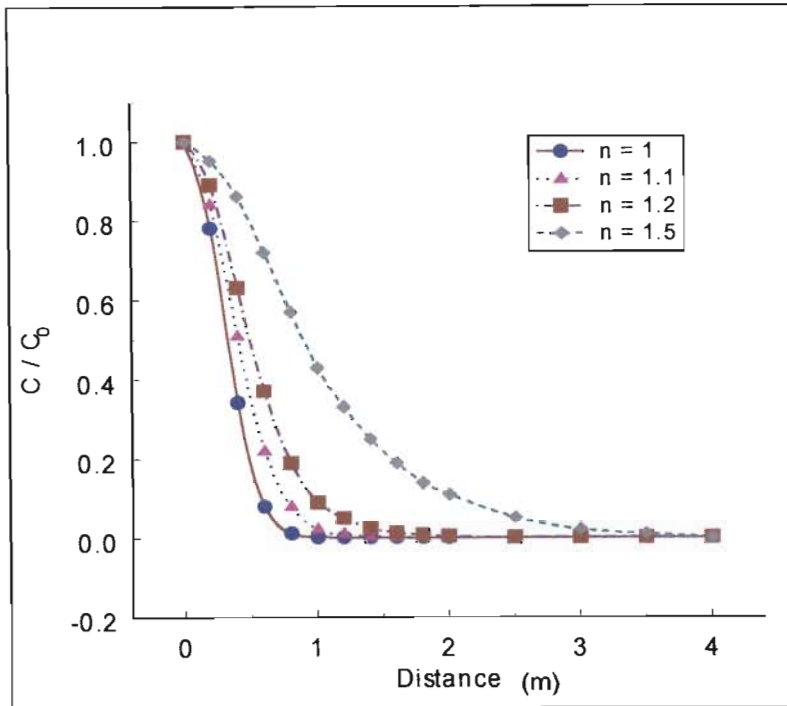


Figure 7.12. The effect of clogging reaction order on the bacteria concentration profile

From equations 7.1 and 7.2 it can be seen that the clogging term is affected by two parameters: the clogging rate constant, as well as the bacteria concentration. Since the clogging process is a function of the bacteria concentration, the degree of retardation will be concentration dependant as has been seen in Figure 7.13. For both the linear and nonlinear models, the effect of higher bacteria concentrations lead to greater retardation of the bacteria plume. From the comparison of Figure 7.13 and Figure 7.7, it is evident that the source concentration will have a greater effect in the nonlinear model than in the linear model. The difference between the models is only in the clogging terms, which is shown below:

the linear model (eqn. 5.13) has a clogging term defined by $k_c C$, and

the nonlinear model (eqn. 5.16) has a clogging term defined by $k_c C^n$.

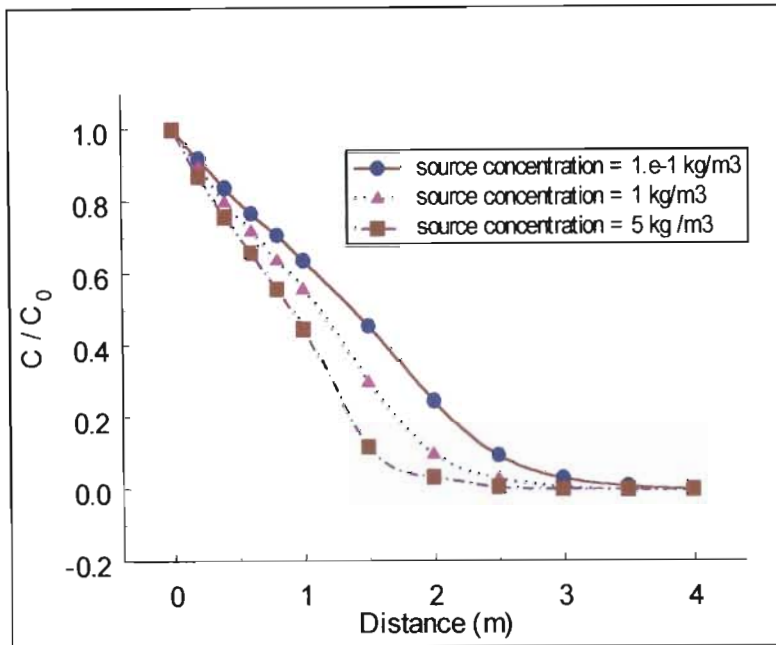


Figure 7.13 Effect of source concentration on nonlinear clogging

7.2.3.7. Effect of Distributed and point sources

One of the strong points of the GEM formulation is its ability to handle both distributed and point sources throughout the problem domain. Here typical bacteria profiles are projected for the following scenarios :

- I. Distributed sources with net growth conditions
- II. Distributed sources with net decay conditions
- III. Point sources with net growth conditions
- IV. Point sources with net decay conditions

For the distributed sources, the following conditions were applied :

- | | | |
|----------------------------------|--------------------------------------|---------------------------|
| initial source concentration | (0.1 kg.m^{-3}) | |
| distributed source concentration | (0.05 kg.m^{-3}) | |
| decay rate constant | $(36 \times 10^{-3} \text{ h}^{-1})$ | For net growth conditions |

decay rate constant	$(36 \times 10^{-2} h^{-1})$	For net decay conditions
domain size	4 meters	

The results obtained are shown in Figure 7.14 and Figure 7.15

For the point sources, the following conditions were applied :

initial source concentration	$(0.1 kg.m^{-3})$	
distributed source concentration	$(0.01 kg.m^{-3})$	
decay rate constant	$(36 \times 10^{-3} h^{-1})$	For net growth conditions
decay rate constant	$(36 \times 10^{-2} h^{-1})$	For net decay conditions
domain size	50 meters	
point source position	25 meters	

The results obtained are shown in Figure 7.16 and Figure 7.17

Whilst the results have not been tested against field data, the results reflect the typical profiles that is expected in this types of application. From a qualitative description, these profiles are consistent with theory.

Since the capacity of the GEM to handle both distributed and point sources throughout the problem domain is one of its greatest advantage over other computational methods, further discussion of this computational procedure is provided here.

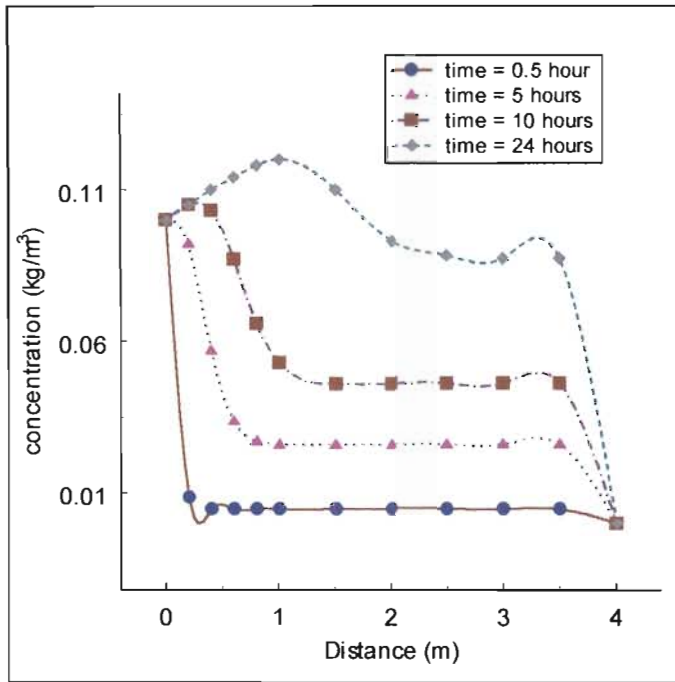


Figure 7.14 Effect of Distributed sources on the bacteria concentration profile under net growth conditions

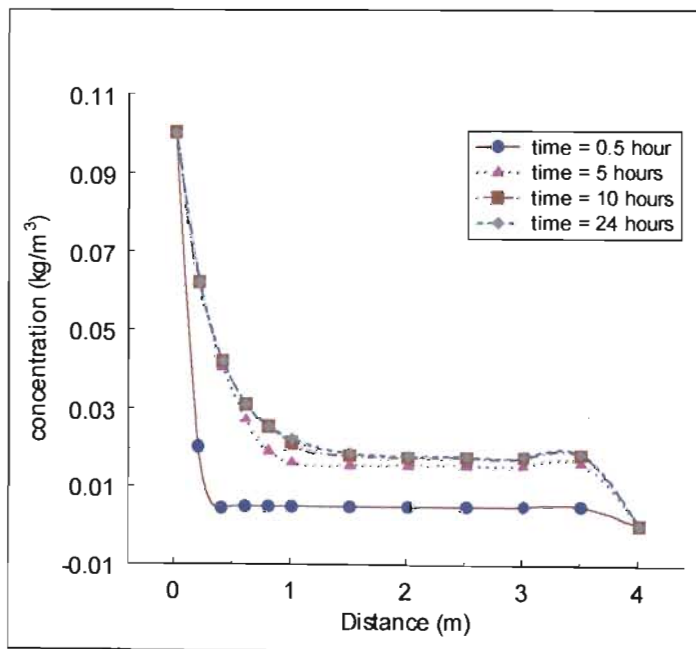


Figure 7.15 Effect of Distributed sources on the bacteria concentration profile under net decay conditions

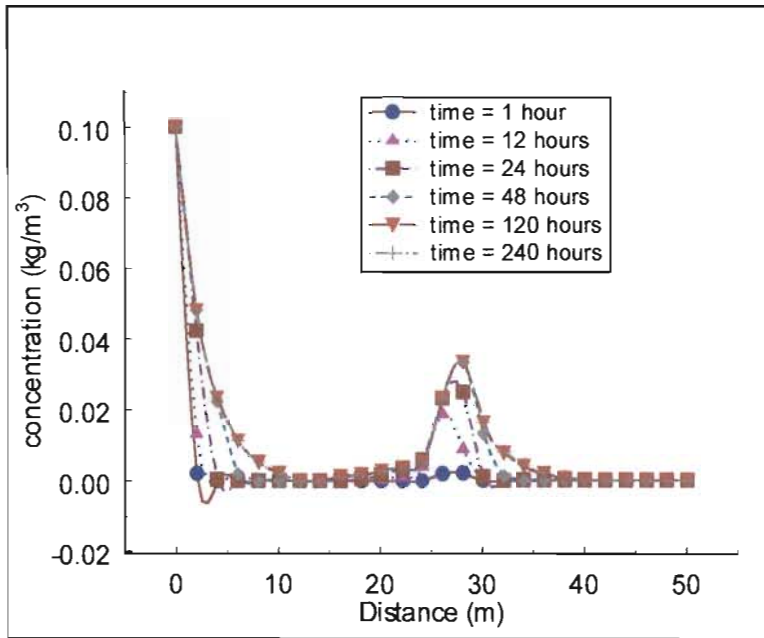


Figure 7.16 Effect of point sources on the bacteria concentration profile under net decay conditions

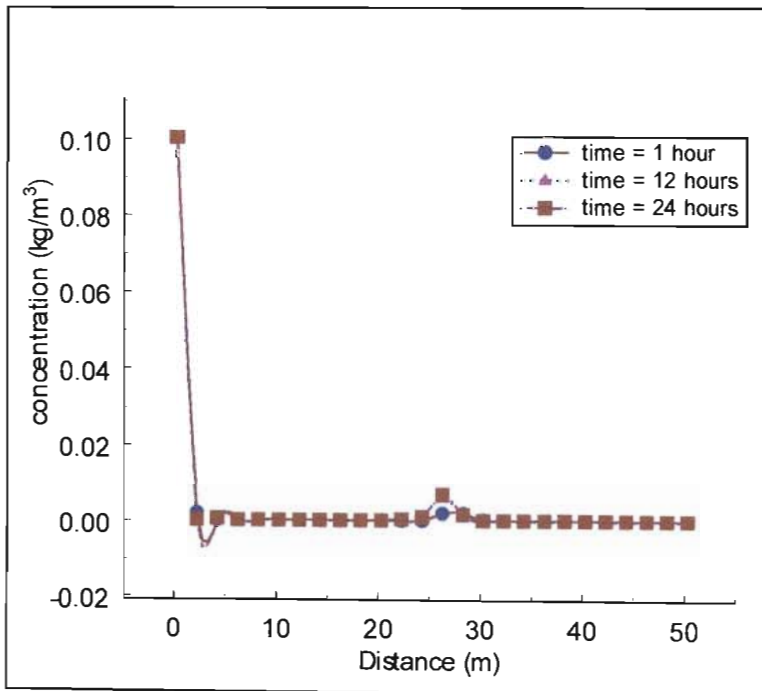


Figure 7.17 Effect of Point sources on the bacteria concentration profile under net decay conditions

The recharge term in all the formulations presented (eqns. 5.12, 5.13, and 5.16) in this work takes into account both concentrated or point and distributed sources / sinks. This can be expressed mathematically as:

$$f(x) = f_p(x) + f_d(x) \quad (7.5)$$

Total Recharge	Point sources / sinks	+	Distributed sources / sinks
-------------------	--------------------------	---	--------------------------------

The Distributed source / sink term is either given as a constant value throughout the domain or it may be expressed as a function of the domain. Whereas point or concentrated sources are represented mathematically as:

$$f_p(x) = \sum_{i=1}^{N_p} Q_i \delta(x - x_i) \quad (7.6)$$

where Q is the strength of the i -th source or sink located at x_i , and N_p is the total number of sources / sinks.

If there are point or concentrated sources / sinks, then we have to ensure that the effects of such sources / sinks are accounted for at the correct nodes and elements. To illustrate the computational method to account for point sources / sinks, consider a typical element R and its adjacent elements in the problem domain as shown in the Figure 7.18.

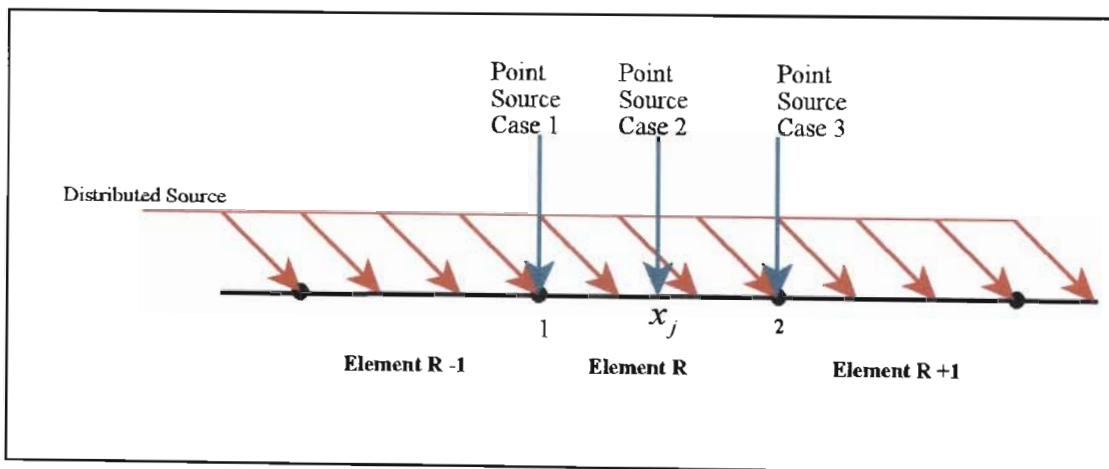


Figure 7.18 The effects of Point sources / sinks on the element / s

In general, the contribution of the point sources to the nodal equations of a typical element can be expressed as:

$$F_{p1}^e = \sum_{j=1}^{N_p^e} Q_j (x_j - x_1^e + \tilde{l})$$

and (7.7)

$$F_{p2}^e = \sum_{j=1}^{N_p^e} Q_j (x_2^e - x_j + \tilde{l})$$

Case 1 - If the point source / sink is at the first node of element R, then, the point source / sink will effect element R -1 and element R. The resulting total recharge term for each of nodal equations will be:

element R - 1

node 1:

$$T_{1j} f_j^{R-1}(x) = T_{11} f_1^{R-1} + T_{12} f_2^{R-1} \quad (7.8)$$

node 2

$$T_{2j} f_j^{R-1}(x) = T_{21} f_1^{R-1} + T_{22} f_2^{R-1}$$

where

$$f_1^{R-1} = F_{d1}^{R-1} + F_{p1}^{R-1} = F_{d1}^{R-1} + \sum_{j=1}^{N_p} Q_j (x_j - x_1^{R-1} + \tilde{l})$$

and (7.9)

$$f_2^{R-1} = F_{d2}^{R-1} + F_{p2}^{R-1} = F_{d2}^{R-1} + \sum_{j=1}^{N_p} Q_j (x_2^{R-1} - x_j + \tilde{l})$$

similarly for element R we have

element R

node 1:

$$T_{1j}f_j^R(x) = T_{11}f_1^R + T_{12}f_2^R \quad (7.10)$$

node 2

$$T_{2j}f_j^R(x) = T_{21}f_1^R + T_{22}f_2^R$$

where

$$f_1^R = F_{d1}^R + F_{p1}^R = F_{d1}^R + \sum_{j=1}^{N_p} Q_j(x_j - x_1^R + \tilde{l})$$

and

$$(7.11)$$

$$f_2^R = F_{d2}^R + F_{p2}^R = F_{d2}^R + \sum_{j=1}^{N_p} Q_j(x_2^R - x_j + \tilde{l})$$

where F_{dj}^e represents the distributed source / sink

Case 2 - If the point sources / sinks are between nodal points, then the only element affected will be the element R. therefore the resulting nodal equations will be:

element R

node 1:

$$T_{1j}f_j^R(x) = T_{11}f_1^R + T_{12}f_2^R \quad (7.12)$$

node 2

$$T_{2j}f_j^R(x) = T_{21}f_1^R + T_{22}f_2^R$$

where

$$f_1^R = F_{d1}^R + F_{p1}^R = F_{d1}^R + \sum_{j=1}^{N_p} Q_j (x_j - x_1^R + \tilde{l})$$

and

(7.13)

$$f_2^R = F_{d2}^R + F_{p2}^R = F_{d2}^R + \sum_{j=1}^{N_p} Q_j (x_2^R - x_j + \tilde{l})$$

Case 3 - If the point source / sink is at the last node of element R, then, the point source / sink will effect element R and element R + 1. The resulting total recharge term for each of nodal equations will be:

element R

node 1:

$$T_{1j} f_j^R(x) = T_{11} f_1^R + T_{12} f_2^R$$
(7.14)

node 2

$$T_{2j} f_j^R(x) = T_{21} f_1^R + T_{22} f_2^R$$

where

$$f_1^R = F_{d1}^R + F_{p1}^R = F_{d1}^R + \sum_{j=1}^{N_p} Q_j (x_j - x_1^R + \tilde{l})$$

and

(7.15)

$$f_2^R = F_{d2}^R + F_{p2}^R = F_{d2}^R + \sum_{j=1}^{N_p} Q_j (x_2^R - x_j + \tilde{l})$$

Similarly for element R +1, we have

element R + 1

node 1:

$$T_{1j} f_j^{R+1}(x) = T_{11} f_1^{R+1} + T_{12} f_2^{R+1}$$
(7.16)

node 2

$$T_{2j} f_j^{R+1}(x) = T_{21} f_1^{R+1} + T_{22} f_2^{R+1}$$

where

$$f_1^{R+1} = F_{d1}^{R+1} + F_{p1}^{R+1} = F_{d1}^{R+1} + \sum_{j=1}^{N_p} Q_j (x_j - x_1^{R+1} + \tilde{l})$$

and

$$f_2^{R+1} = F_{d2}^{R+1} + F_{p2}^{R+1} = F_{d2}^{R+1} + \sum_{j=1}^{N_p} Q_j (x_2^{R+1} - x_j + \tilde{l})$$

(7.17)

7.3 Summary

The results obtained show the general relative trends that could be associated with bacteria transport in porous media. The modelling of bacteria transport is complicated by a number of processes that affect bacterial transport behaviour. Several of these processes show inter-dependance and interactions between various parameters. The general trends observed were :

- ▶ Higher velocities lead to greater bacteria plume migration.
- ▶ Higher source concentrations show retarded plume migration, this results from the decrease in porosity at the beginning of the domain. However, the migrating plume will have a higher bacteria concentration.
- ▶ Substrate concentrations above the minimum promotes bacteria growth within the plume, resulting in higher bacteria concentrations within the plume.
- ▶ The effect of the decay rate constant is dependent on the substrate concentration. If the decay rate is greater than the growth rate, then the migrating plume will have a lower bacteria concentration.
- ▶ The growth and concentration of bacteria have a greater effect in reducing the porosity than the clogging processes of adsorption, sedimentation and sieving.
- ▶ The reaction order of the clogging process greatly influences the migration of the plume. For low source concentrations, higher orders have resulted in greater migration , whereas, for high source concentrations the plume will be more retarded.

Chapter Eight

Conclusion and Recommendations

The objectives of this study were to evaluate the influence of the various processes and parameters related to bacteria transport through porous media, and to broaden the application of the Green Element Method (GEM) to biologically reactive transport systems.

To meet these objectives, the bacteria transport model proposed by Corapcioglu and Haridas(1985) was adopted. The governing partial differential equation was transformed into a Green Element Method Formulation. Three different GEM models were presented:

- a constant porosity model - this model assumed that the porosity of the medium remained unchanged throughout the spatial and temporal domains. This model was used to test the accuracy of the GEM formulation by verifying it against an analytical solution.

- a variable porosity model - this model accounted for changes in porosity and the subsequent changes to velocity. This model was verified against the constant porosity model for an application in which the porosity changes were negligible.

- a non linear clogging model - in this model, the reaction order of the clogging term was changed to orders greater than unity. This resulted in the governing partial differential equation becoming a nonlinear partial differential equation . The numerical and computational procedures had to be modified to facilitate an iterative solution. This was successfully done using the Newton Raphson Algorithm. The model was verified against the constant porosity model in an

application where the changes to porosity were negligible, and the reaction order of clogging was set to unity. This model also accounted for changes to porosity and velocity.

The verified models were simulated in various applications, to evaluate the impact of the various parameters. The following sections summarise the results of these simulations.

Bacteria Transport

The modelling of bacteria transport is complicated by a number of processes that affect bacterial transport behaviour. Several of these processes show inter-dependance and interactions between various parameters. The general trends observed were:

- ▶ Higher velocities lead to greater bacteria plume migration.
- ▶ Higher source concentrations show retarded plume migration, this results from the decrease in porosity at the beginning of the domain. However, the migrating plume will have a higher bacteria concentration.
- ▶ Substrate concentrations above the minimum promotes bacteria growth within the plume, resulting in higher bacteria concentrations within the plume.
- ▶ The effect of the decay rate constant is dependent on the substrate concentration. If the decay rate is greater than the growth rate, then the migrating plume will have a lower bacteria concentration.
- ▶ The growth and concentration of bacteria have a greater effect in reducing the porosity than the clogging processes of adsorption, sedimentation and sieving.
- ▶ The reaction order of the clogging process greatly influences the migration of the plume. For low source concentrations, higher orders have resulted in greater migration, whereas, for high source concentrations the plume will be more retarded.

It is evident that there are several critical and complicating features which need to be considered when modelling bacteria transport. In addition, the various constants and coefficients used in these models are very specific to the type of organism, and the chemical and physical properties of the subsurface environment. Most of these values are not directly measurable and need to be determined from experimental studies.

Green Element Method

- ▶ the governing partial differential equations, both linear and non linear were easily transformed into the GEM formulation with no simplifying assumptions or restrictions,
- ▶ the variation of the various quantities within a typical element were represented by linear interpolation functions.
- ▶ the formulation allows for non uniform discretisation of the problem domain,
- ▶ the non linear model computation was easily facilitated using the Newton Raphson algorithm
- ▶ the formulation has the capacity to accommodate both distributed and point sources /sinks
- ▶ the hand calculations in the appendices show the ease of application of the Method and its extent of application.

These points indicate that the Green Element Method is fairly powerful computational method, that can be used as a solution procedure for many applications, including nonlinear transient problems with multiple sources / sinks in the problem domain.

Further study addressing the following aspects is recommended :

1. Investigate the transport of bacteria in a domain where the substrate concentration is reducing due to consumption by the bacteria i.e a coupled bacteria - substrate system.

2. Development of a two dimensional GEM model, to determine the full extent of plume spreading and migration.
3. Development of radial system formulation to study the effects at injection wells.
4. Testing the models against field or experimental data

References

ADDISCOTT, T., SMITH, J. and BRADBURY, N. (1995), **Critical Evaluation of Models and their Parameters**, *J. Environ. Qual.*, **24**, pp. 803-807.

ARBOGAST, T. and WHEELER, M.F. (1995), **A Characteristics-Mixed Finite Element Method for Advection-Dominated Transport Problems**, *Siam J. Numer. Anal.*, **32**(2),

BALES, R.C., LE, S., MAGUIRE, K.M., YAHYA, M.T., GERBGA, C.P. and HARVEY, R.W. (1995), **Virus and Bacteria Transport in a Sandy Aquifer, Cape Cod, MA**, *Ground Water*, **33**(4). pp. 653-661.

BALES, R.C., LI, S. YEH, T.-C.J., LENCZEWSKI, M.E. and GERBA, C.P. (1997), **Bacteriophage and Microsphere Transport in Saturated Porous Media: Forced-Gradient Experiment at Borden, Ontario**, *Water Resources Research*, **33**(4), pp. 639-648.

BAVEYE, P. and VALOCCHI, A. (1989), **An Evaluation of Mathematical Models of the Transport of Biologically Reacting Solutes in Saturated Soils and Aquifers**, *Water Resources Research*, **25**(6), pp. 1413-1421.

BEAR, J., BELJIN, M.S. and ROSS, R.R. (1992), **Fundamentals of Ground-Water Modeling**, *EPA/540/5 - 92/005*.

BENGTSSON, G. and LINDQUIST, R. (1995), **Transport of Soil Bacteria Controlled by Density Dependent Sorption Kinetics**, *Water Resources Research*, **31**(5), pp. 1247-1256.

BLUE, K.A., LOGAN, B.E. and ARNOLD, R.G. (1995), **Modeling Bacterial Detachment During Transport Through Porous Media as a Residence-Time-Dependent Process**, *Water Resources Research*, **31**(11), pp. 2649-2658.

BOTHA, J.F. (EDITOR) (1990), **Modelling Groundwater Contamination in the Atlantis Aquifer**, *Water Research Commission*, WRC 175/1/90.

BUIKIS, A., RUSAKEVICH, Z. and ULANOVA, N. (1995), **Modelling of Convective Diffusion process with Nonlinear Sorption in Multilayer Aquifer**, *Transport in Porous Media*, **19**, pp. 1-13.

CELIA, M.A., KINDRED, J.S. and HERRERA, I. (1989), **Contaminant Transport and Biodegradation 2. Conceptual Model and Test Simulations**, *Water Resources Research*, **25**(6), pp.1149-1159.

CELIA, M.A., KINDRED, J.S. and HERRERA, I. (1989), **Contaminant Transport and Biodegradation 1. A Numerical Model for Reactive Transport in Porous Media**, *Water Resources Research*, **25**(6), pp.1141-1148.

CLEMENT, T.P., HOOKER, B.S. and SKEEN, R.S. (1996), **Numerical Modeling of Biologically Reactive Transport Near Nutrient Injection Well**, *Journal of Environmental Engineering*, **122**(9), pp. 833-839.

CORAPCIOGLU, M.Y. and HARIDAS, A (1984), **Transport and Fate of Microorganisms in Porous Media - A Theoretical Investigation**, *Journal of Hydrology*, **72**, pp. 149-169.

CORAPCIOGLU, M.Y. and HARIDAS, A (1985), **Microbial Transport in Soil and Groundwater : A Numerical Model**, *Adv. Water Resources*, **8**, pp. 188-199.

CORAPCIOGLU, M.Y. and KIM, S. (1995), **Modeling Facilitated Contaminant Transport by Mobile Bacteria**, *Water Resources Research*, **31**(11), pp. 2639-2647.

DICKINSON, R.A. (1991), **Problems with Using Existing Transport Models to Describe Microbial Transport in Porous Media**, *Modeling the Environmental Fate of Microorganisms*, Edited by Hurst, C.J., American Society for Microbiology, pp. 21-47.

FUGGLE, R.F. and RABBIE, M.A., (1994), *Environmental Management in South Africa*, Juta and Company Ltd.

GOLTZ, N. and ROBERTS, P.V., (1986), **Three dimensional Solutions for Solute Transport in an Infinite medium with Immobile zones**, *Water Resources Research*, **22**(7), pp.1139-1148.

GOTTARDI, G and VENUTELLI, M. (1995), **One dimensional moving finite element program for modelling solute transport in porous media**, *Computers and Geosciences*, **21**(5), pp. 663-685.

GUYMON, G.L., SCOTT, V.H. and HERRMANN, L.R. (1970), **A General Numerical Solution of the Two-Dimensional Diffusion-Convection Equation by the Finite Element Method**, *Water Resources Research*, **6**(6), pp. 1611-1617.

GUYMON, G.L. (1970), **A Finite Element Solution of the One-Dimensional Diffusion-Convection Equation**, *Water Resources Research*, **6**(1), pp.204-210.

HARVEY, R.W. (1991), **Parameters Involved in Modeling Movements of Bacteria in Groundwater**, *Modeling the Environmental Fate of Microorganisms*, Edited by Hurst, C.J., American Society for Microbiology, pp. 89-114.

HARVEY, R.W. and GARABEDIAN, S.P. (1991), **Use of Colloid Filtration Theory in Modeling Movement of Bacteria Through a Contaminated Sandy Aquifer**, *Environmental Science and Technology*, **January**, pp. 178-185.

HARVEY, R.W., METGE, D.W., KINNER, N. and MAYBERRY, N. (1997), **Physiological Considerations in Applying Laboratory-Determined Buoyant Densities to Predictions of Bacterial and Protozoan Transport in Groundwater: Results of In-Situ and Laboratory Tests**, *Environmental Science and Technology*, **31(1)**, pp. 289-295.

HORNBERGER, G.M., MILLS, A.L. and HERMAN, J.S. (1992), **Bacterial Transport in Porous Media: Evaluation of a Model Using Laboratory Observations**, *Water Resources Research*, **28(3)**, pp. 915-938.

HUYAKORN, P.S., UNGS, M.J., MULKEY, L.A. and SUDICKY, E.A. (1987), **A Three-Dimensional Method for Predicting Leachate Migration**, *Ground Water*, **25(5)**, pp. 588-598.

JEWETT, D.G., HILBERT, T.A., LOGAN, B.E., ARNOLD, R.G. and BALES, R.C. (1995), **Bacterial Transport in Laboratory Columns and Filters: Influence of Ionic Strength and pH on Collision Efficiency**, *Wat. Res.*, **29(7)**, pp. 1673-1680.

JOHNSON, W.P., BLUE, K.A., LOGAN, B.E. and ARNOLD, R.G. (1995), **Modeling Bacterial Detachment During Transport Through Porous Media as a Residence-Time-Dependent Process**, *Water Resources Research*, **31(11)**, pp. 2649-2658.

KEELEY, A., RUSSELL, H.H. and SEWELL, G.W. (1999), **Microbial Processes Affecting Monitored Natural Attenuation of Contaminants in the Subsurface**, *EPA/540/5 - 99/01*.

KINNER, N.E., HARVEY, R.W., BLAKESLEE, K., NOVARINO, G. and MEEKER, L.D. (1998), **Size-Selective Predation on Groundwater Bacteria by Nanoflagellates in an Organic-Contaminated Aquifer**, *Applied and Environmental Microbiology*, **64**(2),

Le BLANC, D.R. (1993), **Overview of Research at the Cape Cod Site : Field and Laboratory Studies of Physical, Chemical, and Microbiological Processes Affecting Transport in a Sewage-Contaminated Aquifer**, *US Geological Survey of Toxic Substance Hydrology Program Proceedings*, Colorado Springs, Colorado, September.

LEIJ, F.J. and DANE, J.H.(1990), **Analytical Solutions of the One-Dimensional Advection Equation and Two- or Three-Dimensional Dispersion Equation**, *Water Resources Research*, **26**(7), pp. 1475-1482.

McDOWELL-BOYER, L.M., HUNT, J.R. and SITAR, N. (1986), **Particle Transport Through Porous Media**, *Water Resources Research*, **22**(13), pp. 1901-1921.

McINERNEY, M.J. (1991), **Use of Models to Predict Bacterial Penetration and Movement Within a Subsurface Matrix**, *Modeling the Environmental Fate of Microorganisms*, Edited by Hurst, C.J., *American Society for Microbiology*, pp.115-136.

MOLZ, F.J., WIDDOWSON, M.A. and BENEFIELD, L.D. (1986), **Simulation of Microbial Growth Dynamics Coupled to Nutrient and Oxygen Transport in Porous Media**, *Water Resources Research*, **22**(8), pp. 1207-1216.

MORSLED, J. and KALUARACHCHI, J.J. (1995), **Critical Assessment of the Operator-Splitting Technique in Solving the Advection-Dispersion-Reaction Equation: 2. Monod Kinetics and Coupled Transport**, *Advances in Water Resources*, **18**(2), pp. 101-110.

NACHABE, M.H., ISLAS, A.L. and ILLANGASEKARE, T.H. (1995), **Analytical Solutions for Water Flow and Solute Transport in the Unsaturated Zone**, *Ground Water*, **33**(2),

NATIONAL RESEARCH COUNCIL (1990), *Groundwater Models - Scientific and Regulatory Applications*, National Academy Press.

ONYEJEKWE, O.O. (1995), **A Simmplified Numerical Treatment of the Solute Transport Equation**, *Seventh South African National Hydrology Symposium, Grahamstown, 4th - 6th Sept.*, pp.13.

ONYEJEKEWE, O.O. (1996a), **Green Element Description of Mass Transfer in Reacting Systems**, *Numerical Heat Transfer, Part B*, **30**, pp. 483-498.

ONYEJEKWE, O.O. (1996b), **A Green Element Formulation Applied to Advection-Diffusion-Reaction Problems**, *Proceed. 1st South African Conf. on Appld. Mecmh. (SACAM'96) July 1-5, Midrand, South Africa*,

ONYEJEKEWE, O.O. (1997a), **A green element treatment of isothermal flow with second order reaction**, *Int. Comm. Heat and Mass Transfer*, **97**, pp. 251-264.

ONYEJEKEWE, O.O. (1997b), **Green element computation of Sturm-Liouville equations**, *Advances in Engineering Software*, **28**, pp. 615-620.

ONYEJEKEWE, O.O. (1998a), **A Boundary Element - Finite Element Equation Solutions to Flow in Heterogeneous Porous Media**, *Transport in Porous Media*, **31**, pp. 293-312.

ONYEJEKWE, O.O. (1998b), **A Green-Element Implementation of Nonlinear Transport Equation**, *Proceed. 12th Engrn. Mech. Conf. La jolla, California, May 17-20*, pp. 1645-1648.

ONYEJEKWE, O.O. (1998c), **Boundary Integral Procedures for Unsaturated Flow Problems**, *Transport in Porous Media*, **31**, pp. 313-330.

ONYEJEKWE, O.O. (1998d), **Solution of Nonlinear Transient Conduction Equation by a Modified Boundary Integral Procedure**, *Int. Comm. Heat and Mass Transfer*, **25**,

ONYEJEKWE, O.O. (2000), Personnel Communication

ONYEJEKWE, O.O., KARAMA, A.B. and TESHOME, D.S. (1998), **Changes in Water Table Induced by Transient Boundary condition and Space-dependent Recharge - A Green Element Approach**, *Water SA*, **24**(4), pp. 309-313.

ONYEJEKWE, O.O., KARAMA, A.B. and KUWORNOO, D.K. (1999), **A Modified Boundary Integral Solution of Recharging and Dewatering of an Unconfined Homogeneous Aquifer**, *Water SA*, **25**(1), pp. 9-13.

OSTER, C.A., SONNICHSEN, J.C. and JASKE, R.T. (1970), **Numerical Solution to the Convective Diffusion Equation**, *Water Resources Research*, **6**(6), pp.1746-1752.

PEPPER, D.W. and STEPHENSON, D.E. (1995), **An Adaptive Finite-Element Model for Calculating Subsurface Transport of Contaminant**, *Ground Water*, **33**(3), pp. 486-496.

RAMACHANDRAN, P.A (1994), *Boundary Element Methods in Transport Phenomena*, Computational Mechanics Publication.

ROWE, R.K. and BOOKER, K.R. (1995), **A Finite Layer Technique of Modelling Complex Landfill History**, *Can. Geotech. J.*, **32**, pp. 660-676.

RYAN, J.N., ELECH, M.E., ARD, R.A., HARVEY, R.W. and JOHNSON, P.R. (1999), **Bacteriophage PRD1 and Silica Colloid Transport and Recovery in an Iron Oxide-Coated Sand Aquifer**, *Environ. Sci. Technol.*, **33**, pp. 63-73.

RYAN, J.N. and ELIMELECH, M. (1996), *Colloid Mobilization and Transport in Groundwater - A Review*, Elsevier Science.

SAIERS, J.E. and HORNBERGER, G.M. (1994), **First and Second Order Kinetic Approaches for Modelling the Transport of Colloidal Particles in Porous Media**, *Water Resources Research*, **30**(9), pp. 2499-2506.

SATO, K (1992), **Accelerated Perturbation Boundary Element Model for Flow Problems in Heterogeneous Reservoirs**, *PhD Thesis*, Stanford University.

SCHOLL, M.A. and HARVEY, R.W. (1992), **Laboratory Investigations on the Role of Sediment Surface and Groundwater Chemistry in Transport of Bacteria Through a Contaminated Sandy Aquifer**, *Environ. Sci. Technol.*, **26**(7), pp. 1410-1417.

SUN, Y. and CHRYSIKOPOULOS, C.V. (1995), **Analytical Models for One-Dimensional Virus Transport in Saturated Porous Media**, *Water Resources Research*, **31**(5),

SIMS, J.L., SUFLITA, J.M. and RUSSELL, H.H. (1992), **In-Situ Bioremediation of Contaminated Ground Water**, *EPA/540/5 - 92/003*.

STRAUB, W.A. and LYNCH, R.D. (1982), **Models of landfill leaching :Moisture Flow and Inorganic Strength**, *Journal of Environmental Engineering*, **108**(EE2), pp. 231-249.

TAIGBENU, A. (1998), **Hermitian Green Element Calculations of Contaminant Transport**, *Water SA*, **24**(4), pp. 303-307.

- TAIGBENU, A.E (1999), *The Green Element Method*, Kluwer Academic Publishers.
- TAIGBENU, A. and LIGGETT, J.A. (1986), **An Integral Solution for the Diffusion-Advection Equation**, *Water Resources Research*, **22**(8), pp. 1237-1246.
- TAIGBENU, A.E. and ONYEJEKWE, O.O. (1995), **Green element simulations of nonlinear unsaturated flow**, *Appld. Math. Mod.*, **19**, pp. 675-684.
- TAIGBENU, A.E. and ONYEJEKWE, O.O. (1997a), **Transient 1-D Transport Equation Simulated by a Mixed Green Element Formulation**, *Int. Jnl. Numerical Mthds. In Fluids*,
- TAIGBENU, A.E. and ONYEJEKWE, O.O. (1997b), **A mixed Green element formulation for transient Burgers equation**, *Int. Jnl. Numerical Mthds. In Fluids*, **24**, pp. 437-454.
- TAIGBENU, A.E. and ONYEJEKWE, O.O. (1998), **Green's Function-Based Integral Approaches to Linear Transient Boundary-Value Problems and Their Stability Characteristics (I)**, *Appld. Math. Mod.*, **22**, pp. 687-702.
- TAIGBENU, A.E. and ONYEJEKWE, O.O. (1999), **Green's Function-Based Integral Approaches to Linear Transient Boundary-Value Problems and Their Stability Characteristics (II)**, *Appld. Math. Mod.*, **23**, pp. 241-253.
- TAN, T., GANNON, J.T., BAVEYE, P. and ALEXANDER, M. (1994), **Transport of Bacteria in an Aquifer Sand: Experiments and Model Simulations**, *Water Resources Research*, **30**(12), pp. 3243-3252.
- TAN, Y., GANNON, J.T., BAVEYE, P. and ALEXANDER M. (1994), **Transport of Bacteria in an Aquifer Sand: Experiments and Model Simulations**, *Water Resources Research*, **30**(12), pp. 3243-3252.

TAYLOR, S.W. and JAFFE, P.R. (1990), **Biofilm Growth and the Related Changes in the Physical Properties of a Porous Medium 3. Dispersivity and Model Verification**, *Water Resources Research*, **26**(9), pp. 2171-2180.

TAYLOR, S.W., MILLY, P.C.D. and JAFFE, P.R. (1990), **Biofilm Growth and the Related Changes in the Physical Properties of a Porous Medium 2. Permeability**, *Water Resources Research*, **26**(9), pp. 2161-2169.

TAYLOR, S.W. and JAFFE, P.R. (1990), **Biofilm Growth and the Related Changes in the Physical Properties of a Porous Medium 1. Experimental Investigation**, *Water Resources Research*, **26**(9), pp. 2153-2159.

TAYLOR, S.W. and JAFFE, P.R. (1990), **Substrate and Biomass Transport in a Porous Medium**, *Water Resources Research*, **26**(9), pp. 2181-2194.

UNITED STATES ENVIRONMENTAL PROTECTION AGENCY (1997), **Ground-water Model Testing : Systematic Evaluation and Testing of Code Functionality and Performance**, *EPA/600/R-97/007*.

VAN ZYL, H.D (1998), **Ex Situ Bioremediation of Hydrocarbon Contaminated Soil Using the Biopile Technique**, *MSc Thesis*, University of Stellenbosch.

VANDEVIVERE, P., BAVEYE, P., de LLOZADA, D.S. and DELEO, P. (1995), **Microbial Clogging of Saturated Soils and Aquifer Materials: Evaluation of Mathematical Models**, *Water Resources Research*, **31**(9), pp. 2173-2180.

WAN, J., TOKUNAGA, T.K. and TSANG, C-F. (1995), **Bacterial Sedimentation Through a Porous Medium**, *Water Resources Research*, **31**(7), pp. 1672-1636.

WATER RESEARCH COMMISSION (1999a), **Groundwater Contamination as a Result of Third World Type Urbanisations**, *Technical Report, Project No. 514*.

WATER RESEARCH COMMISSION (1999b), **Technology Adaption for Successful Application of Septic Tank Systems in the Coastal Zone**, *Technical Report, Project No. 597*.

WATER RESEARCH COMMISSION (1999c), **Assessment of the Impact of Agricultural Practises of the Quality of Groundwater Resources in South Africa**, *Technical Report, Project No. 641*.

WEISS, T.H., MILLS, A.L., HORNBERGER, G.M. and HERMAN, J.S. (1995), **Effect of Bacterial Cell Shape on Transport of Bacteria in Porous Media**, *Environ. Sci. Technol.*, **29**,

YATES, M.V. and YATES, S.R. (1991), **Modeling Microbial Transport in the Subsurface: A Mathematical Discussion**, *Modeling the Environmental Fate of Microorganisms*, Edited by Hurst, C.J., American Society for Microbiology, pp. 48-76.

YATES, M.V. and JURY, W.A. (1995), **On the Use of Virus Transport Modeling for Determining Regulatory Compliance**, *J. Environ. Qual.*, **24**, pp. 1051-1055.

ZHANG, R. (1995), **Prediction of Solute Transport using a Transfer Function Model and the Convection-Dispersion Equation**, *Soil Science*, **160**(1), pp.18-27.

ZYSSET, A., STAUFFER, F. and DRACOS, T. (1994), **Modeling of Reactive Groundwater Transport Governed by Biodegradation**, *Water Resources Research*, **30**(8), pp. 2423-2434.

Appendix A

Worked Example - Heterogenous Heat Transfer

This example serves to illustrate the ease with which heterogenous problems can be solved using GEM. This example clearly shows the computational advantages and resulting accuracies achieved when compared to FEM. The GEM solution is compared to FEM solution presented by Burnett (1987).

Statement of Problem

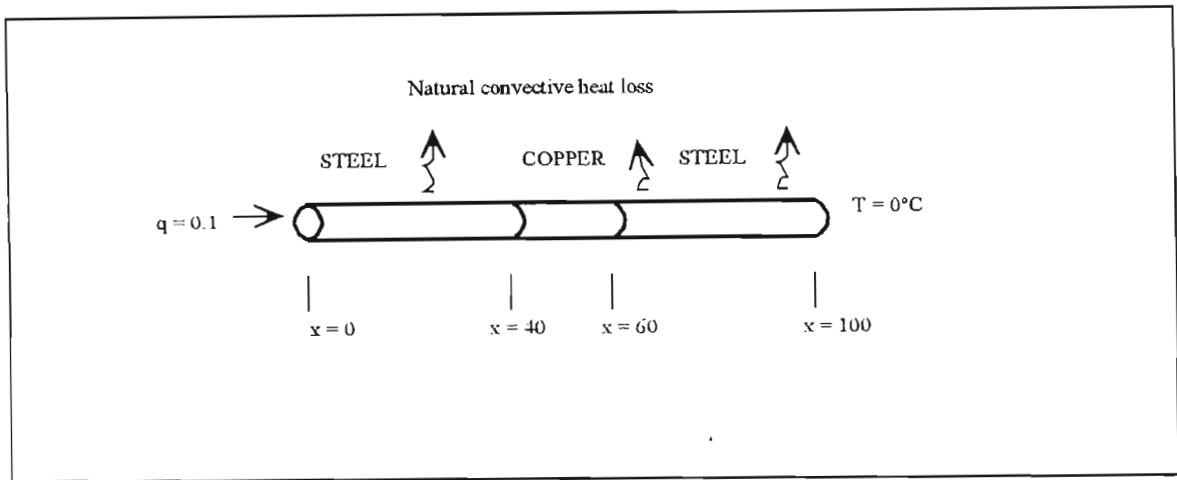


Figure A.1. Heat Conduction along a heterogenous rod, with convection from the lateral surface

Figure A.1 depicts a thin, cylindrical rod, 1 m long, composed of two different materials: a center section 20 cm long made of copper, and two end sections, each 40 cm long made of steel. The circular cross section, with a radius of 2 cm. Heat is flowing into the left end at a steady rate of $0.1 \text{ cal / sec-cm}^2$. The temperature of the right end is maintained at a constant 0°C . The rod is in contact with air at an ambient temperature of 20°C , so there is free convection from the lateral surface. The governing differential equation is can be expressed as :

$$-\frac{d}{dx} \left[K(x) \frac{dT(x)}{dx} \right] + \frac{hl}{A} [T(x) - T_{\infty}] = Q(x) \quad \text{B.1}$$

where, $Q(x)$ is the internal heat source and is equal to zero.

$$K(x) = \begin{cases} k_{steel} = 0.12 \frac{cal - cm}{sec - cm^2 \text{ } ^\circ C} & 0 < x < 40 \\ k_{copper} = 0.92 \frac{cal - cm}{sec - cm^2 \text{ } ^\circ C} & 40 < x < 60 \\ k_{steel} = 0.12 \frac{cal - cm}{sec - cm^2 \text{ } ^\circ C} & 60 < x < 100 \end{cases}$$

and

$$\frac{hl}{A} = 1.5 \times 10^{-4} \frac{cal}{sec - cm^3 \text{ } ^\circ C} \quad \text{and} \quad \frac{hlT_{\infty}}{A} = 3 \times 10^{-3} \frac{cal}{sec - cm^3}$$

GEM Solution

Since one of the boundary conditions is given in terms of flux, i.e.

$$q(0) = 0.1 \text{ cal} \cdot \text{s}^{-1} \cdot \text{cm}^{-2},$$

the GEM formulation will be developed to include the flux term. This formulation will be referred to as the GEM -Flux Formulation.

Consider the situation where the diffusivity (K) varies with distance (x). Mathematically this could be represented by :

$$\frac{d}{dx}(K(x))\frac{d\phi}{dx} \pm f(x) = 0$$

i.e.

$$\frac{dK(x)}{dx} \cdot \frac{d\phi}{dx} + K(x) \cdot \frac{d^2\phi}{dx^2} \pm F(x) = 0$$

therefore

$$\Rightarrow \frac{d^2\phi}{dx^2} = \pm \frac{f(x)}{K(x)} - \frac{dK(x)}{dx} \cdot \frac{d\phi}{dx} \cdot \frac{1}{K(x)}$$

Application of the Green Element Method to the above problem:

As before, the GEM formulation converts a differential equation (that is at least twice differentiable) into an integral form using Greens Second Identity. The application of GEM to solve the above differential equation requires the following steps :

- ▶ Integral representation of the governing differential equation
- ▶ Discretisation of the resulting integral equation over the problem domain
- ▶ A finite element type solution to determine the field variables

We start by converting the governing differential equation into its integral form, using Greens 2nd Identity, which is formally represented as:

$$\int_{x_1}^{x_2} \left[\phi \frac{d^2G}{dx^2} - G \frac{d^2\phi}{dx^2} \right] dx = \phi \frac{dG}{dx} \Big|_{x_1}^{x_2} - G \frac{d\phi}{dx} \Big|_{x_1}^{x_2}$$

rearranging

$$- \int_{x_1}^{x_2} \phi \frac{d^2G}{dx^2} dx + \int_{x_1}^{x_2} G \frac{d^2\phi}{dx^2} dx + \phi \frac{dG}{dx} \Big|_{x_1}^{x_2} - G \frac{d\phi}{dx} \Big|_{x_1}^{x_2} = 0$$

As before,

$$-\int_{x_1}^{x_2} \phi \frac{dG}{dx^2} dx = -\int_{x_1}^{x_2} \phi \delta(x - x_i) dx = -\lambda \phi_i$$

where

$$\lambda = 1 \quad x_i \in [x_o, x_L]$$

$$\lambda = 0.5 \quad x_i = x_0 \quad \text{or} \quad x_i = x_L$$

NOTE : This is where the flux term is introduced

$$\begin{aligned} -G \frac{d\phi}{dx} \Big|_{x_1}^{x_2} &= \left[(G) \cdot \frac{-K(x)}{K(x)} \cdot \frac{d\phi}{dx} \right]_{x_1}^{x_2} = \left[\frac{G}{K(x)} \cdot q \right]_{x_1}^{x_2} \\ &= \frac{1}{2} (|x_2 - x_i| + k) \left(\frac{q}{K(x)} \right)_2 - \frac{1}{2} (|x_1 - x_i| + k) \left(\frac{q}{K(x)} \right)_1 \end{aligned}$$

and

$$\begin{aligned} \int_{x_1}^{x_2} G \frac{d^2\phi}{dx^2} &= \int_{x_1}^{x_2} G \left(\pm \frac{f(x)}{K(x)} - \frac{1}{K(x)} \cdot \frac{dK(x)}{dx} \cdot \frac{d\phi}{dx} \right) dx \\ &= \int_{x_1}^{x_2} G \frac{f(x)}{K(x)} dx - \int_{x_1}^{x_2} \left(\frac{G}{K(x)} \cdot \frac{dK(x)}{dx} \cdot \frac{d\phi}{dx} \right) dx \\ &= \int_{x_1}^{x_2} \frac{G}{K(x)} \left[\frac{h\phi(x)}{A} - \frac{hT_x}{A} \right] dx - \int_{x_1}^{x_2} \left(\frac{G}{K(x)} \cdot \frac{dK(x)}{dx} \cdot \frac{d\phi}{dx} \right) dx \end{aligned}$$

The resulting equations from the above equation will depend on the type variation the Diffusivity (K), and temperature (ϕ) has within the domain (x). In this regard, the following types of variations are considered in this problem :

- ▶ for the temperature, we elect to use the linear interpolation function of :

$$\phi(x) = \Omega_j \phi_j = \Omega_1^e \phi_1^e + \Omega_2^e \phi_2^e$$

- ▶ for the diffusivity , we elect to use

$$\tilde{K}^e = \frac{K_1^e + K_2^e}{2}$$

This implies that K is constant within an element.

$$\Rightarrow \frac{dK(x)}{dx} = 0$$

$$\Rightarrow \int_{x_1}^{x_2} \left(\frac{G}{K(x)} \cdot \frac{dK(x)}{dx} \cdot \frac{d\phi}{dx} \right) dx = 0$$

$$\int_{x_2}^{x_2} G \frac{d^2\phi}{dx^2} dx = \frac{1}{\tilde{K}_e} \int_{x_1}^{x_2} G \cdot \left[\frac{hl\phi(x)}{A} - \frac{hlT_\infty}{A} \right] dx$$

$$= \frac{1}{\tilde{K}_e} \int_{x_1}^{x_2} (|x - x_i| + k) \left(\frac{hl}{A} \right) \Omega_j \phi_j dx - \frac{1}{\tilde{K}_e} \int_{x_1}^{x_2} (|x - x_i| + k) \left(\frac{hlT_\infty}{A} \right) dx$$

$$= T_{ij} (B^e) \phi_j - \frac{F_j^e}{\tilde{K}_e}$$

where $B^e = \frac{hl}{A\tilde{K}_e}$

and

$$-G \frac{d\phi}{dx} \Big|_{x_1}^{x_2} = \frac{1}{2} (|x_2 - x_i| + k) \left(\frac{q}{\tilde{K}_e} \right)_2 - \frac{1}{2} (|x_1 - x_i| + k) \left(\frac{q}{\tilde{K}_e} \right)_1$$

at node 1

$$-G \frac{d\phi}{dx} \Big|_{x_1}^{x_2} = \frac{1}{2} \left[(2l) \left(\frac{q}{\tilde{K}_e} \right)_2 - l \left(\frac{q}{\tilde{K}_e} \right)_1 \right]$$

at node 2

$$-G \frac{d\phi}{dx} \Big|_{x_1}^{x_2} = \frac{1}{2} \left[(l) \left(\frac{q}{\tilde{K}_e} \right)_2 - 2l \left(\frac{q}{\tilde{K}_e} \right)_1 \right]$$

Therefore, the resulting GEM-Flux formulation for this application is

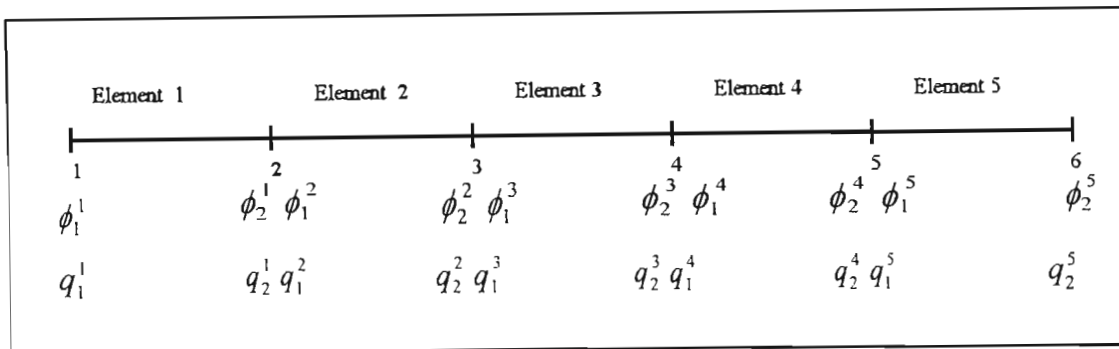
$$\left(R_{ij} + BT_{ij} \right) \phi_j + \frac{L_{ij}}{\tilde{K}_e} \cdot q_j - \frac{1}{\tilde{K}_e} F_i = 0$$

where

$$L_{ij} = \begin{bmatrix} -l & 2l \\ -2l & l \end{bmatrix} \quad R_{ij} = \begin{bmatrix} -1 & 1 \\ 1 & -1 \end{bmatrix}$$

$$T_{ij} = l \int_0^1 \Omega_j G(\zeta, \zeta_1) d\zeta = \frac{l}{6} \begin{bmatrix} 3\tilde{l} + l & 3\tilde{l} + 2l \\ 3\tilde{l} + 2l & 3\tilde{l} + 2l \end{bmatrix}$$

Discretising the problem domain into five equal elements, we have:



Since **continuity exists between the adjacent elements**, this implies

$$\begin{aligned} \phi_1^1 &= \phi_1 & q_1^1 &= q_1 \\ \phi_2^1 &= \phi_1^2 = \phi_2 & q_2^1 &= q_1^2 = q_2 \\ \phi_2^2 &= \phi_1^3 = \phi_3 & q_2^2 &= q_1^3 = q_3 \\ \phi_2^3 &= \phi_1^4 = \phi_4 & q_2^3 &= q_1^4 = q_4 \\ \phi_2^4 &= \phi_1^5 = \phi_5 & q_2^4 &= q_1^5 = q_5 \\ \phi_2^5 &= \phi_6 & q_2^5 &= q_6 \end{aligned}$$

Note : If a domain is discretised into M elements, then the number of nodes = M+1.

Since there are 2 equations per element, the number of equations will be 2 M.

Taking continuity between adjacent elements into account, the resulting number of unknowns will be 2 X (M+1). This implies that at least two of the “unknowns”

need to supplied as boundary conditions.

For the diffusivity interpolation chosen for this problem, we have

$$\frac{\tilde{K}^1}{K} = \frac{K_1^1 + K_2^1}{2} = 0.12$$

$$\frac{\tilde{K}^2}{K} = \frac{K_1^2 + K_2^2}{2} = 0.12$$

$$\frac{\tilde{K}^3}{K} = \frac{K_1^3 + K_2^3}{2} = 0.92$$

$$\frac{\tilde{K}^4}{K} = \frac{K_1^4 + K_2^4}{2} = 0.12$$

$$\frac{\tilde{K}^5}{K} = \frac{K_1^5 + K_2^5}{2} = 0.12$$

Since the recharge is a constant, this implies

$$F_1^e = F_2^e = a_0 l^e \left(\tilde{l} + \frac{l^e}{2} \right) = (3 \times 10^{-3}) 20 \left(20 + \frac{20}{2} \right) = 1.8$$

Therefore

$$\frac{F_1^1}{\tilde{K}^1} = \frac{F_2^1}{\tilde{K}^1} = \frac{F_1^2}{\tilde{K}^2} = \frac{F_2^2}{\tilde{K}^2} = \frac{F_1^4}{\tilde{K}^4} = \frac{F_2^4}{\tilde{K}^4} = \frac{F_1^5}{\tilde{K}^5} = \frac{F_2^5}{\tilde{K}^5} = \frac{1.8}{0.12} = 15$$

$$\frac{F_1^3}{\tilde{K}^3} = \frac{F_2^3}{\tilde{K}^3} = \frac{1.8}{0.92} = 1.957$$

Therefore,

$$L_{ij} = \begin{bmatrix} -20 & 40 \\ -40 & 20 \end{bmatrix}$$

$$R_{ij} = \begin{bmatrix} -1 & 1 \\ 1 & -1 \end{bmatrix}$$

$$T_{ij} = \frac{20}{6} \begin{bmatrix} 80 & 100 \\ 100 & 100 \end{bmatrix}$$

A step by step procedure showing how the element equations and the global matrix are assembled, is now given. Restating the GEM-Flux formulation for this application in matrix notation, we have

$$\left(R_{ij} + BT_{ij}\right)\phi_j + \frac{L_{ij}}{\tilde{K}_e} \cdot q_j - \frac{1}{\tilde{K}_e} F_i = 0$$

Therefore the equations for a typical element N will be as follows :

at node 1

$$\left(R_{11} + BT_{11}\right)\phi_n + \frac{L_{11}}{\tilde{K}_n} \cdot q_n + \left(R_{12} + BT_{12}\right)\phi_{n+1} + \frac{L_{12}}{\tilde{K}_n} \cdot q_{n+1} = \frac{1}{\tilde{K}_n} F_1^n$$

at node 2

$$\left(R_{21} + BT_{21}\right)\phi_n + \frac{L_{21}}{\tilde{K}_n} \cdot q_n + \left(R_{22} + BT_{22}\right)\phi_{n+1} + \frac{L_{22}}{\tilde{K}_n} \cdot q_{n+1} = \frac{1}{\tilde{K}_n} F_2^n$$

The resulting system of equations for the whole problem domain will be:

Element 1

node 1

$$\begin{aligned} \left(R_{11} + BT_{11}\right)\phi_1 + \left(R_{12} + BT_{12}\right)\phi_2 + \frac{L_{12}}{\tilde{K}_1} \cdot q_2 &= \frac{1}{\tilde{K}_1} F_1^1 - \frac{L_{11}}{\tilde{K}_1} \cdot q_1 \\ - 0.667\phi_1 + 1.417\phi_2 + 333.33q_2 &= 166.67 \times 0.1 + 15 \end{aligned}$$

node 2

$$\begin{aligned} \left(R_{21} + BT_{21}\right)\phi_1 + \left(R_{22} + BT_{22}\right)\phi_2 + \frac{L_{22}}{\tilde{K}_1} \cdot q_2 &= \frac{1}{\tilde{K}_1} F_2^1 - \frac{L_{21}}{\tilde{K}_1} \cdot q_1 \\ 1.417\phi_1 - 0.667\phi_2 + 166.67q_2 &= 333.33 \times 0.1 + 15 \end{aligned}$$

Note: the entry of the known boundary conditions into the right hand side i.e all known quantities will be transferred onto the right hand side

Element 2**node 1**

$$\begin{aligned} (R_{11} + BT_{11})\phi_2 + \frac{L_{11}}{\tilde{K}_2} \cdot q_2 + (R_{12} + BT_{12})\phi_3 + \frac{L_{12}}{\tilde{K}_2} \cdot q_3 &= \frac{1}{\tilde{K}_2} F_1^2 \\ -0.667\phi_2 - 166.67q_2 + 1.417\phi_3 + 333.33q_3 &= 15 \end{aligned}$$

node 2

$$\begin{aligned} (R_{21} + BT_{21})\phi_2 + \frac{L_{21}}{\tilde{K}_2} \cdot q_2 + (R_{22} + BT_{22})\phi_3 + \frac{L_{22}}{\tilde{K}_2} \cdot q_3 &= \frac{1}{\tilde{K}_2} F_2^2 \\ 1.417\phi_2 - 333.33q_2 - 0.667\phi_3 + 166.67q_3 &= 15 \end{aligned}$$

Element 3**node 1**

$$\begin{aligned} (R_{11} + BT_{11})\phi_3 + \frac{L_{11}}{\tilde{K}_3} \cdot q_3 + (R_{12} + BT_{12})\phi_4 + \frac{L_{12}}{\tilde{K}_3} \cdot q_4 &= \frac{1}{\tilde{K}_3} F_1^3 \\ -0.957\phi_3 - 21.74q_3 + 1.05\phi_4 + 43.478q_4 &= 1.957 \end{aligned}$$

node 2

$$\begin{aligned} (R_{21} + BT_{21})\phi_3 + \frac{L_{21}}{\tilde{K}_3} \cdot q_3 + (R_{22} + BT_{22})\phi_4 + \frac{L_{22}}{\tilde{K}_3} \cdot q_4 &= \frac{1}{\tilde{K}_3} F_2^3 \\ 1.05\phi_3 - 43.478q_3 - 0.957\phi_4 + 21.74q_4 &= 1.957 \end{aligned}$$

Element 4**node 1**

$$\begin{aligned} (R_{11} + BT_{11})\phi_4 + \frac{L_{11}}{\tilde{K}_4} \cdot q_4 + (R_{12} + BT_{12})\phi_5 + \frac{L_{12}}{\tilde{K}_4} \cdot q_5 &= \frac{1}{\tilde{K}_4} F_1^4 \\ -0.667\phi_4 - 166.67q_4 + 1.417\phi_5 + 333.33q_5 &= 15 \end{aligned}$$

node 2

$$\begin{aligned} (R_{21} + BT_{21})\phi_4 + \frac{L_{21}}{\tilde{K}_4} \cdot q_4 + (R_{22} + BT_{22})\phi_5 + \frac{L_{22}}{\tilde{K}_4} \cdot q_5 &= \frac{1}{\tilde{K}_4} F_2^4 \\ 1.417\phi_4 - 333.33q_4 - 0.667\phi_5 + 166.67q_5 &= 15 \end{aligned}$$

Element 5

node 1

$$\begin{aligned} (R_{11} + BT_{11})\phi_5 + \frac{L_{11}}{\widetilde{K}_5} \cdot q_5 + \frac{L_{12}}{\widetilde{K}_5} \cdot q_6 &= \frac{1}{\widetilde{K}_5} F_1^5 - (R_{12} + BT_{12})\phi_6 \\ -0.667\phi_5 - 166.67q_5 + 333.33q_6 &= 15 + 0 \end{aligned}$$

node 2

$$\begin{aligned} (R_{21} + BT_{21})\phi_5 + \frac{L_{21}}{\widetilde{K}_5} \cdot q_5 + \frac{L_{22}}{\widetilde{K}_5} \cdot q_6 &= \frac{1}{\widetilde{K}_5} F_2^5 - (R_{22} + BT_{22})\phi_6 \\ 1.417\phi_5 - 333.33q_5 + 166.67q_6 &= 15 + 0 \end{aligned}$$

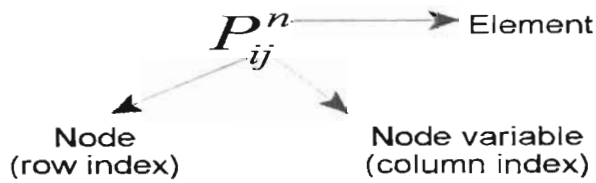
Note : known values are transferred onto the right hand side of the equality.

Here we demonstrate how the global matrix is assembled

Let

$$\begin{aligned} (R_{11} + T_{11}B)^n &= P_{11}^n & (R_{12} + T_{12}B)^n &= P_{12}^n \\ (R_{21} + T_{21}B)^n &= P_{21}^n & (R_{22} + T_{22}B)^n &= P_{22}^n \end{aligned}$$

where the following notation will apply



Applying this notation to the current problem, where q_1 and ϕ_6 are given as the boundary conditions, we will show how the global matrix is constructed. Following standard matrix notation implies :

- ▶ all the coefficients of the unknown variables are entered into the coefficient matrix

- ▶ the unknown variables form the vector matrix
- ▶ all the known quantities including the boundary conditions are entered into the right hand side matrix

Coefficient Matrix										Vector of Unknowns	Vector of Known Quantities
↓										↓	↓
P_{11}^1	P_{12}^1	$\frac{L_{12}^1}{\tilde{K}_1}$	0	0	0	0	0	0	0	$\begin{bmatrix} \phi_1 \\ \phi_2 \\ q_2 \\ \phi_3 \\ q_3 \\ \phi_4 \\ q_4 \\ \phi_5 \\ q_5 \\ q_6 \end{bmatrix}$	$\frac{F_1^1}{\tilde{K}_1} - \frac{L_{11}^1}{\tilde{K}_1} q_1$
P_{21}^1	P_{22}^1	$\frac{L_{22}^1}{\tilde{K}_1}$	0	0	0	0	0	0	0		$\frac{F_2^1}{\tilde{K}_1} - \frac{L_{21}^1}{\tilde{K}_1} q_1$
0	P_{11}^2	$\frac{L_{11}^2}{\tilde{K}_1}$	P_{12}^2	$\frac{L_{12}^2}{\tilde{K}_1}$	0	0	0	0	0		$\frac{F_1^2}{\tilde{K}_2}$
0	P_{21}^2	$\frac{L_{21}^2}{\tilde{K}_2}$	P_{22}^2	$\frac{L_{22}^2}{\tilde{K}_2}$	0	0	0	0	0		$\frac{F_2^2}{\tilde{K}_2}$
0	0	0	P_{11}^3	$\frac{L_{11}^3}{\tilde{K}_3}$	P_{12}^3	$\frac{L_{12}^3}{\tilde{K}_3}$	0	0	0		$\frac{F_1^3}{\tilde{K}_3}$
0	0	0	P_{21}^3	$\frac{L_{21}^3}{\tilde{K}_3}$	P_{22}^3	$\frac{L_{22}^3}{\tilde{K}_3}$	0	0	0		$\frac{F_2^3}{\tilde{K}_3}$
0	0	0	0	0	P_{11}^4	$\frac{L_{11}^4}{\tilde{K}_4}$	P_{12}^4	$\frac{L_{12}^4}{\tilde{K}_4}$	0		$\frac{F_1^4}{\tilde{K}_4}$
0	0	0	0	0	P_{21}^4	$\frac{L_{21}^4}{\tilde{K}_4}$	P_{22}^4	$\frac{L_{22}^4}{\tilde{K}_4}$	0		$\frac{F_2^4}{\tilde{K}_4}$
0	0	0	0	0	0	0	P_{11}^5	$\frac{L_{11}^5}{\tilde{K}_5}$	$\frac{L_{12}^5}{\tilde{K}_5}$		$\frac{F_1^5}{\tilde{K}_5} - P_{12}^5 \phi_6$
0	0	0	0	0	0	0	P_{21}^5	$\frac{L_{21}^5}{\tilde{K}_5}$	$\frac{L_{22}^5}{\tilde{K}_5}$		$\frac{F_2^5}{\tilde{K}_5} - P_{22}^5 \phi_6$

The resulting global matrix is

$$\begin{bmatrix}
 -0.667 & 1.417 & 333.33 & 0 & 0 & 0 & 0 & 0 & 0 & 0 \\
 1.417 & -0.667 & 166.67 & 0 & 0 & 0 & 0 & 0 & 0 & 0 \\
 0 & -0.667 & -166.67 & 1.417 & 333.33 & 0 & 0 & 0 & 0 & 0 \\
 0 & 1.417 & -333.33 & -0.667 & 166.67 & 0 & 0 & 0 & 0 & 0 \\
 0 & 0 & 0 & -0.957 & -21.74 & 1.05 & 43.478 & 0 & 0 & 0 \\
 0 & 0 & 0 & 1.05 & -43.478 & -0.957 & 21.74 & 0 & 0 & 0 \\
 0 & 0 & 0 & 0 & 0 & -0.667 & -166.67 & 1.417 & 333.33 & 0 \\
 0 & 0 & 0 & 0 & 0 & 1.417 & -333.33 & -0.667 & 166.67 & 0 \\
 0 & 0 & 0 & 0 & 0 & 0 & 0 & -0.667 & -166.67 & 333.33 \\
 0 & 0 & 0 & 0 & 0 & 0 & 0 & 1.417 & -333.33 & 166.67
 \end{bmatrix}
 \cdot
 \begin{bmatrix}
 \phi_1 \\
 \phi_2 \\
 q_2 \\
 \phi_3 \\
 q_3 \\
 \phi_4 \\
 q_4 \\
 \phi_{53} \\
 q_5 \\
 q_6
 \end{bmatrix}
 =
 \begin{bmatrix}
 31.67 \\
 48.33 \\
 15.00 \\
 15.00 \\
 1.957 \\
 1.957 \\
 15.00 \\
 15.00 \\
 15.00 \\
 15.00
 \end{bmatrix}$$

Table A.1. Table of GEM Results and FEM results (Burnett,1987)

Node	GEM 5 elements discretization		FEM 5 elements discretization		FEM 44 elements discretization	
	Temperature	Flux	Temperature	Flux	Temperature	Flux
1	40.95	1	40.94	0.074	40.94	0.098
2	28.49	0.056	28.47	0.061	28.47	0.058
3	20.66	0.042	20.61	0.044	20.61	0.042
4	19.75	0.042	19.71	0.044	19.71	0.042
5	12.04	0.054	12.03	0.059	12.03	0.054
6	0	0.096	0	0.072	0	0.092

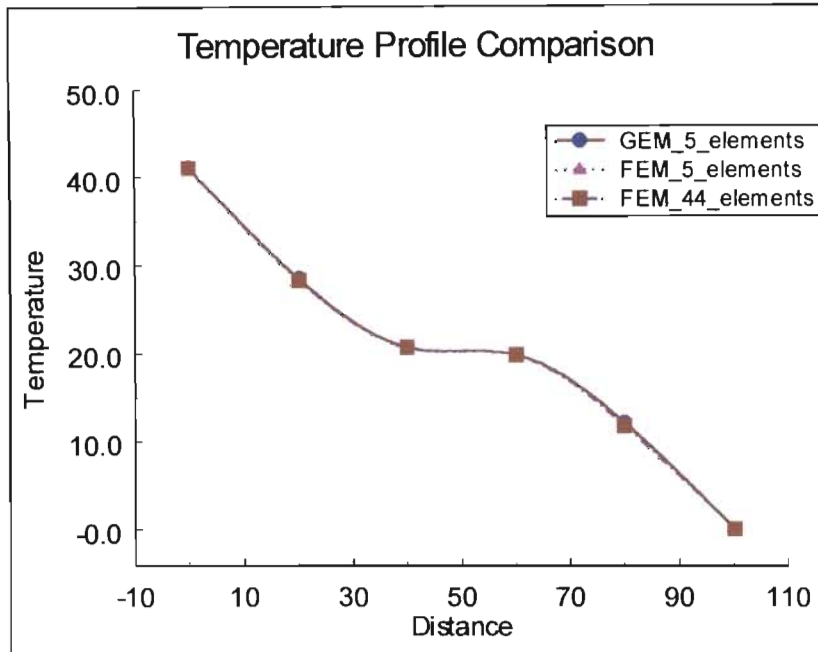


Figure A.1 Temperature Profile Comparison of GEM and FEM Results

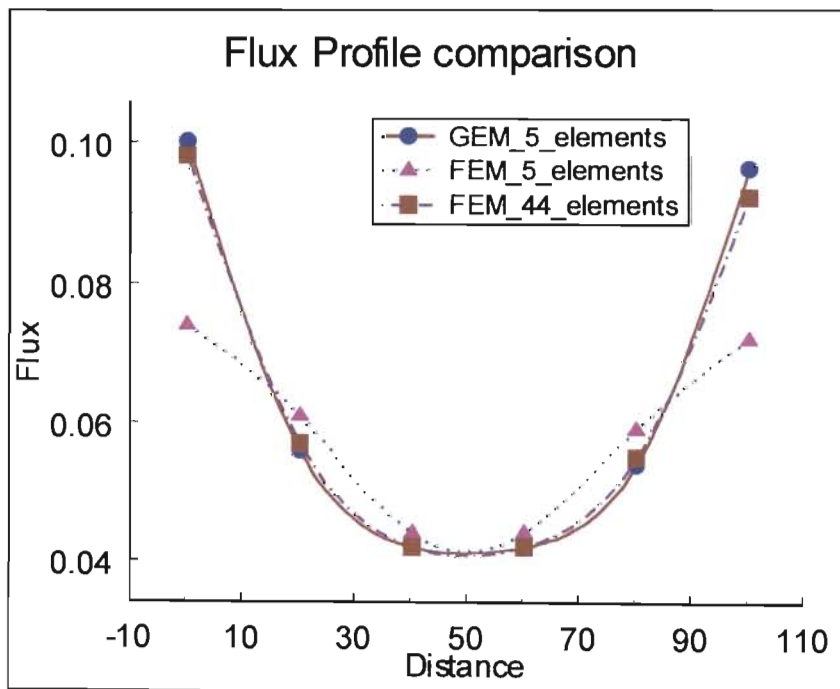


Figure A.2 Flux Profile Comparison of GEM and FEM Results

General Comments :

It can be clearly seen from Figure B.2, some of the advantages offered by the Green element method, in particular :

- ▶ It offers the same accuracy of the computer generated FEM solution compared to the hand calculations of the GEM
- ▶ A simple 5 element discretisation in the GEM formulation offers the same accuracy of a 44 element discretisation in the FEM formulation in the computation of the flux. Note that this is achieved with even the most basic interpolation relationship for the diffusion coefficient term (i.e. average values within the element)
- ▶ The GEM Flux formulation overcomes the problem of discontinuities that is generally experienced with the typical gradient formulation $\frac{d\phi}{dx}$.

Appendix B

Worked Example - Biofilm Mass Transfer

A biofilm is a mixed population of micro-organisms that are part of a stable thin film. Inside the biofilm, organic substrates are decomposed. The substrate must diffuse from the exterior solution into the biofilm. In certain biofilms along solid surfaces, the decomposition of the substrate within the biofilm can be assumed to be zero order when the substrate concentration is very high, i.e.

$$r_a = -k_A^0 \quad \text{where A is the substrate}$$

The differential equation governing the concentration of the substrate within the biofilm is :

$$D_{eff} \frac{d^2 C_A}{dx^2} - k_A^0 = 0$$

for the following boundary conditions of :

$$C_A(0) = C_{A0},$$
$$\frac{dC_A}{dx}(L) = 0$$

the analytical solution is given by :

$$C_A = \frac{k_A^0}{D_{eff}} \left[\frac{x^2}{L} - Lx \right] + C_{A0}$$

$$\frac{dC_A}{dx} = \frac{k_A^0}{D_{eff}} \left[\frac{x}{L} - 1 \right]$$

GEM Solution:

The GEM formulation converts a differential equation (that is at least twice differentiable) into an integral form using Greens 2nd Identity. The application of GEM to solve the above differential equation requires the following steps :

- Integral representation of the governing differential equation
- Discretisation of the resulting integral equation over the problem domain
- A finite element type solution to determine the field variables.

We start by converting the governing differential equation into its integral form, using Green's second identity , which is formally represented as:

$$\int_{x_0}^{x_i} \left[\phi \frac{d^2 G}{dx^2} - G \frac{d^2 \phi}{dx^2} \right] dx = \phi \frac{dG}{dx} \Big|_{x_0}^{x_i} - G \frac{d\phi}{dx} \Big|_{x_0}^{x_i}$$

where $\frac{d^2 G}{dx^2}$ is the complementary differential equation, and is given by

$$\frac{d^2 G}{dx^2} = \delta(x - x_i), \text{ and which has a fundamental solution of}$$

$$G = \frac{1}{2} (|x - x_i| + k), \text{ and its first derivative with respect to } x \text{ is :}$$

$$\frac{dG}{dx} = \frac{1}{2} [H(x - x_i) - H(x_i - x)], \text{ where, } H \text{ is the Heaviside function, and has the}$$

following properties :

$$H(x - x_i) = \begin{cases} 1 & x \succ x_i \\ 0 & x \prec x_i \end{cases}$$

Therefore Green's second function becomes

$$\int_{x_0}^{x_i} \phi \delta(x - x_i) dx - \int_{x_0}^{x_i} \frac{1}{2} (|x - x_i| + k) \frac{k_A^0}{D_{eff}} dx$$

$$= \frac{\phi}{2} [H(x - x_i) - H(x_i - x)]_{x_0}^{x_i} - \frac{1}{2} \left[(|x - x_i| + k) \frac{d\phi}{dx} \right]_{x_0}^{x_i}$$

where, by the properties of the Dirac-Delta function, we have

$$\int_{x_0}^x \phi \delta(x - x_i) dx = \phi(x_i)$$

also, let $\frac{d\phi}{dx} \Big|_{x_0} = \varphi_0$, and, $\frac{d\phi}{dx} \Big|_{x_i} = \varphi_L$, therefore we have

$$-2\lambda\phi_i + [H(x_L - x_i) - H(x_i - x_L)]\varphi_L - [[H(x_0 - x_i) - H(x_i - x_0)]\varphi_0] - (|x_L - x_i| + k)\varphi_L$$

$$+ (|x_0 - x_i| + k)\varphi_0 + \frac{k_A^0}{D_{eff}} \int_{x_0}^{x_L} (|x - x_i| + k) dx = 0$$

Discretising the domain into M elements , we have,

$$\sum_{e=1}^M \left[-2\lambda\phi_i^e + [H(x_L^e - x_i^e) - H(x_i^e - x_L^e)]\varphi_L^e - [H(x_0^e - x_i^e) - H(x_i^e - x_0^e)]\varphi_0^e \right]$$

$$\left[-(|x_L^e - x_i^e| + k^e)\varphi_L^e + (|x_0^e - x_i^e| + k^e)\varphi_0^e + \frac{k_A^0}{D_{eff}} \int_{x_0}^{x_L} (|x^e - x_i^e| + k^e) dx \right] = 0$$

For equally discretised elements of length l (i.e $k = l$), a node by node analysis will result in the following :

at node 1, where $x_i = x_1$, we have

$$\sum_{e=1}^M \left[-\phi_1^e + \phi_2^e - 2l^e\varphi_2^e + l^e\varphi_1^e + \frac{k_A^0}{D_{eff}} \int_{x_1}^{x_2} (|x^e - x_1^e| + k^e) dx \right] = 0$$

at node 2, where $x_i = x_2$, we have

$$\sum_{e=1}^M \left[-\phi_2^e + \phi_1^e - l^e \phi_2^e + 2l^e \phi_1^e + \frac{k_A^0}{D_{eff}} \int_{x_1}^{x_2} (|x^e - x_2^e| + k^e) dx \right] = 0$$

In matrix notation, the above equations can be represented as

$$\sum_{e=1}^M R_{ij} \phi_j + L_{ij} \phi_j + F_i = 0$$

where

$$R_{ij} = \begin{bmatrix} -1 & 1 \\ 1 & -1 \end{bmatrix} \quad \text{and} \quad L_{ij} = \begin{bmatrix} l & -2l \\ 2l & -l \end{bmatrix}$$

For constant source / sink, we have that,

$$F_1^e = a_0 l^e \left(\tilde{l} + \frac{l^e}{2} \right)$$

$$F_2^e = a_0 l^e \left(\tilde{l} + \frac{l^e}{2} \right)$$

$$\text{where, } a_0 = \frac{k_A^0}{D_{eff}}$$

Discretising the problem domain into 4 equal elements, we have $l^e = \tilde{l} = k = 0.25L$

Applying the following conditions to the example:

$$\frac{k_A^0}{D_{eff}} = 0.1, \quad L = 1, \quad C_{,10} = 1$$

Therefore

$$L_{ij} = \begin{bmatrix} 0.25 & -0.50 \\ 0.50 & -0.25 \end{bmatrix}$$

$$F_1^e = F_2^e = 0.0094$$

The resulting global matrix is

$$\begin{bmatrix} 0.25 & 1 & -0.50 & 0 & 0 & 0 & 0 & 0 \\ 0.50 & -1 & -0.25 & 0 & 0 & 0 & 0 & 0 \\ 0 & -1 & 0.25 & 1 & -0.50 & 0 & 0 & 0 \\ 0 & 1 & 0.50 & -1 & -0.25 & 0 & 0 & 0 \\ 0 & 0 & 0 & -1 & 0.25 & 1 & -0.50 & 0 \\ 0 & 0 & 0 & 1 & 0.50 & -1 & -0.25 & 0 \\ 0 & 0 & 0 & 0 & 0 & -1 & 0.25 & 1 \\ 0 & 0 & 0 & 0 & 0 & 1 & 0.50 & -1 \end{bmatrix} \cdot \begin{bmatrix} \phi_1 \\ \phi_2 \\ \phi_2 \\ \phi_3 \\ \phi_3 \\ \phi_4 \\ \phi_4 \\ \phi_5 \end{bmatrix} = \begin{bmatrix} 0.0094 \\ -1.0094 \\ -0.0094 \\ -0.0094 \\ -0.0094 \\ -0.0094 \\ -0.0094 \\ -0.0094 \end{bmatrix}$$

A matrix solver is used to find a solution to the above matrix.

Table B.1 Comparison of Results of GEM Solution and Analytical Solution

Domain Size	Analytical Solution		GEM Solution	
L	Primary Variable ϕ	Flux φ	Primary Variable ϕ	Flux φ
0.00	1.00	-0.100	1.00	-0.100
0.25	0.978	-0.075	0.978	-0.075
0.50	0.962	-0.050	0.962	-0.050
0.75	0.953	-0.025	0.953	-0.025
1.00	0.950	0.00	0.950	0.00

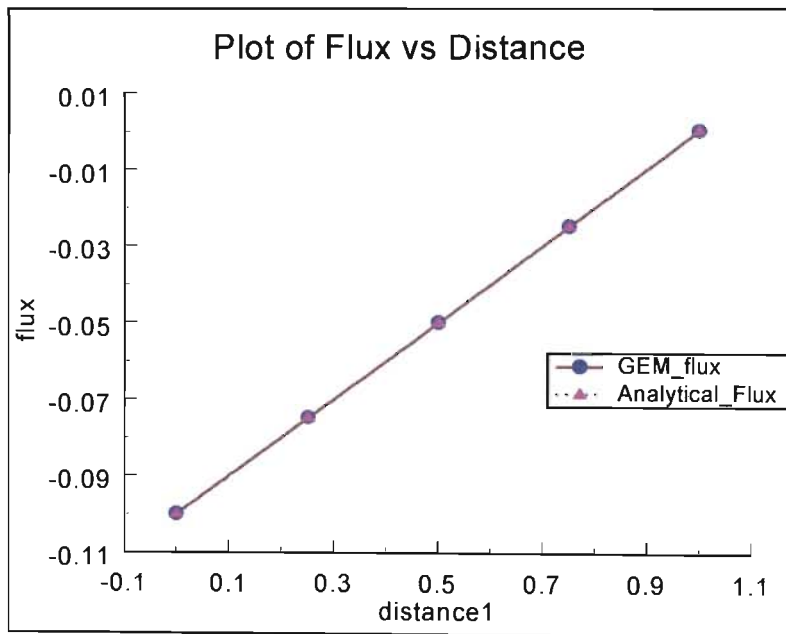
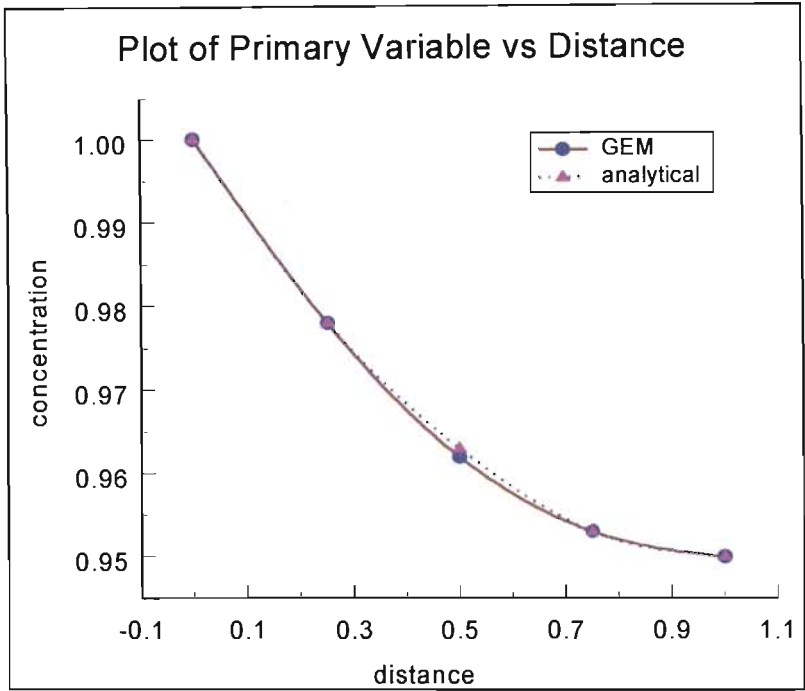


Figure B.1 Graphical Comparison of GEM and Analytical Solutions

Appendix C

Programme Details

In this work, three computer programmes were developed to simulate the three GEM formulated models for bacteria transport through porous media. Herein a brief description of the three programmes, and sample input and output files are provided. These programmes, coded in Fortran, were developed from a core programme developed by Onyejekwe (2000). All three programmes and the relevant input data files are provided in the attached diskette.

Programme 1: BactCP

This programme simulated the constant porosity bacteria transport model which was developed to test the accuracy of the GEM formulation against analytical solutions. This model described by equation 5.12, assumed that the porosity of the porous media (aquifer) remained unchanged throughout the spatial and temporal domains. In this programme two coupled equations are solved simultaneously:

- ▶ the governing transport model (linear PDE) described by equation 5.12, and
- ▶ the adsorbed species continuity equation (initial value ODE) described by equation 5.7.

The computational algorithm and programme flowsheet are given in Figure 5.3 and Figure 5.5 respectively. The results obtained from this programme are shown graphically as the GEM solutions in Figures 6.1 and 6.2.

Programme 2: BactVaripor

This programme simulated the variable porosity bacteria transport model. This model described by equation 5.13, accounted for the changes in porosity of the porous media (aquifer) and the subsequent changes to the flow velocity throughout the spatial and temporal domains. In this programme a set of coupled equations are solved simultaneously:

- ▶ the governing transport model (linear PDE) described by equation 5.13,
- ▶ the adsorbed species continuity equation (initial value ODE) described by equation 5.7,
- ▶ equation 5.9, which calculates changes to the porosity due to bacteria growth and the clogging process,
- ▶ equation 5.11, which calculates the change to flow velocity due to porosity changes.

The computational algorithm and programme flowsheet are given in Figure 5.3 and Figure 5.5 respectively. Sample input data files and resulting output files shown in Figures C.1 and C.2 respectively.

Programme 3: BactNLclog

This programme simulated the nonlinear clogging bacteria transport model. This model described by equation 5.16, is based on the assumption that the clogging process is described by a nonlinear clogging term. In addition, this model also accounts for the changes in porosity of the porous media (aquifer) and the subsequent changes to the flow velocity throughout the spatial and temporal domains. In this programme a set of coupled equations are solved simultaneously:

- ▶ the governing transport model (nonlinear PDE) described by equation 5.16,
- ▶ the adsorbed species continuity equation (initial value ODE) described by equation 5.14,
- ▶ equation 5.9, which calculates changes to the porosity due to bacteria growth and the clogging process,
- ▶ equation 5.11, which calculates the change to flow velocity due to porosity changes.

The governing transport equation is a nonlinear partial differential equation . This requires an iterative numerical and computational procedures to facilitate a solution. This was successfully done using the Newton Raphson Algorithm. The computational algorithm and programme flowsheet are given in Figure 5.4 and Figure 5.6 respectively. The results obtained from this programme are shown graphically in Figure 7.12 and Figure 7.13.

List of Typical Input Requirements for Bacteria Transport Programmes

1.	READ (5, '(A)') TITLE		
2.	READ (ICR, *) KEY1, KEY2, KEY3		
3.	READ(5, *)	DIFFS	= substrate diffusivity
4.	READ(5, *)	DIFFB	= bacteria diffusivity
5.	READ(5, *)	velx	= velocity
6.	READ(5, *)	xmgr	= maximum growth rate constant
7.	READ(5, *)	xpore	= porosity of medium
8.	READ(5, *)	chmgr	= K_s = conc. At which growth rate is half the maximum
9.	READ(5, *)	tcy	= true cell yield
10.	READ(5, *)	bdr	= bacteria decay rate
11.	READ(5, *)	clog	= clogging rate
12.	READ(5, *)	sden	= soil density
13.	READ(5, *)	bden	= bacteria density
14.	READ(5, *)	xka	= adsorption coefficient
15.	READ(5, *)	cs	= substrate concentration
16.	READ(5, *)	xky	= declogging rate
17.	READ(5, *)	xn	= clogging reaction order
18.	READ(5, *)	RMS	= Convergence tolerance ,
		NSTOP	= Maximum number of iterations allowed
19.	READ(5, *)	INAT	= 1 if it is a time-dependent problem; = 0 if it is steady state
	IF(INAT .EQ. 1) THEN		
20.	READ(ICR, *)	NSUB	= Number of divisions of the time dimension ,
		TIME	= Initial time ,
		ICOND	= 1 if the boundary data change with time; = 0 if boundary data are steady
21.	READ(ICR, *)	NWRITE(I)	= the number of time steps to skip before solution is printed,
		TDIV(I)	= is the time step of each time subdivision,
		TLEVEL(I)	= is the time limit of each time subdivision,
22.	READ(5, *)	ISCHEME	= 2 for the 2-level time scheme; = 3 for the 3-level time scheme
23.	READ(5, *)	THETA	= Finite difference time weighing factor; it takes any value between 0.0 and 1.0 for the 2-level scheme and between 1.0 and 2.0 for the 3-level scheme.
24.	READ(5, *)	NSEG	= Number of segments into which the 1-D spatial dimension is divided
25.	READ (5, *)	X(1), NSP(1)	
26.	READ (5, *)	X(IEND), NSP(M)	

*X is the x-coordinate of the node of the segment
NSP = Number of additional nodes generated excluding the end nodes*

27)	READ(5,*) NTYP(1),TMP		<i>for first node for first equation</i>
28)	READ(5,*) NTYP(2),TMP		<i>for last node for first equation</i>
		NTYP =	<i>1 if the external node is a flux type, or 2 if it is a Dirichlet type</i>
		TMP =	<i>is the value of the boundary data at the external node</i>
29)	READ(5,*) NFINIT	=	<i>1 if the data at initial time at the nodes are read from the data file; = 0 if the data at initial time are uniform or given by a functional relationship.</i>
	IF(NFINIT .EQ. 0) THEN		
30)	READ(5,*) POT	ELSE	READ(5,*) (CHI0(I),I=1,NGLOBE)
31)	READ(5,*) NNODES	=	<i>No. of external of nodes at which initial flux values should be specified</i>
	IF(NNODES .GE. 1) THEN		
32)	READ(5,*) J,U		<i>Specify node number, and initial flux value the where J = Node number; U = flux Value</i>
33)	READ(5,*) nrech		
	IF(NRECH .EQ. 0) THEN		
	READ(5,*) RAIN		
	READ(5,*) npoint		
	IF(NPOINT .GE. 1) THEN		
34)	READ(5,*) K,V		<i>then identify the strength and position of the point sources where K is the location and V is the magnitude of the point source</i>

```

1-D. Bacteria Transport - variable porosity
0 0 0 Key1, Key2, key3
2.e-2 DIFFS
2.e-2 DIFFB
1.0 VELX
15.e-2 XMGR
0.6 XPORE
2 XKS
0.04 TCY
36.e-3 BDR
23.4 CLOG
1740 SDEN
1000 BDEN
1 XKA
1.e-2 CS
1.566 XKY
1.e-6 4 convergence tolerance number of iterations
1 Inat
1 0 0 Nsub initialtime ICOND
1 0.5 24 nwrite tdiv tlevel
2 ISCHEME
0.67 theta
1 Nseg
0.0 39 XminAddnode
4 0 length nodes generated
2 1.e-1 bc(1), node1 ntyp(1)= 1 or 2(flux/dirichlet)
2 0.000 bc(2), node2 ntyp(2)=1 or 2(flux/dirichlet)
0 nfinite
0.0 pot
0 nnodes
1 nrech
1 number of point sources
2 1.e-1

```

Figure C.1 Sample Input Data File for BactVaripor

1-D. Coupled Bacteria Transport problem- Variable porosity

substrate diffusivity = 2.000000E-02
 bacteria diffusivity = 2.000000E-02
 velocity = 1.000000
 max.growth rate contant = 1.500000E-01
 porosity = 6.000000E-01
 Xks = 2.000000
 true cell yield = 4.000000E-02
 bacteria decay rate = 3.600000E-02
 clogging rate = 23.400000
 soil density = 1740.000000
 bacteria density = 1000.000000
 adsorption coefficient = 1.000000
 substrate concentration = 1.000000E-02
 declogging rate = 1.566000
 NUMBER OF NODES = 41

..... NATURE OF BOUNDARY CONDS. (STEADY=0; UNSTEADY=1) = 0
 INITIAL TIME = .0000; TIME LIMIT = 24.0000

..... TIME= 24.0000

Node No.	Location	Primary Variable	Flux	Porosity
1	.000	.1000E+00	-.5453E-01	.5991E+00
2	.100	.9469E-01	-.5163E-01	.5992E+00
3	.200	.8967E-01	-.4889E-01	.5992E+00
4	.300	.8491E-01	-.4630E-01	.5993E+00
5	.400	.8040E-01	-.4386E-01	.5993E+00
6	.500	.7613E-01	-.4163E-01	.5993E+00
7	.600	.7207E-01	-.3975E-01	.5994E+00
8	.700	.6816E-01	-.3857E-01	.5994E+00
9	.800	.6431E-01	-.3855E-01	.5994E+00
10	.900	.6039E-01	-.4021E-01	.5995E+00
11	1.000	.5621E-01	-.4371E-01	.5995E+00
12	1.100	.5160E-01	-.4882E-01	.5996E+00
13	1.200	.4643E-01	-.5436E-01	.5996E+00
14	1.300	.4074E-01	-.5936E-01	.5997E+00

Figure C.2 Sample Output File for BactVaripor

15	1.400	.3466E-01	-.6142E-01	.5997E+00
16	1.500	.2851E-01	-.6194E-01	.5998E+00
17	1.600	.2251E-01	-.5528E-01	.5998E+00
18	1.700	.1724E-01	-.5490E-01	.5999E+00
19	1.800	.1230E-01	-.3143E-01	.5999E+00
20	1.900	.1109E-01	-.3978E-02	.5999E+00
21	2.000	.1022E-01	-.1514E-01	.5999E+00
22	2.100	.8277E-02	-.1987E-01	.5999E+00
23	2.200	.6594E-02	-.1405E-01	.5999E+00
24	2.300	.5417E-02	-.9729E-02	.6000E+00
25	2.400	.4604E-02	-.6708E-02	.6000E+00
26	2.500	.4041E-02	-.4714E-02	.6000E+00
27	2.600	.3636E-02	-.3482E-02	.6000E+00
28	2.700	.3326E-02	-.2798E-02	.6000E+00
29	2.800	.3064E-02	-.2505E-02	.6000E+00
30	2.900	.2816E-02	-.2484E-02	.6000E+00
31	3.000	.2561E-02	-.2631E-02	.6000E+00
32	3.100	.2288E-02	-.2849E-02	.6000E+00
33	3.200	.1993E-02	-.3026E-02	.6000E+00
34	3.300	.1685E-02	-.3126E-02	.6000E+00
35	3.400	.1375E-02	-.2996E-02	.6000E+00
36	3.500	.1084E-02	-.2906E-02	.6000E+00
37	3.600	.8150E-03	-.2190E-02	.6000E+00
38	3.700	.6061E-03	-.2680E-02	.6000E+00
39	3.800	.3880E-03	.1014E-03	.6000E+00
40	3.900	.3486E-03	-.5451E-02	.6000E+00
41	4.000	.0000E+00	.1006E-01	.6000E+00

Figure C.2 Sample Output Data File for BactVaripor - continued